Towards deployable analytical systems for nutrient monitoring in natural waters

Eoin Murray (M.Sc.)

Thesis submitted in partial fulfilment of the requirements for the degree of

Doctor of Philosophy

January 2020

Supervisors: Dr Aoife Morrin, Prof Dermot Diamond

School of Chemical Sciences / National Centre for Sensor Research

Dublin City University

Declaration

I hereby certify that this material, which I now submit for assessment on the program of study leading to the award of Doctor of Philosophy is entirely my own work, and that I have exercised reasonable care to ensure that the work is original, and does not to the best of my knowledge breach any law of copyright, and has not been taken from the work of others save and to the extent that such work has been cited and acknowledged within the text of my work.

Signed: _____

Eoin Murray

ID No: 15211877

Date: 6 January 2020

For my parents

Acknowledgments

Firstly, I would like to thank Mark Bowkett and Breda Moore for providing me with the opportunity to carry out this PhD with TelLab. I gratefully acknowledge my Employment-Based Scholarship received from the Irish Research Council.

I would like to thank my colleagues and friends, Patrick Roche, Kevin Harrington, Sandra Lacey and Mathieu Briet for their invaluable assistance and advice. I would also like to thank Padraig Kelly for his generosity during my time at TelLab.

I thank my supervisor, Dr. Aoife Morrin, for her continuous encouragement and guidance throughout the PhD process. I also thank Prof. Dermot Diamond; his advice and expertise during the PhD were indispensable and greatly appreciated.

I would like to extend my thanks and appreciation to Prof. Brett Paull for all his support and for providing me with the opportunity to work at the Australian Centre for Research on Separation Science, UTas. I also acknowledge the Endeavour Research Fellowship received from the Australian Government.

I owe a debt of gratitude to my parents, and I thank them and my aunt, Philomena, for being there through the innumerable ups and downs of the PhD.

Most of all, I would like to give a special thanks to my best friend and partner, Niamh. I am immensely grateful for your support, kindness and everything you do for me.

List of Publications

Journal Publications

1. E.P. Nesterenko, B. Murphy, E. Murray, B. Moore and D. Diamond (2016) 'Solid-phase test reagent for determination of nitrite and nitrate,' *Analytical Methods*, Volume 8, (35), pp. 6520-6528

2. E. Murray, E.P. Nesterenko, M. McCaul, A. Morrin, D. Diamond and B. Moore (2017) 'A colorimetric method for use within portable test kits for nitrate determination in various water matrices,' *Analytical Methods*, 9, 680-687

3. E. Murray, Y. Li, S. Currivan, B. Moore, A. Morrin, D. Diamond, M. Macka and B. Paull (2018) 'Miniaturised capillary ion chromatograph with indirect UV LED based detection for anion analysis in potable and environmental waters', *Journal of Separation Science*, 41, 3224–3231, Journal Cover.

4. E. Murray, P. Roche, K. Harrington, M. McCaul, B. Moore, A. Morrin, D. Diamond, B. Paull (2019) 'Low cost 235 nm UV Light-emitting diode-based absorbance detector for application in a portable ion chromatography system for nitrite and nitrate monitoring', *Journal of Chromatography A*. 1603, 8-14.

5. E. Fornells, E. Murray, S. Waheed, A. Morrin, D. Diamond, B. Paull, M. Breadmore (2019) 'Integrated 3D printed heaters for microfluidic applications: ammonium analysis within environmental water', *Analytica Chimica Acta.*

6. E. Murray, P. Roche, M. Briet, B. Moore, A. Morrin, D. Diamond, B. Paull (2019) 'Fully automated, low-cost ion chromatography system for *in-situ* analysis of nitrite and nitrate in water', *Analytica Chimica Acta,* submitted.

Conference Proceedings

1. E. Murray, P. Roche, A. Morrin, D. Diamond and B. Paull (2019) 'Low-cost, portable, fully automated ion chromatography system with 235 nm UV-LED based microfluidic optical detector for *in-situ* monitoring of nitrite and nitrate', *35th International Symposium on Microscale Separations and Bioanalysis*, Oregon, USA, 25-28 March 2019.

2. E. Murray, P. Roche, S.C Lam, M. Briet, M. McCaul, B. Moore, M. Macka, A. Morrin, D. Diamond and B. Paull (2018) 'Monitoring of nitrate and nitrite in aquatic environments using ion chromatography with low-cost, portable UV optical detection', *32nd International Symposium on Chromatography ISC 2018*, Cannes-Mandelieu, France, 23-27 September, 2018

3. P. Roche and E. Murray (2017) 'Developing smart sensor systems for the detection of nutrients in water', *International Conference and Exhibition on Integration Issues of Miniaturized Systems* (SSI 2017), Cork, Ireland, 8-9 Mar 2017

Oral Presentations

1. E. Murray, P. Roche, A. Morrin, D. Diamond and B. Paull (2019) 'Low-cost, portable, fully automated ion chromatography system with 235 nm UV-LED based microfluidic optical detector for *in-situ* monitoring of nitrite and nitrate', *35th International Symposium on Microscale Separations and Bioanalysis*, Oregon, USA, 25-28 March 2019.

2. E. Murray, P. Roche, A. Morrin, D. Diamond and B. Paull (2018) 'Planning for the successful commercialisation of the first low-cost, deployable nitrate analyser', *ICE-AQUA workshop – Instrumentation and environmental sensors: needs and fronts of knowledge in in situ measurement of inland and marine waters*, Toulouse, France, 26-27 November 2018.

3. E. Murray, P. Roche, S.C. Lam, M. Briet, M. McCaul, B. Moore, M. Macka, A. Morrin, D. Diamond and B. Paull (2018) 'Monitoring of nitrate and nitrite in aquatic environments using ion chromatography with low-cost, portable UV optical detection', *32nd International Symposium on Chromatography ISC*, Cannes-Mandelieu, France, 23-27 September, 2018

4. E. Murray, R. Cunningham, A. Sweetman, A. Morrin, B. Moore, M. Bowkett (2017) 'Monitoring of metals in Irish Rivers using DGT passive samplers', *DGT 2017*, Gold Coast, Australia, 6-8 Sept 2017

5. E. Murray, Y. Li, S. Currivan, B. Moore, M. Macka, B. Paull, D. Diamond and A. Morrin (2017) 'Low cost, autonomous sensor systems for the monitoring of

nutrients in water', *Sensors for Water Interest Group - Low Cost Water Sensors*, University of Southampton, United Kingdom, 5 July 2017

6. E. Murray, Y. Li, S. Currivan, B. Moore, A. Morrin, D. Diamond, M. Macka, and B. Paull (2017) 'Miniaturised capillary ion chromatography with indirect UV detection for anion analysis', *Royal Society of Chemistry Analytical Research Forum*, London, United Kingdom, 7 July 2017

7. E. Murray (2016) 'PhD research within industry: A personal perspective', *The George Guilbault annual analytical symposium*, University College Cork, Ireland, 27 -30 Sept 2016

Poster Presentations

1. E. Murray, B. Moore, D. Diamond, A. Morrin (2016) 'Developing a portable Ion Chromatography System for Freshwater Analysis', *The 8th Conference on Analytical Sciences Ireland* (CASi 2016), Dublin City University, Ireland, 14 - 15 April 2016

2. E. Murray, B. Moore, D. Diamond, A. Morrin (2016) 'Developing a portable Ion Chromatography system for freshwater analysis', *International Symposium on Chromatography* (ISC 2016), University College Cork, Ireland, 28-1 Sept 2016

3. E. Murray, B. Moore, D. Diamond and A. Morrin (2016) 'Developing a portable Ion Chromatography system for freshwater analysis', *Ecobalt 2016*, Tartu, Estonia, 9-12 Oct 2016

4. E. Murray, B. Moore, M. Macka, B. Paull, D. Diamond and A. Morrin, (2017) 'Developing multi-analyte detection systems for *in-situ* monitoring of water chemistry,' *ACES Conference: International Electromaterials Science Symposium*, Wollongong, Australia, 8-10 Feb 2017

5. P. Roche and E. Murray (2017) 'Developing smart sensor systems for the detection of nutrients in water', *International Conference and Exhibition on Integration Issues of Miniaturised Systems* (SSI 2017), Cork, Ireland, 8-9 March 2017

6. E. Murray, Y. Li, S. Currivan, B. Moore, D. Diamond, A. Morrin, M. Macka, B. Paull (2017) 'A miniaturised capillary ion chromatography system with indirect UV

detection', *NAPES Workshop - Sensing our Environment: From Innovative Materials to Autonomous Sensors and Earth Observation*, Dublin, Ireland, 27-28 March 2017

7. E. Murray, Y. Li, S. Currivan, B. Moore, D. Diamond, A. Morrin, M. Macka, B. Paull (2017) 'A miniaturised ion chromatography system for anion analysis in water', *ACES: Collaborate to Innovate Workshop*, Dublin, Ireland, 25 June 2017

8. E. Murray, P. Roche, A. Morrin, B. Moore and M. Bowkett (2017) 'Developing smart sensor systems for the detection of nutrients in water', *International MicroNano Conference*, Amsterdam, Netherlands, 12-13 Dec 2017

Awards

1. Endeavour Research Fellowship Award (2018), awarded by the Australian Government.

2. Travel bursary to attend and present at the Royal Society of Chemistry Analytical Research Forum, received from the Royal Society of Chemistry London, United Kingdom, July 2017

Patent

1. E. Murray, P. Roche, K. Harrington, M. Briet, *Optical detection cell and system for the detection of inorganic analytes*, International Patent - PCT/EP2019/055206, Filed 1st March 2019.

Aims of this Thesis

This project is driven by the current global commercial demand which exists for effective, low-cost portable analytical systems for nutrient monitoring in environmental waters. The overall focus of this research is to develop low-cost analytical solutions and platforms which facilitate and enable on-site and *in-situ* monitoring of various nutrients within freshwater environments. Two strategies will be investigated to achieve this overall aim. The primary strategy of interest is the development of a field deployable, automated ion chromatography (IC) system for nitrate and nitrite analysis. The IC will be comprised of miniaturised, low-cost components and will use LED based optical detection. Rapid prototyping techniques, such as 3D printing and micromilling, will also be assessed as a route to component fabrication. As a complimentary strategy, portable systems incorporating colorimetric chemistries to achieve nutrient analysis platforms will also be explored. Colorimetry integrated within microfluidic platforms, or within simple portable test kit formats will be investigated.

Selected Publications and Author Contribution

This thesis is comprised of five original manuscripts; four published in peer-reviewed journals, and one submitted to a peer-reviewed journal. The central theme of the thesis is the development of low-cost, portable analytical systems and strategies for nutrient analysis in water matrices. The primary approach is concerned with the development of an ion chromatography system for analysis of the anionic nutrient pollutants, nitrite and nitrate. The secondary approach relates to the use of colorimetric chemistries, either in simple test kit form or in combination with microfluidic technology, towards achieving nutrient analysis in the field and *in-situ*. The ideas, construction and writing of manuscripts, along with the generation and interpretation of data, were the responsibility of the candidate. This work was carried out within the R&D laboratories of TelLab, the School of Chemical Sciences, DCU and the Australian Centre for Research on Separation Science, UTas. Supervision and research advice were provided by Dr Aoife Morrin, Prof. Dermot Diamond and Prof Brett Paull. Industrial advice and commercial direction were provided by Mrs Breda Moore and Mr Mark Bowkett of TelLab. The inclusion of various co-authors and the work which the candidate was enabled to carry out within the three collaborating organisations, highlights a collaborative link between DCU, UTas and TelLab which has been strengthened as a result of this PhD. The candidate's contribution to the work reported in chapters 2 to 6 is as follows:

Thesis Chapter	Publications	Publication Status	Candidate's Contribution
2	A colorimetric method for use within portable test kits for nitrate determination in various water matrices	Published, Analytical Methods, 2017	First author, overall concept and initiation, experimentation and analysis, data generation and interpretation, writing of manuscript.
3	Portable capillary ion chromatography with indirect UV LED based detection for anion analysis in potable and environmental waters	Published, Journal of Separation Science (Cover), 2018	First author, key ideas, method development and integration, column fabrication, data generation and analysis, writing of manuscript and design of journal front cover.
4	Low cost 235 nm UV Light-emitting diode-based absorbance detector for application in a portable ion chromatography system for nitrite and nitrate monitoring	Published, Journal of Chromatography A, 2019	First author, overall concept and initiation, design and fabrication of optical cell, method development and experimentation, data generation and analysis, writing of manuscript.
5	Integrated 3D printed heaters for microfluidic applications: ammonium analysis within environmental water	Published, Analytica Chimica Acta, 2019	Co-First author, key ideas, input into reactor design, integration of reactor with method, data generation and interpretation, shared writing of manuscript.
6	Fully automated, low-cost ion chromatography system for *in-situ* analysis of nitrite and nitrate in natural waters	Submitted, Analytica Chimica Acta, 2019	First author, overall concept and initiation, input into system design, data generation and interpretation, deployment of system and writing of manuscript.

Signed: _____ Date:

Eoin Murray

Signed: _____ Date:

Dr. Aoife Morrin

Thesis Structure and Outline

This thesis is structured into eight chapters, an overview of each chapter is given below:

Chapter 1

This chapter can be seen as the introduction and provides a background to the research undertaken. The occurrence and effect of nutrients in the aquatic environment are discussed. Relevant legislation and the typical strategies and techniques employed for nutrient monitoring in the context of legislative compliance are highlighted. State-of-the-art and commercially available *in-situ* analytical systems for nutrient monitoring are explored. The aim is to inform the reader of the current situation within the water monitoring marketplace, and the need which exists for low-cost portable nutrient sensing platforms.

Chapter 2

This chapter is a study on the development, optimisation and validation of a colorimetric method for nitrate determination in various water matrices. The study aims to develop a simple, fast and low-cost method which can be integrated into a portable test kit format for direct on-site analysis. The developed method was accredited according to ISO 17025 accreditation guidelines and demonstrated excellent correlation to an accredited IC.

Chapter 3

This chapter works towards achieving a low-cost, portable nutrient analysis system through the application of chromatography. The chapter highlights the development and analytical assessment of a novel miniaturised capillary IC which employs indirect UV LED based detection for anion analysis in environmental waters. The IC is light weight and the modular design enables ease of modification. The miniaturised IC system allows for the analysis of nitrate, nitrite and other small inorganic anions in various water matrices. This work was carried out within the Australian Centre of Research on Separation Science (ACROSS) at the University of Tasmania.

Chapter 4

Building on the lessons learned in chapter 3. This chapter details the design and development of a novel, low cost, UV absorbance detector incorporating a 235 nm light emitting diode (LED) for use with portable ion chromatography. The optical cell was fabricated using rapid prototyping techniques such as micromilling and 3D printing. A chromatographic method for the direct detection of nitrate and nitrite using the UV LED detector was developed and a simple portable IC configuration was built and tested analysing an extensive range of water samples.

Chapter 5

This chapter describes the development of a multi-material 3D printed microfluidic reactor with integrated heating. This reactor was demonstrated with colorimetric determination of ammonium. Using such a reactor, the acceleration of colorimetric reactions to achieve fast determination of ammonium was investigated. A simple flow injection analysis set up was built and ammonium analysis was carried out. A system such as this offers potential when considering integration with the developed UV-LED detector reported in chapter 4, in order to generate a portable total nitrogen analysis system.

Chapter 6

This chapter draws from the developments and work described in the prior chapters. An automated, low-cost portable IC system was generated employing 3D printed pumps and the optical detector described in chapter 4. The system was validated in the lab and was deployed in the US, Finland and Ireland. The performance of the system was established and compared to grab sample data and accredited instrumentation.

Chapter 7

This chapter discusses experimentation and work which was carried out at the early stages of the PhD. The observations associated with this work are reported and the way in which they informed the direction of the research is elucidated. This chapter demonstrates how the generation of unexpected results can provoke a new direction of focus which can ultimately lead to fruitful outcomes.

Chapter 8

This chapter summarises the work carried out and presents the conclusions which have arisen. The next steps for the portable IC system in terms of manufacturing and commercialisation are discussed and the potential impact which the system has on the market place is highlighted. In addition, the challenges and hurdles which lie ahead are set out and the strategies to overcome these challenges are conveyed.

Table of Contents

Declaration i
Acknowledgments iii
List of Publications iv
Aims of this Thesis viii
Selected Publications and Author Contribution ix
Thesis Structure and Outline xii
List of Abbreviations xix
Abstract xxi

Chapter 1
Introduction 1
1.1 Water quality 2
1.2 Nutrient pollution 2
1.3 Towards point-of-use water analysis 4
1.4 Current *in-situ* nutrient monitoring 4
1.4.1 Analysers based on direct optical detection 5
1.4.2 Colorimetric based nutrient analysers 6
1.4.3 Electrochemical based systems 12
1.4.4 Chromatography based analysers 15
1.5 Conclusions 22
1.6 References 23

Chapter 2
A colorimetric method for use within portable test kits for nitrate determination in various water matrices 31
2.1 Introduction 33
2.2 Experimental 35
2.2.1 Materials and reagents 35
2.2.2 Instrumentation 36
2.2.3 Methods 36
2.3 Results and Discussion 38
2.3.1 Determination of optimum working conditions for the Zn powder method 38
2.3.2 Method Validation 39

2.3.3 Comparison of Zn powder method against accredited IC analysis 45
2.3.4 Comparison against alternative colorimetric method 46
2.4 Conclusions 47
2.5 Acknowledgements 48
2.6 References 49

Chapter 3

Miniaturised capillary ion chromatograph with indirect UV LED based detection for anion analysis in potable and environmental waters 51
3.1. Introduction 54
3.2. Materials and methods 55
3.2.1 Reagents and materials 55
3.2.2 Packing of capillary anion exchange column 56
3.2.3 Capillary ion chromatography platform 56
3.3. Results and discussions 59
3.3.1 LED comparison and assessment 59
3.3.2 Chromatographic repeatability 61
3.3.3 Capillary IC analytical performance 62
3.3.4 Water sample analysis 63
3.4 Conclusions 65
3.5 Acknowledgements 65
3.6 References 66

Chapter 4

Low cost 235 nm UV-LED based absorbance detector for application in a portable ion chromatography system for nitrite and nitrate monitoring. 68
4.1. Introduction 70
4.2. Experimental 72
4.2.1. Chemicals and Reagents 72
4.2.2. Instrumentation 73
4.2.3. UV Optical Detector 74
4.2.4. Stray Light and Effective Path Length Determination 75
4.3. Results and Discussions 76
4.3.1. Thermal Study of LED and Detector 76
4.3.2. Detector Stray Light and Effective Optical Path Length 77
4.3.3. Chromatography Repeatability 78

4.3.4. Assessment of Interfering Anions 80
4.3.5. Analytical performance and sample analysis 81
4.3.6. Integration of detector with low pressure syringe pump 82
4.4. Conclusion 84
4.5. Acknowledgements 85
4.6. References 86

Chapter 5

Integrated 3D printed heaters for microfluidic applications: ammonium analysis within environmental water 90

5.1. Introduction 92
5.2. Experimental 95
5.2.1. Chemicals and Reagents 95
5.2.2. Heating chip design and printing 95
5.2.3. System configuration and measurement procedures 96
5.2.4. Thermal study for ammonium analysis 97
5.3. Results and Discussions 98
5.3.1. Heater fabrication and thermal characterisation 98
5.3.2. Assessment of mixing on chip 102
5.3.3. Temperature study with simplified Berthelot method 103
5.3.4. Sample Analysis 104
5.4. Conclusion 106
5.5 Acknowledgements 106
5.6 References 107

Chapter 6

Fully automated, low-cost ion chromatography system for *in-situ* analysis of nitrite and nitrate in natural waters 112

6.1. Introduction 114
6.2. Materials and methods 116
6.2.1. Chemicals and reagents 116
6.2.2. Portable IC system 116
6.2.3. Fluidic configuration 118
6.2.4. Sample intake system 120
6.2.5. System control and data acquisition 121
6.3. Results and Discussions 123

6.3.1 Chromatographic Repeatability 123
6.3.2. Analytical Performance 124
6.3.3. *In-situ* analysis 125
6.4. Conclusions 128
6.5. Acknowledgements 129
6.6. References 130

Chapter 7
Other experimentation and observations 133
7.1 Monolithic columns and conductivity detection 134
7.2 LED-based optical detection 137
7.3 Conclusion 139
7.4 References 141

Chapter 8: Conclusions and future perspectives 142
8.1 Overall summary and conclusions 142
8.2 Next Steps 145
8.3 Towards Commercialisation 147
8.4 Other Analytes 149
8.5 References 151

Supplementary Information A A1
Supplementary Information B B1
Supplementary Information C C1
Supplementary Information D D1
Supplementary Information E E1

List of Abbreviations

IC	Ion chromatography
UV	Ultraviolet
LED	Light emitting diode
FIA	Flow injection analysis
LOC	Lab-on-a-chip
PMMA	Poly(methylmethacrylate)
ISE	Ion selective electrode
OTIC	Open tubular ion chromatography
CPC	Cetylpyridinium chloride
LOD	Limit of detection
WRC	Water research centre
SFI	Science foundation Ireland
LOQ	Limit of quantification
S/N	Signal to noise
WFD	Water framework directive
EPA	Environmental protection agency
CSV	Comma separated value
ESI	Electronic supplementary information
RSD	Relative standard deviation
R_S	Resolution
SSR	Sum of squared residuals
HPLC	High performance liquid chromatography
ABS	Acrylonitrile butadiene styrene

PCR	Polymerase chain reaction
FDM	Fused deposition modelling
HTHP	High pressure and high temperature
CWA	Clean water act
D-ABS	Diamond infilled acrylonitrile butadiene styrene
PLA	Polylactic acid
PID	Proportional-integral-derivative
µTAS	Micro total analysis systems
ACT	Alliance for coastal technologies
PWM	Pulse width modulation
DDAB	Didodecyldimethylammonium bromide
SEM	Scanning electron microscope
PD	Photodiode
TRL	Technology readiness level
R^2	Coefficient of correlation
WHO	World health organisation
WWTP	Waste water treatment plant
SLA	Stereolithography
NPD	New product development
IoT	Internet of things

Abstract

The freshwater environment is intrinsically linked to human, animal and plant life and is an indispensable resource for the economy. Effective water quality monitoring is therefore one of the cornerstones of environmental protection and this importance is reflected within both European and global legislation. Nutrient pollution in water bodies can be seen as one of the largest global problems which effects the freshwater environment. Current legislation and policies governing water quality depend on grab sampling techniques, providing only instantaneous data which can result in a non-representative estimate of the nutrient pollution load status of a water body. In order to fully satisfy the water sectors need for comprehensive analysis, management and protection, effective portable *in-situ* nutrient monitoring systems are required.

The focal point of this research was based around the current need which exists for inexpensive, robust *in-situ* nutrient monitoring solutions for the freshwater environment. The primary goal was to develop a low-cost, field deployable, automated IC system for nutrient anion analysis. Complimentary to this work, portable systems based on colorimetry for nutrient analysis were also explored. Through this research, a portable low-cost nitrate test kit has been developed which is based on a modified version of the Griess assay and employs zinc as a reducing agent. The developed method was validated according to ISO17025 accreditation guidelines and reliably detected nitrate in a range of freshwater samples. A portable, lightweight capillary IC system for anion analysis in water was also developed and demonstrated in a laboratory setting. The IC uses low-cost, miniaturised components and through a modular design enables flexible system modification.

Progressing from this capillary system, a new low-cost, UV absorbance detector incorporating a 235 nm light emitting diode (LED) was developed for portable ion chromatography. The detector enabled selective, fast determination of nitrite and nitrate in a range of natural waters. In an attempt to develop a portable system for ammonium analysis, a multi-material 3D printed microfluidic reactor with integrated heating was fabricated and used with colorimetry to facilitate fast ammonium determination. Although the analytical range for ammonium

determination was narrow, the developed 3D printed heater represents a novel contribution in the area of 3D printed analytical systems. Finally, an IC which is low-cost, automated and fully deployable was developed which allows for *in-situ* analysis of nitrite and nitrate in a wide variety of natural waters. The system employed 3D printed pumps for eluent delivery and the 235 nm LED based optical detector which was developed during the course of the research. The system was deployed at various locations around the world and achieved an analytical performance comparable to accredited benchtop instrumentation.

Chapter 1:

Introduction

Chapter Overview

This chapter highlights the impact nutrient pollution has on the freshwater environment, both economically and ecologically. Environmental legislation which is in place to battle this problem, the limitations associated with grab or spot sampling, and the need which exists for portable; *in-situ* analytical systems are discussed. Current state-of-the-art and commercial *in-situ* analytical systems for the analysis of nutrients in the freshwater environment are reviewed. Optical based sensor systems, microfluidic lab-on-chip (LOC), electrochemical and chromatography-based sensor systems are discussed. The key theme of this thesis, arises from the current lack of low-cost, *in-situ* nutrient analysis systems available on the market. Through chapter 1, we gain an insight into the systems currently available on the market, and the shortcomings which these systems exhibit. In the subsequent chapters complimentary low-cost approaches are introduced exploring both colorimetric and chromatographic approaches towards achieving low-cost *in-situ* nutrient analysers.

1.1 Water quality

Water is a crucial natural resource upon which all social and economic activities and ecosystem functions depend [1]. Despite the importance of water, over 80 % of used water worldwide is discharged untreated into water bodies [2]. Water pollution arises when substances build up to such an extent that the water becomes unfit for its natural or intended use. Pollutant pressures can be divided into two main sources: point sources and diffuse sources. Point sources can be defined as fixed or stationary facilities from which pollutants are discharged. Examples of this type of source include wastewater treatment plants and industrial discharges. Diffuse pollution arises from activities which have no specific point of discharge. Agriculture is a leading example of diffuse pollution along with anthropogenic landscapes. In Europe, 38% of surface waters are said to be under significant pressures from diffuse pollution, while 32% of freshwater bodies are under significant pressure from point sources [3]. Within the US, it is reported that in 2015, U.S. industries and businesses discharged 86.6 million kg of chemicals into rivers and streams [4]. Water is often regarded as the "universal solvent" due its capability of dissolving more substances than any other liquid. As a consequence of this trait, water readily dissolves the substances originating from the numerous pollutant sources, which ultimately results in water pollution. Of the various types of water contamination, nutrient pollution, caused by excess nitrogen and phosphorus in water, can be seen as a leading treat to water quality worldwide [2].

1.2 Nutrient pollution

Globally, the most prevalent water quality problem results from high nutrient loads entering water bodies [5]. Nitrogen and phosphorus, predominantly in the form of nitrite (NO_2^-), nitrate (NO_3^-) and phosphate (PO_4^{3-}), are nutrients naturally found in aquatic ecosystems. These nutrients play an essential role for the growth of algae and aquatic plants which provide food and habitat for aquatic organisms. Despite the intrinsic nature of nutrients within natural processes, excessive levels in water bodies can arise as a consequence of anthropogenic activities such as agriculture, wastewater discharges and sewage disposal. This often has a detrimental impact, both from an environmental and economic

perspective. The key environmental issue associated with nutrient pollution of water bodies is eutrophication. This condition results in the overproduction of algae and aquatic plants as shown in Figure 1.1. Algal blooms can severely reduce oxygen levels in water which results in fish kills. In addition to environmental impacts, significant economic impacts are associated with nutrient pollution. In European countries such as Spain and the Netherlands, eutrophication costs the economy hundreds of millions of euro per year, mainly as a consequence of loss of water function. While in the U.S., nutrient pollution can cost the economy $2.2 billion per year [6].

Figure 1.1: Satellite image of toxic algae bloom in Lake Erie, USA [7]

As a response to the impacts associated with nutrient pollution, a range of regulatory and legislative documentation exists both in Europe and globally which requires the monitoring of chemical nutrients in water bodies (EU Water Framework Directive 2000/60/EC; Council Directive 91/271/EC; Blueprint to Safeguard Europe's Water Resources, Clean Water Act 1972).

1.3 Towards point-of-use water analysis

At present, nutrient analysis and monitoring, in compliance with legislation, predominantly involves grab sampling. Grab sampling refers to the act of manually collecting a water sample for either on site analysis or subsequent laboratory analysis. This methodology is well established and has been accepted for regulatory and legislation purposes. However, numerous shortcomings are associated with this approach. When taking a grab sample, sample composition can change at any time during sampling, transportation, preservation or storage. While the magnitude of the change may be minimised, it cannot be eliminated completely. Grab sampling only provides instantaneous data, and when monitoring for regulatory purposes the use of infrequent grab sampling often results in non-representative estimates of pollution loads. As nutrient concentrations fluctuate in water systems, grab sampling may either miss recurring pollution episodes leading to underestimation of pollution, or catch a pollution episode as it occurs leading to overestimation of the total pollution load [8]. To overcome the issues associated with grab sampling, and to effectively manage nutrient pollution, *in-situ* analysers are required. Through the use of these analysers, the measurement of nutrients directly in the environmental medium is enabled, providing real-time observations of nutrient levels [9].

1.4 Current *in-situ* nutrient monitoring

Over the years, various technologies and analytical techniques have been explored in order to achieve *in-situ* sensors and instruments for nutrient monitoring in aquatic environments [9]. This chapter aims to provide an overview of current commercially available technologies along with developments in the area of *in-situ* monitoring of nutrients in freshwater systems. The review focuses on analytical systems based on optical detection, including LOC systems, electrochemistry and chromatographic techniques. Information on the systems in terms of analytical operation, portability, deployment demonstration, longevity in the field and cost is provided. In addition, it should also be noted that further detail on *in-situ* nutrient analysers is also provided and discussed within the introduction sections of the papers reported in each of the subsequent thesis chapters.

1.4.1 Analysers based on direct optical detection

The development of *in-situ* nutrient sensing systems has predominantly focused on optical-based detection mechanisms. Optical methods refer to those techniques which involve the interaction of electromagnetic radiation with atoms or molecules. Nitrate and nitrite anions have natural absorbance peaks within the ultraviolet (UV) electromagnetic spectrum. By measuring optical absorption at specific wavelengths, nitrate and nitrite concentrations within water media can be determined. This approach does not require any reagents and provides fast response times. Over the past decade, *in-situ* UV-spectrophotometers for nitrate and nitrite analysis have been used for waste water monitoring [10, 11] and have been deployed successfully in various marine and oceanographic studies [12, 13]. Direct UV nitrate and nitrite sensors have also gained broad application within a range of freshwater matrices [14-16].

A number of *in-situ* UV spectrophotometers are commercially available which have suitable deployment capabilities and performance characteristics to yield high resolution nitrate and nitrite measurements in freshwater and other aquatic environments. YSI Incorporated (Yellow Springs, USA) provide an *in-situ* UV nitrate sensor called the NitraVis which provides real-time nitrate analysis in aquatic environments. Figure 1.2 (left) shows the NitraVis probe. In addition, Sea-Bird Scientific produce the 'SUNA' UV nitrate sensor which is more suited to turbid waters and is virtually applicable to any aquatic environment. The SUNA V2 UV sensor system is shown in Figure 1.2 (right). Other examples of *in-situ* spectrophotometers which can achieve high resolution nitrate and nitrite monitoring in freshwater environments, as reported by Huebsch *et al.* [16], include the Nitratax plus sc sensor (Hach Lange GmbH, Germany) and the spectro::lyser™ (s::can Messtechnik GmbH, Austria). Despite the demonstrated suitability of *in-situ* UV spectrophotometers in terms of continuous nitrate and nitrite monitoring in freshwaters, these systems are considerably expensive. Costs to purchase a UV nitrate sensor can range from $ 15,000 - $25,000 per unit and additional expenses are also related to instrument service and maintenance [17]. When considering phosphate analysis, direct optical detection sensors are not applicable, as the phosphate anion does not absorb UV light directly. To

enable spectrophotometric detection of phosphate, a reagent can be added which reacts with phosphate to form a new molecule capable of absorbing light at a specific wavelength. This is the basis of colorimetric chemistry, where following the addition of reagents, the formation of an absorbing dye which incorporates the analyte results. The optical absorption of this dye is linearly proportional to the target analyte concentration [18]. A wide range of colorimetric based *in-situ* nutrient analysis systems have been developed over the years and a number of high-performance systems are currently available on the market.

Figure 1.2: (Left) YSI SensorNet NitraVis® optical sensor for *in-situ* nitrate analysis. Dimensions: Length 80 cm; diameter 6 cm with a weight of ~ 4 kg [19] (Right) SUNA V2 UV nitrate sensor. Dimensions: Length 70 cm; diameter 7 cm with a weight of ~ 3 kg [20].

1.4.2 Colorimetric based nutrient analysers

Colorimetric and spectroscopic techniques are very well-established techniques, and many standard methods exist for the analysis of nitrate, nitrite and phosphate in the laboratory [21, 22]. As a result of this extensive knowledge concerning optical methods, in addition to developments in the fields of light-emitting diode (LED) technology, communications and rapid prototyping techniques, the generation of colorimetric based *in-situ* nutrient analysers has been facilitated.

The concept of flow injection analysis (FIA) employing colorimetry represents a typical approach which is adopted to achieve *in-situ* nutrient analysers. FIA refers to continuous flow analysis that uses an analytical stream into which reproducible volumes of sample are injected. *In-situ* analysers based on flow analysis methods incorporate a pump, detector and a narrow bore tube manifold. The pump propels the sample through the tube manifold where mixing with reagent occurs to form detectable species [23]. The first flow injection analysis systems were focused within the field of electrochemistry. In 1970, Nagy *et al.* published their first of a series of papers relating to the injection of a sample into a flowing stream of electrolyte [24]. Soon after, colorimetric analysis of nutrients in water matrices using FIA configurations were carried out [25]. Since the 1990's, a variety of field analysers based on FIA and colorimetry have been developed for the detection of nutrient analyte species in a range of aquatic media [26-29].

A number of *in-situ* and online colorimetric based flow analysers for nutrient monitoring have been developed and are commercially available. For example, the YSI 9600 (YSI Inc., USA) allows for continuous recording of nitrate at variable intervals in a range of waters, while the Liquiline System from Endress+Hauser offers precise online measurement of nitrite. The Sea-Bird Scientific HydroCycle – Phosphate Sensor is an example of a miniaturised colorimetric based sensor which enables *in-situ* phosphate monitoring. The Systea WIZ probe (Systea S.p.A Analytical Technologies, Italy), depicted in Figure 1.3, is a leading state-of-the-art *in-situ* probe for monitoring fresh and marine aquatic environments. The system can detect phosphate, nitrate, nitrite and ammonia. Similar to the aforementioned colorimetric sensors, the Systea WIZ analyzer is deployed with on-board reagents along with standard solutions to enable *in-situ* calibrations.

Figure 1.3: Photograph of the Systea WIZ probe prior to nitrate monitoring deployment to assess system performance in the field. Dimensions: 140 mm diameter x 520 mm height (analytical unit); 70 mm diameter x 200 mm height (reagents container) [30].

When considering *in-situ* nutrient analysis based on colorimetry and optical detection, the application of microfluidic technology represents a promising avenue towards achieving miniaturised analysers. From a low-cost, miniaturisation perspective, microfluidics serves to miniaturise and integrate processes previously employed at a larger scale in separate operation. This integration and miniaturisation falls under the concept of lab-on-a-chip (LOC). When applied to colorimetric nutrient analysis, LOC systems potentially allow for high performance analysis while reducing reagent volumes and power consumption in comparison to larger *in-situ* analysers [18]. Microfluidics is also well-suited to rapid-prototyping and micro-fabrication techniques such as micromilling and 3D printing. As a consequence, a potential exists to develop and manufacture analytical systems which are much lower cost than that of macroscale instruments.

A variety of microfluidic based nutrient analysers, employing the principles of colorimetry, have been demonstrated in recent years. For a description of microfluidic systems employed for *in-situ* chemical analysis in water, including nutrient analysis, along with technical developments in this area, Nightingale *et al.* has reported a comprehensive review [31].

An overview of nutrient analysis prototypes which have been developed over the past decade are briefly discussed in the succeeding paragraphs. In 2010, Cleary *et al.* reported an autonomous microfluidic sensor for phosphate detection in environmental waters. The system used the vanadomolybdate method within a microfluidic manifold where mixing, reaction and detection took place. Optical detection was performed using a LED light source and photodiode detector [32]. Hwang *et al.* (2013) described a platform based on centrifugal microfluidics for the simultaneous determination of NO_2^-, NO_3^-, NH_4^+, PO_4^{2-}, and silicate in water. All processes were integrated and automatically performed on the rotating disc device. The system incorporated a number of novel aspects such as the control of liquid transfer by laser irradiation on ferrowax-based microvalves. However, poor long-term deployment capabilities were noted due to the limited number of samples which could be processed simultaneously on a single disc [33].

Several examples of *in-situ* microfluidic devices for nutrient monitoring in water bodies have been reported by the National Oceanographic Centre (NOC), Southampton, UK [34, 35]. One such example is the system reported by Beaton *et al.* (2012). This microfluidic based system enabled effective, automated *in-situ* colorimetric detection of nitrate and nitrite in natural waters. The Griess assay was employed for nitrite detection, and reduction of nitrate to nitrite was achieved through the use of a cadmium column. The system was deployed in a range of water matrices and demonstrated effective monitoring of nitrate and nitrite [36]. Additionally, an example of a high-performance microfluidic analyser for phosphate monitoring was reported by Legiret *et al.* [37]. The system used the vanadomolybdate method in combination with a microfluidic chip manufactured from tinted poly (methyl methacrylate) (PMMA), custom syringe pumps and on-board standards and control electronics. Although this system was applied within the marine environment, the system could also find application within freshwater monitoring. In 2017, Clinton-Bailey *et al.* from NOC, reported a LOC analyser for *in-situ* phosphate monitoring based on an improved molybdenum blue colorimetric method. The system, depicted in Figure 1.4, was successfully continuously deployed for 9 weeks in a fluvial system, autonomously monitoring phosphate levels *in-situ* [38]. This system can be seen as an important step towards generating high resolution sensors for effective *in-*

situ nutrient monitoring, yet this platform still had a total manufacturing cost of ~ €10,000. A cost-effective *in-situ* phosphate analyser was described and tested by Donohoe *et al.* (2018). The system employed the vanadomolybdate colorimetric method for phosphate analysis on a microfluidic chip with LED-based optical detection. The system was deployed at a freshwater lake for several days and successfully generated phosphate data [39].

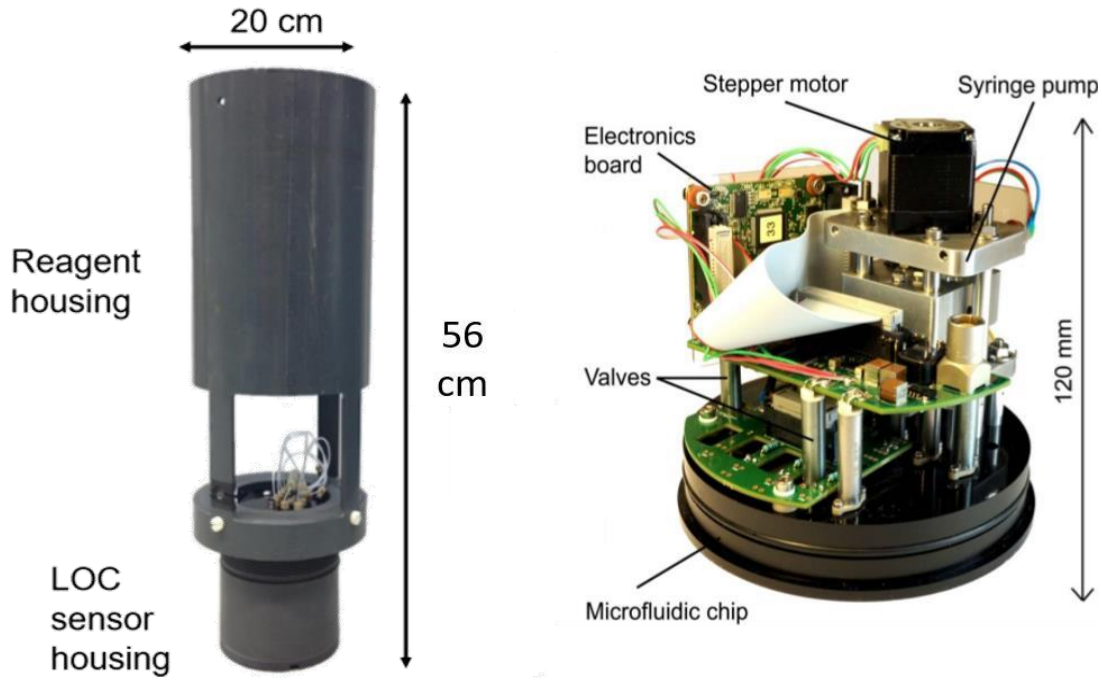

Figure 1.4: (Left) Complete sensor system with reagent and LOC sensor housings developed by NOC. (Right) Phosphate LOC microfluidic configuration. The platform can be adapted for other absorbance-based assays such as nitrate or nitrite [38].

A very promising area in terms of achieving low-cost *in-situ* nutrient analysers is that of droplet-based microfluidics. Within these systems, aqueous samples and reagents are carried as discrete droplets within an immiscible oil. By using this approach instead of a typical microfluidic flow approach, dispersion effects and surface interactions at channel walls can be reduced. In addition, measurement throughput can be significantly increased. A prototype nitrate and nitrite sensor combining this approach with colorimetric chemistry (Figure 1.5) has been developed and reported by SouthWestSensor Ltd. The system has the potential to achieve high frequency monitoring in a range of environmental waters and is currently in its final stages of development before market launch.

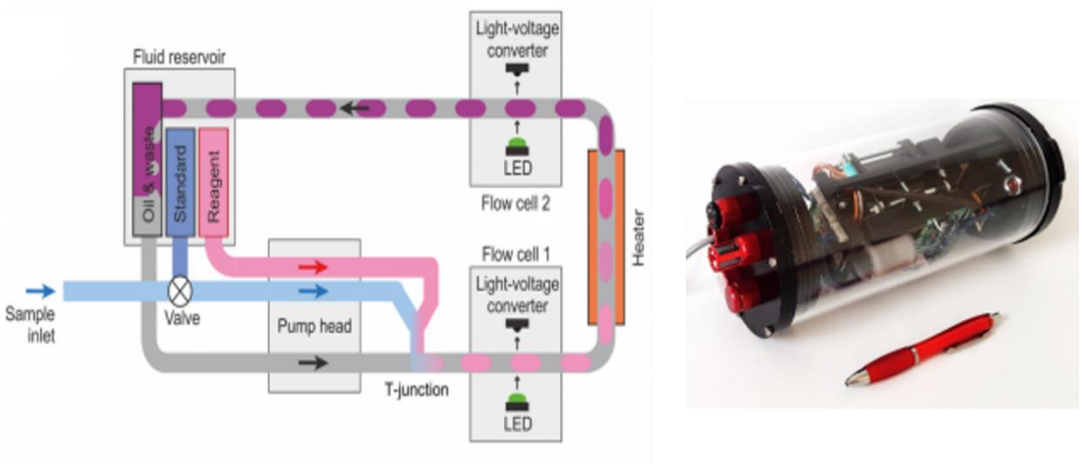

Figure 1.5: Field deployable nitrite and nitrate sensor based on novel droplet microfluidics developed for SouthWestSensor Ltd. (Left) Schematic showing fluidics of sensor and mode of operation. (Right) Image of finished sensor incorporating fluidics, heater, flow cells, and control electronics with a pen shown for scale [40].

1.4.3 Electrochemical based systems

Electrochemical approaches have been extensively used for the analysis of major and minor elements in aquatic environments [41]. Electroanalytical systems for the analysis of environmental waters has greatly progressed in recent years. Notable advances in terms of cost, assay time, minimal sample preparation, sensitivity and selectivity have been achieved. A key focus of development over the past number of decades has been towards the development of electrochemical based devices for *in-situ* measurements [42].

A wide variety of electrode substrates and strategies have been employed for the determination of nitrate and nitrite including copper [43], cadmium [44], boron doped electrodes [45], and gold [46] just to name a few. This abundance of electrode materials suggests that the electroanalytical determination of nitrate and nitrite at bare electrodes is simply achieved, however it is far from facile. Using bare electrodes, the kinetics of the charge transfer are slow which leads to poor sensitivity and reproducibility. Modification of electrodes make reduction more feasible and facilitates improved analyte detection. However, these modifications can be fragile, expensive and procedurally complex limiting use for *in-situ* deployment [47]. Of the modifications, copper electroplating may be seen as one of the more simplistic and inexpensive ways of functionalising electrodes for nitrate and nitrite detection [48]. Ion selective membrane electrodes (ISEs) have also showed a lot of promise when considering portable or *in-situ* sensing platforms for environmental water analysis [49]. An example of a commercial ion-selective electrode (ISE) for nitrate analysis in freshwaters is the WQ-Nitrate sensor (Figure 1.6) developed by NEXSENSE Technologies. This ISE probe has a USB interface allowing for analysis directly in the field. Although this system is portable and well-suited to on-site analysis, the system is not autonomous or deployable.

Figure 1.6: (Left) Photograph of WQ-Nitrate ISE Sensor. (Right) Construction of ISE sensor. The electrode can be used within lab and field applications. The probe is ~ 15 cm in length and 1.5 cm in diameter [50]

Enzymatic-based biosensors have also been shown to be an effective means of electrochemical nitrate detection in water matrices. Typically, within these systems nitrate reductase is used for the reduction of nitrate to nitrite and the reducing current is used to determine nitrate concentration [51]. However, enzymes require storage under ideal conditions and degrade overtime which makes them poorly suited for long-term *in-situ* deployment. An alternative, more robust approach to enzyme-based biosensors for nitrate and nitrite is the use of biosensors based on denitrifying bacteria. A commercially available bacteria-based biosensor, referred to as the NO_x^- Biosensor is produced by Unisense (Unisense A/S, Denmark). Using this sensor, NO_3^- or NO_2^- anions enter the sensor through an ion-permeable membrane. Active denitrifying bacteria, present in a chamber within the sensor, reduce nitrate or nitrite to N_2O. This N_2O is then detected electrochemically by a N_2O transducer. Denitrification is facilitated by electron donors contained in a reservoir within the sensor. As a result of this reservoir, bacteria growth is continuous, enabling greater robustness as opposed to enzyme-based systems. The NO_x^- Biosensor, shown in Figure 1.7, is well-suited to freshwater analysis and can measure nitrate and nitrite at concentrations below 0.5 µM showing good stability over days [52]. However, the sensor is not suited to long term *in-situ* analyses for weeks or months due to loss of stability and fouling issues.

Figure 1.7: Unisense NOx^- biosensor for nitrate and nitrite analysis in environmental waters. NO_x^- or NO_2^- ions diffuse across an ion-permeable membrane. Active denitrifying bacteria secured behind the membrane reduces NO_x^- or NO_2^- to N_2O, which is then detected by a N_2O transducer. The total length of the probe is 20 cm and the shaft diameter is 1.5 cm [52].

Similar to nitrate and nitrite, a variety of electrode substrates have been demonstrated for phosphate determination. Such approaches include metal electrodes, gold and glassy carbon modified electrodes [53], modified carbon paste electrodes [54], lead ion selective electrodes [55] and cobalt-based electrodes [56, 57]. A comprehensive review of potentiometric, voltammetric and amperometric methods for phosphate determination is reported by Berchmans *et al.* [58], with a further review on the analysis of soluble phosphates in environmental samples reported by Warwick *et al.* [59]. Recently, reagentless paper-based electrochemical sensors have shown impressive potential as a route to low-cost, rapid nutrient analysis. For example, Cinti *et al.* demonstrated a paper-based screen-printed electrochemical sensor for phosphate detection in freshwater. Through a three-step process consisting of wax patterning, paper chemical modification using acidic molybdate solution containing supporting electrolyte, and electrode screen-printing, the filter paper provided an effective electroanalytical platform for phosphate detection through cyclic voltammetry [60]. Although this system represents a simple and affordable approach to phosphate detection, the system is yet to be tested in the field and is not suited to long term, autonomous, *in-situ* deployment in environmental water systems.

Overall, electrochemical based systems are inexpensive and easy to use. However, when considering long term *in-situ* deployments in environmental waters, electrochemical probes have not seen any level of significant adoption in terms of nutrient analysis. This is mainly due to high drift over time, ionic interferences and biofouling as probes are most typically directly exposed to the sample during analysis [61].

1.4.4 Chromatography based analysers

Ion chromatography (IC) is a leading standard method for the analysis of nutrient anions in freshwater samples and a range of standard methods are available and widely used for regulatory monitoring purposes [62]. Although various approaches are available for the separation of inorganic ionic species such as ion interaction, chelation and ion exclusion chromatography, ion-exchange can be seen as the primary separation mode used in IC [63]. In ion-exchange chromatography, most typically the stationary phase is comprised of a porous, insoluble resin containing fixed charged groups and mobile counter ions of opposite charge. As the mobile phase passes through the column, these counter ions are reversibly exchanged for analyte ions carrying the same charge, Variations in the interaction and the affinity of the analyte ions with the stationary phase results in differential migration rates and in turn analyte separation.

For the analysis of nitrate, nitrite and phosphate using IC, suppressed conductivity detection is regarded as the standard method of detection. Electrolytic conductivity detection is well suited to IC as conductivity is a property shared by all ions. As the eluent used in IC is comprised of high amounts of salt, it exhibits a high conductivity. To enable efficient conductivity detection of analyte ions eluted from the system, the amount of background dissolved ions present in the eluent must be decreased after the column. This reduction in background eluent conductivity is achieved through the use of a suppressor. In a suppressor, eluent is neutralised by continuous flow ion exchange through a membrane. The eluent flows inside the membrane, while a regenerant, typically an acid, flows on the outside of the membrane in the opposite direction. For the separation of nutrient anions using alkaline eluent a cation exchange takes place across the membrane. Thus, eluent Na^+ or K^+ cations are exchanged with regenerant H^+ cations. The membrane incorporates covalently bound sulfonic acid groups which enables the selective transportation of the cations. Analyte anions are prevented from passing through the membrane due to electrostatic repulsion [64]. Although less common, direct conductivity or nonsuppressed conductivity can also be utilised with IC. Nonsuppressed conductivity methods

require low capacity stationary phases and dilute eluents to achieve low background conductivity and in turn analyte anion detection. As both NO_2^- and NO_3^- are UV-absorbing electroactive species, UV/VIS detection represents another direct detection method which can be used with IC. Alternatively, indirect UV-VIS detection can be used to detect nitrate, nitrite and phosphate along with other inorganic anions. For indirect UV-VIS, a highly UV absorbing eluent is used so analyte anions reduce detector signal following elution. As each analyte ion elutes from the column, eluent ions are displaced allowing more light to reach the photodiode detector. This decrease in absorbance appears as an inverse peak and is directly proportional to analyte concentration.

Despite the widespread application of IC for nutrient analysis and the broad range of detection modes available, analysis has predominantly been confined to a laboratory setting and there has been a lack of successful commercial development of automated, *in-situ* IC systems. The physical size, significant weight, eluent and power requirements of bench-top IC systems have hindered the uptake of IC for portable, autonomous applications. Over the past 30 years, a number of prototype portable IC systems, employing a range of strategies, for monitoring of ionic analytes in aquatic media have been reported. One of the earliest attempts towards portable IC was that of Tsitouridou and Puxbaum [65]. Using a single column IC with conventional bench-top components and non-suppressed conductivity detection, anion concentrations, such as nitrite and nitrate, of fog water and atmospheric aerosols were determined in the field. Although the system was applied in the field, the system weighted 20 kg and still had the cost and power requirements associated with traditional systems. Over the years, others have also demonstrated portable IC systems for anion analysis using predominantly standard IC components [66-68]. However, these systems were not automated, *in-situ* devices and required manual interaction.

An example of a commercial portable IC for online anion and cation analysis has been provided by Qingdao Sheng-Han Chromatography, China, since 2013. This system is sold as a portable instrument, but uses typical system components, thus the system is not low-cost and although portable, the system cannot be deployed autonomously *in-situ* for long deployment periods [69]. In 2014, Elkin

successfully demonstrated an automated, battery powered portable IC which allowed for autonomous operation in the field for a period of one month. The IC used a commercial guard column, an eluent reflux device for eluent regeneration and suppression, a small diaphragm pump and a capacitively-coupled contactless conductivity detector. The system used standard suppressed IC using KOH eluent and analysed nutrients and other anions in freshwater streams. The total weight of the portable IC device was 27.5 kg including the battery and solar cell [70]. A schematic representation of the system is shown in Figure 1.8.

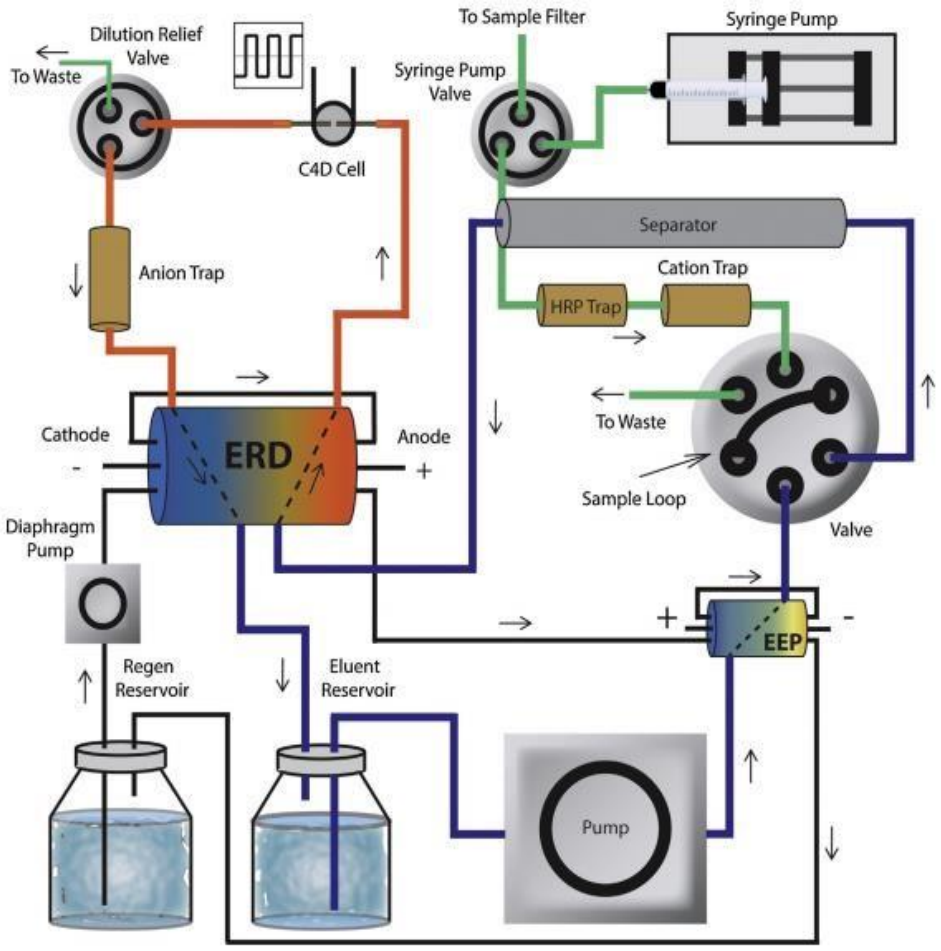

Figure 1.8: Schematic of portable IC, based on suppressed conductivity detection, reported by Elkin. KOH eluent flow is shown in blue, suppressed eluent in orange, flow outside the chromatography system in green, and electrode rinse water in black. Dashed lines in the eluent reflux device (ERD) and electrolytic eluent purifier (EEP) depict the general flow direction. The net ionic movements in the electrodialytic devices are denoted by the device polarities. The 3-port dilution relief valve (DRV) removes excess water from the system to maintain a precise eluent concentration [70].

An approach which has shown promise in terms of generating low power, portable IC systems is open tubular IC (OTIC) [71]. The OTIC reported by Yang *et al.* for ionic analysis, albeit in the context of extraterrestrial exploration as opposed to aquatic monitoring, clearly demonstrates this promise [72]. This OTIC, schematically shown in Figure 1.9, uses AS18 latex coated 9.8 µm radius PMMA capillaries. The anion exchange particles bind strongly to the oppositely charged –COOH groups on the hydrolyzed PMMA surface generating the anion exchange open tubular column. The eluent used was sodium benzoate and detection was achieved through admittance detection of the charged analytes. Using this platform, a wide range of anionic species, including NO_2^- and NO_3^-, have been detected in a laboratory setting. Further advancements building on this work have focused on achieving OTIC for suppressed anion chromatography, recently an electrodialytic capillary suppressor and novel functionalized cycloolefin polymer capillaries for OTIC have been reported, illustrating a potential route to suppressed hydroxide eluent OTIC for nutrients and other ions [73, 74].

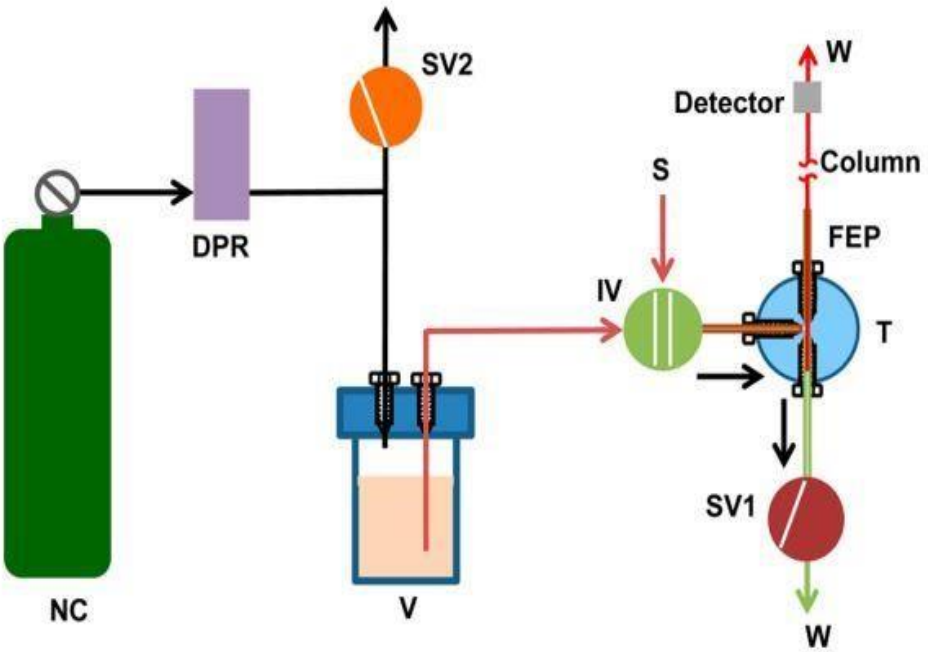

Figure 1.9: Schematic illustration of OTIC: NC, nitrogen cylinder; DPR, digital pressure regulator; IV, injection valve; SV, solenoid valve; OTC, open tubular capillary; W, waste [72].

Monolithic columns may be seen as an intermediate between open tubular and packed columns, albeit they are more closely related to the latter. As monolithic columns have a porous structure, it is possible to achieve higher flow rates at lower back pressures compared to particulate columns. This provides the opportunity for low pressure or ultra-fast chromatography, which are attractive characteristics when considering the development of a low-cost, portable IC system. In order to produce monolithic ion exchange columns, modification of the monolith is required. This can be achieved through the use of ion-interaction reagents, surfactant coatings applied to reverse phase monoliths or by covalently binding reagents to bare monoliths. Although both silica and polymeric monolithic columns are available, for small inorganic anions, such as aquatic nutrients, silica monoliths are most suitable due to their macroporous and mesoporous nature. Miniaturisation of IC and rapid separations have been demonstrated through the use of short silica monolithic columns. Through the application of these monoliths, low pressure IC systems which use small pumps, less power and small volumes of eluent have been generated [75]. Using a syringe pump, a Chromolith RP18e silica monolith (1 cm) coated with didodecyldimethylammonium bromide (DDAB) in suppressed IC mode, Pelltier and Lucy successfully separated and detected five anions, including nitrate and nitrite, in under 2.5 min [76]. The back pressure observed within the system was 4.8 bar, with 2.8 bar attributed to the suppressor. An example of a chromatogram generated by the system is shown in Figure 1.10.

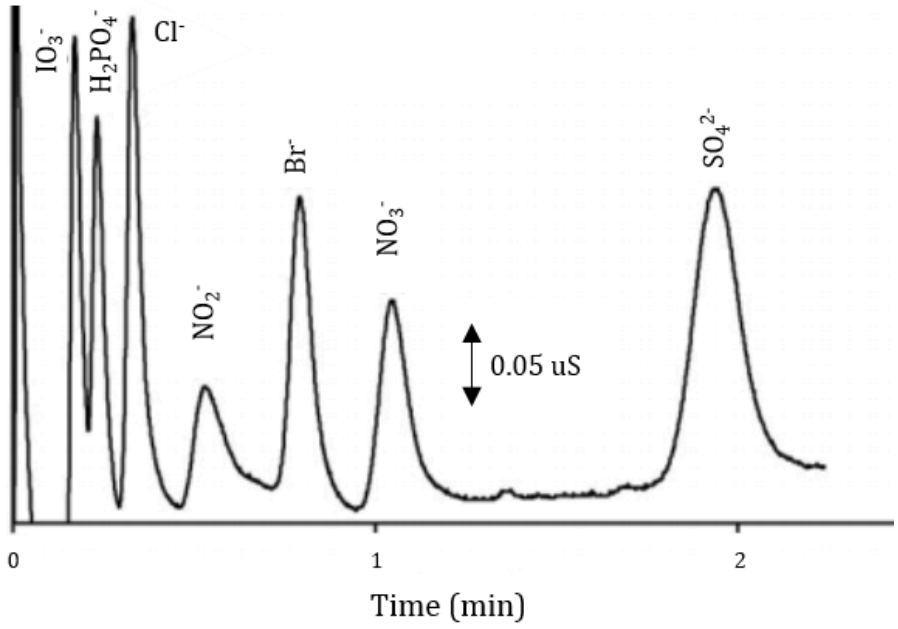

Figure 1.10: Suppressed anion separations using 1 cm silica monolith coated with DDAB using the coating solution of DDAB 1 mM/1% acetonitrile. The eluent used was 5 mM 4-hydroxybenzoic acid (pH 5.6) eluent. The flow rate was 2 mL/min and an injection volume of 0.5 µL was used [76].

Despite these promising results, the coating stability of the DDAB is an issue and over time reduction in retention times is observed. To improve the longevity of these columns, DDAB may be added to the eluent. Alternatively, cetylpyridinium chloride (CPC) has been used as a coating for anion analysis. Li *et al.* produced and anion exchange (2.5 cm x 4.6 mm) reverse phase silica monolith through coating with CPC, and an excellent coating stability for 3 months continuous use was observed, with a retention time variability of 0.17 %. Six anions, including nitrate and nitrite, were separated and detected in under 1 min. An eluent of 10 mM Na_2SO_4 at a flow rate of 3 mL/min was used with direct UV detection at 210 nm [77]. Although a range of developments have taken place in terms of monolithic phases for IC and the application of coated monoliths for nutrient analysis in both freshwater and seawater has been demonstrated [78], no portable, automated, *in-situ* IC system for the analysis of nutrients has been developed using monolithic columns thus far. Despite this, the use of these columns still represents good potential when it comes to low-cost, portable liquid chromatography. This is exemplified by the hand-portable liquid chromatography instrument developed by Sharma *et al.* [79]. However, this

system employed a capillary reversed-phase monolithic column with UV detection for organic compound analysis. Similarly, a portable high-performance liquid chromatograph (HPLC) has recently been developed by Axcend Corporation, Provo, USA. The system, shown in Figure 1.11, employs a capillary based column packed with reverse-phase particles with LED-based UV detection for organic analysis. However, anion exchange particles could potentially be used to pack the column to enable ion chromatography. The system can be operated for 10 hours using battery power and has the potential to perform gradient eluent. This LC unit represents a significant advancement in the area of on-site high-performance analytical instrumentation, however when considering *in-situ* analysis of environmental waters, system cost and deployability are still restrictive.

Figure 1.11: Portable, high-performance liquid chromatograph facilitating on-the-spot analysis. A 150 µm internal diameter (ID) capillary column filled with 1.7 - 3 µm fused silica particles is used within the system. Detection is achieved using a UV-LED based optical detector. System dimensions are 32 x 23 x 20 cm [80].

1.5 Conclusions

The importance which freshwater quality has both environmentally and economically is widely recognised and this is reflected by global legislation. A key global water quality issue is that of eutrophication and as such a clear need for reliable and widespread information regarding nitrate, nitrite, ammonium and phosphate levels in freshwater environments is required. In order to achieve truly representative, real-time or near real-time nutrient levels in aquatic environments, the typical strategy of spot or grab sampling is not sufficient and the application of *in-situ* monitoring systems is required. Through progress and developments within the fields of rapid prototyping, microfluidics, electrochemistry and chromatography, tremendous strides towards *in-situ* nutrient monitoring systems have taken place. When considering autonomous deployments of sensor systems, biofouling, power requirements and reliability issues and cost are key challenges which must be overcome. Despite this, a number of commercial and prototype systems have been produced for *in-situ* nutrient monitoring in the freshwater environment. In order to achieve mass adoption and application of *in-situ* analysers, system and operation costs are essential. Development priorities should focus on *in-situ* nutrient measurements which can be achieved in a cost-effective manner. At present, few commercial autonomous, reliable sensing systems for long term *in-situ* nutrient monitoring exist, and those which do cost tens of thousands of euros. It is clear there is a need for low-cost, reliable monitoring systems which are capable of measuring nutrients *in-situ* over long periods of time. As the overall cost of sensing systems reduce, this would potentially enable the deployment of larger numbers of devices and thereby improve the spatial and temporal resolution and extent of freshwater nutrient monitoring activities.

1.6 References

[1] UNESCO (2012) *Managing water under uncertainty and risk: The United Nations world water development report 4*, Luxembourg: UNESCO

[2] NRDC (2018) *Water Pollution: Everything You Need to Know* [online], Available: https://www.nrdc.org/stories/water-pollution-everything-you-need-know [Accessed 17 June 2019].

[3] EEA (2018) *Pressures and impacts* [online], Available: https://www.eea.europa.eu/themes/water/european-waters/water-quality-and-water-assessment/water-assessments/pressures-and-impacts-of-water-bodies [Accessed 9 Oct. 2017].

[4] US Environmental Protection Agency (2017) *TRI National Analysis 2015: Intro.* [online], Available: www.epa.gov/sites/production/files/2017-01/documents/tri_na_2015_complete_english.pdf [Accessed 17 June 2019].

[5] United Nations (2014) *International decade for action 2005-2015* [online], available: http://www.un.org/waterforlifedecade/quality.shtml [accessed 6 Dec 2016]

[6] A. Moxey (2012), *Agriculture and Water Quality: Monetary Costs and Benefits across OECD Countries,* Pareto Consulting, Edinburgh

[7] Wall Street Journal (2018), *Researchers Race to Thwart Toxic Algae Outbreaks* [online], Available: https://www.wsj.com/articles/researchers-race-to-thwart-toxic-algae-outbreaks-1523102400 (accessed 18 June 2019).

[8] Knutsson, J. (2013) Passive sampling for monitoring of inorganic pollutants in water, published thesis (PhD), Chalmers University of Technology

[9] Mills, G. and Fones, G. (2012) 'A review of *in situ* methods and sensors for monitoring the marine environment', *Sensor Review*, 32(1), 17-28

[10] Drolc, A. and Vrtovšek, J. (2010) 'Nitrate and nitrite nitrogen determination in waste water using on-line UV spectrometric method', *Bioresource Technology*, 101, 42284233

[11] Rieger, L., Vanrolleghem, P. A., Langergraber, G., Kaelin, D., and Siegrist, H. (2008) 'Long-term evaluation of a spectral sensor for nitrite and nitrate', *Water Science and Technology*, 10, 1563-1569

[12] Johnson, K.S. (2010) 'Simultaneous measurements of nitrate, oxygen, and carbon dioxide on oceanographic moorings: Observing the Redfield ratio in real time', *Limnology and Oceanography*, 55(2), 615-627

[13] Frank, C., Meier, D., Voß, D. and Zielinski, O. (2014) 'Computation of nitrate concentrations in coastal waters using an in situ ultraviolet spectrophotometer: Behaviour of different computation methods in a case study a steep salinity gradient in the southern North Sea', *Methods in Oceanography*, 9, 34-43

[14] Heffernan, J.B. and Cohen, M.J. (2010) 'Direct and indirect coupling of primary production and diel nitrate dynamics in a subtropical spring-fed river', *Limnology and Oceanography*, 55(2), 677-688.

[15] Cohen, M.J., Kurz, M.J., Heffernan, J.B., Martin, J.B., Dou-glass, R.L., Foster, C.R. and Thomas, R.G. (2013) 'Diel Phosphorus Variation and the Stoichiometry of Ecosystem Metabolism in a Large Spring-Fed River', *Ecological Monographs*, 83(2), 155-176

[16] Huebsch, M., Grimmeisen, F., Zemann, M., Fenton, O., Richards, K.G., Jordan, P., Sawarieh, A., Blum, P. and Goldscheider, N. (2015) 'Field experiences using UV/VIS sensors for high-resolution monitoring of nitrate in groundwater', Hydrology and Earth System Sciences., 19, 1589–1598

[17] Pellerin, B.A., Bergamaschi, B.A., Downing, B.D., Saraceno, J.F., Garrett, J.A. and Olsen, L.D. (2013) *Optical techniques for the determination of nitrate in environmental waters: Guidelines for instrument selection, operation, deployment, maintenance, quality assurance, and data reporting,* Virginia: US Geological Survey

[18] Bagshaw, E.A., Beaton, A., Wadham, J.L., Mowlem, M., Hawkings, J.R. and Tranter M. (2016) 'Chemical sensors for *in situ* data collection in the cryosphere', *Trends in Analytical Chemistry*, 82, 348–357

[19] YSI incorporated, IQ SensorNet NitraVis® Sensors https://www.ysi.com/nitravis, (accessed 12 June 2019).

[20] Sea Bird Scientific, SUNA V2 Nitrate Sensor https://www.seabird.com/nutrient-sensors/suna-v2-nitrate-sensor/family?productCategoryId=54627869922, 2018 (accessed 07 May 2019).

[21] USEPA (1993) *Method 353.2: Determination of nitrate-nitrite nitrogen by automated colorimetry*, Cincinnati: United States Environmental Protection Agency

[22] USEPA (1978) *Method 356.3: Phosphorous, All forms (colorimetric, ascorbic acid, two reagent)*, Cincinnati: United States Environmental Protection Agency

[23] Vuillemin, R., LeRoux, D., Dorval, P., Bucas, K., Sudreau, J.P., Hamon, M., LeGall, C. and Sarradin, P.M. (2009), 'CHEMINI: a new in situ CHEmical MINIaturized analyzer', *DeepSea Research Part I*, 56, 1391-1399.

[24] Nagy, G., Feher, Z. and Pungor, E. (1970) 'Application of silicone rubber-based graphite electrodes for continuous flow measurements: Part II. Voltammetric study of active substances injected into electrolyte streams', *Analytica Chimica Acta*, 52(1), 47-54

[25] Anderson, L. (1979) 'Simultaneous spectrophotometric determination of nitrite and nitrate by flow injection analysis', *Analytica Chimica Acta*, 110(1), 123-128.

[26] Jannasch, H.W., Johnson, K.S. and Sakamoto, C.M. (1994) 'Submersible, osmotically pumped analyzer for continuous determination of nitrate in situ*', Analytical Chemistry*, 66(20), 3352–3361.

[27] Vuillemin, R., Thouron, D., Gallou, G., Pares, L., Brient, B., Dubreule, A. and Garcon, V. (1999) 'ANAIS: autonomous nutrient analyzer *in-situ'*, *Sea Technology*, 40(4), 75–78.

[28] Ellis, P., Shabani, A., Gentle B. and Mckelvie I. (2011) 'Field measurement of nitrate in marine and estuarine waters with a flow analysis system utilizing on-line zinc reduction', *Talanta*, 84(1), 98-103

[29] Mesquitaa, R.B.R., Ferreira, M.T.S.O.B, Tóthc, I.V., Bordalo, A.A., McKelvie, I.D. and Rangel, A.O.S.S. (2011) 'Development of a flow method for the determination of phosphate in estuarine and freshwaters—Comparison of flow cells in spectrophotometric sequential injection analysis', *Analytica Chimica Acta*, 701, 15–22

[30] Alliance for Coastal Technologies - ACT (2017) *Photograph of Systea nitrate instrument prior to and following the CBL field trial* [image], available: http://www.actus.info/Download/Evaluations/NextGenNutrient/SysteaNitrate/#32 [accessed 08/July/2017].

[31] Nightingale, A.M., Beaton, A.D. and Mowlem M.C. (2015) 'Trends in microfluidic systems for in situ chemical analysis of natural waters', *Sensors and Actuators B*, 221, 1398–1405.

[32] Cleary, J., Maher, D., Slater C. and Diamond D. (2010) 'In situ monitoring of environmental water quality using an autonomous microfluidic sensor', *IEEE Sensors Applications Symposium*, Limerick, Ireland, 23-25 Feb, 2010, IEEE Instrumentation and Measurement Society, 36–40.

[33] Hwang, H. Kim, Y. Cho, J. Lee, J. Choi M. and Cho, Y. (2013) 'Lab-on-a-Disc for Simultaneous Determination of Nutrients in Water', *Analytical Chemistry*, 85, 29542960

[34] Sieben, V.J. Floquet, C.F.A. Ogilvie, I.R.G., Mowlem M.C. and Morgan H. (2010) 'Microfluidic colourimetric chemical analysis system: Application to nitrite detection', *Analytical Methods*, 2, 484-491.

[35] Beaton, A.D., Sieben, V.J., Floquet, C.F.A., Waugh, E.M., Abi Kaed Bey, S., Ogilivie, I.R.G., Mowlem, M.C. and Morgan, H. (2011) 'An automated microfluidic colorimetric sensor applied *in situ* to determine nitrite concentration', *Sensors and Actuators B: Chemical*, 156, 1009-1014.

[36] Beaton, A.D., Cardwell, C.L., Thomas, R.S., Sieben, V.J., Legiret, F., Waugh, E.M., Statham, P.J., Mowlem, M.C. and Morgan H. (2012) 'Lab-on-chip measurement of nitrate and nitrite for In Situ analysis of natural waters', *Environmental Science and Technology*, 46, 9548-9556.

[37] Legiret, F.E., Sieben, V.J., Woodward, E.M.S., Abi Kaed Bey, S.K., Mowlem, M.C., Connelly, D.P. and Achterberg, E.P. (2013) 'A high performance microfluidic analyser for phosphate measurements in marine waters using the vanadomolybdate method', *Talanta*, 116, 382–387.

[38] Clinton-Bailey, G., Grand, M., Beaton, A., Nightingale, A., Owsianka, D., Slavik, G., Connelly, D., Cardwell, C. and Mowlem, M. (2017) 'A Lab-on-Chip Analyzer for in Situ measurement of Soluble Reactive Phosphate: Improved Phosphate Blue Assay and Application to Fluvial Monitoring', *Environ. Sci. Technol.*, 51 (17), 9989–9995

[39] A. Donohoe, G. Lacour, P. McCluskey, D. Diamond, M. McCaul (2018), 'Development of a Cost-Effective Sensing Platform for Monitoring Phosphate in Natural Waters', *Chemosensors* 6, 57.

[40] A.M. Nightingale, S. Hassan, B.M. Warren, K. Makris, G.W.H. Evans, E. Papadopoulou, S. Coleman, X. Niu (2019) 'A Droplet Microfluidic-Based Sensor for Simultaneous in Situ Monitoring of Nitrate and Nitrite in Natural Waters', *Environ. Sci. Technol.* 53, 9677−9685.

[41] Nollet, L.M.L. and De Gelder, L.S.P. (2011) *Handbook of Water Analysis*, 3rd ed., Florida: CRC Press

[42] Moretto, L.M. and Kalcher, K. (2014) *Environmental Analysis by Electrochemical Sensors and Biosensors*, New York: Springer

[43] Pletcher, D. and Poorabedi, Z. (1979) 'The reduction of nitrate at a copper cathode in aqueous acid', *Electrochimica Acta*, 24, 1253–1256.

[44] Davenport R. J. and Johnson D. C. (1973) 'Voltammetric determination of nitrate and nitrite ions using a rotating cadmium disk electrode', *Analytical Chemistry*, 45, 1979– 1980.

[45] Lévy-Clément, C., Ndao, N.A., Katty, A., Bernard, M., Deneuville, A., Comninellis, C. and Fujishima, A. (2003) 'Boron Doped Diamond Electrodes for Nitrate Elimination in Concentrated Wastewater', *Diamond and Related Materials*, 12, 606-612.

[46] Da Silva, S.M. and Mazo, L.H. (1998) 'Differential pulse voltammetric determination of nitrite with gold ultramicroelectrode', *Electroanalysis,* 10, 1200–1203.

[47] Tatka, L. and Kim, U. (2016) 'Affordable, rapid, electrochemical nitrate detection towards point-of-use water quality monitoring', *IEEE Global Humanitarian Technology Conference*, Dayalbagh Agra, India, 21-23 Dec, 2016, IEEE Advancing Technology for Humanity, 761-764.

[48] Davis, J., Moorcroft, M.J., Wilkins, S.J., Compton, R.G. and Cardosi, M.F. (2000) 'Electrochemical detection of nitrate and nitrite at a copper modified electrode', *Analyst*, 125, 737-742.

[49] Crespo, G. (2017) 'Recent Advances in Ion-selective membrane electrodes for in situ environmental water analysis', *Electrochimica Acta*, 245, 1023-1034.

[50] NexSens Technology Inc. (2017) *WQ-NO3 Nitrate Smart USB Sensor Overview - NexSens Technology Inc.*. [online] Available at: http://www.nexsens.com/knowledgebase/legacy-products/wqsensors/wq-no3-nitrate-smart-usb-sensor/wq-no3nitrate-smart-usb-sensor-overview.htm [Accessed 9 Oct. 2017]

[51] Cosnier, S., Innocent, C. and Jouanneau, Y. (1994) 'Amperometric detection of nitrate via nitrate reductase immobilized and electrically wired at the electrode surface,' *Analytical Chemistry*, 66, 3198-3201

[52] UNISENSE (2017) *NO_X Biosensor* [online], available: http://www.unisense.com/NOx [accessed 12 July 2017].

[53] Jońca, J., León Fernández, V., Thouron, D., Paulmier, A., Graco, M. and Garçon, V. (2011) 'Phosphate determination in seawater: Toward an autonomous electrochemical method', *Talanta*, 87, 161-167.

[54] Ejhieh, A.N. and Masoudipour, N. (2010) 'Application of a new potentiometric method for determination of phosphate based on a surfactant-modified zeolite carbon-paste electrode (SMZ-CPE)', *Analytica Chimica Acta*, 658, 68-74.

[55] Hara, H. and Kusu, S. (1992) 'Continuous-flow determination of phosphate using a lead ion-selective electrode', *Analytica Chimica Acta*, 261, 411-417.

[56] Gilbert, L., Jenkins, A.T.A., Browning, S. and Hart, J.P. (2009) 'Development of an amperometric assay for phosphate ions in urine based on a chemically modified screenprinted carbon electrode', *Analytical Biochemistry*, 393, 242-247.

[57] K. Xu, Y. Kitazumi, K. Kano, O. Shirai (2018), 'Phosphate ion sensor using a cobalt phosphate coated cobalt electrode', Electrochimica Acta, 282, 242-246.

[58] Berchmans, S., Issa, T.B., Singh, P. (2012) 'Determination of inorganic phosphate by electroanalytical methods: A review', *Analytica Chimica Acta*, 729, 7-20.

[59] Warwick, C., Guerreiro, A. and Soares, A. (2013) 'Sensing and analysis of soluble phosphates in environmental samples: A review', *Biosensors and Bioelectronics*, 41, 111

[60] Cinti, S., Talarico, D., Palleschi, G., Moscone, D. and Arduini, F. (2016) 'Novel reagentless paper-based screen-printed electrochemical sensor to detect phosphate', *Analytica Chimica Acta*, 919, 78-84.

[61] USGS, Continuous Monitoring for Nutrients: State of the Technology and State of the Science. https://acwi.gov/monitoring/webinars/national_monitoring_council_webinar_092414b_Pellerin.pdf (accessed 14 January 2019).

[62] U.S. EPA, *Method 300.0: Determination of Inorganic Anions by Ion Chromatography,* Cincinnati: Environmental Protection Agency, 1993.

[63] Jackson, P.E. (2000) *Encyclopaedia of Analytical Chemistry: Ion Chromatography in Environmental Analysis*, Chichester: Wiley & Sons

[64] SeQuant (2007) *A practical guide to ion chromatography: An introduction and troubleshooting manual*, Sweden: SeQuant AB

[65] Tsitouridou, R. and Puxbaum, H. (1987) 'Application of a portable ion chromatograph for field site measurements of the ionic composition of fog water and atmospheric aerosols', *lnt. J Environ. Anat*., 31, 11-22.

[66] Baram, G.I. (1996) 'Portable liquid chromatograph for mobile laboratories: I. Aims', *J. Chromatogr. A*, 728, 387-399.

[67] Tanaka, K., Ohta, K., Haddad, P.R., Fritz, J.S., Lee, K.P., Hasebe, K., Ieuji, A. and Miyanaga, A. (1999) 'Acid-rain monitoring in East Asia with a portable-type ion-exclusion– cation-exchange chromatographic analyser', *J. Chromatogr. A*, 850, 311-317

[68] Boring, C.B. Dasgupta, P.K. and Sjogren, A. (1998) 'Compact, field-portable capillary ion chromatograph', *J. Chromatogr. A*, 804, 45-54

[69] Qingdao Sheng-Han Chromatograph Technology company (2013) CIC-H180 Portable ion chromatograph [online], available: http://www.sheng-han.com/en/products_detail.aspx?nid=222&q=2 [accessed 10 June 2019].

[70] Elkin, K.R. (2014) 'Portable, fully autonomous, ion chromatography system for on-site analyses', *J. Chromatogr. A*, 1352, 38-45

[71] Kiplagat, I.K., Kubán, P., Pelcováa, P. and Kubán, V. (2010) 'Portable, lightweight, low power, ion chromatographic system with open tubular capillary columns', *J. Chromatogr. A*, 1217, 5116–512

[72] Yang, B., Zhang, M., Kanyanee, T., Stamos, B. and Dasgupta, P. (2014) 'An Open Tubular Ion Chromatograph', *Anal. Chem.*, 86(23), 11554-11561

[73] Huang, W. and Dasgupta, P. (2016) 'Electrodialytic Capillary Suppressor for Open Tubular Ion Chromatography', *Anal. Chem.*, 88(24), 12021-12027.

[74] Huang, W., Seetasang, S., Azizi, M. and Dasgupta, P. (2016) 'Functionalized Cycloolefin Polymer Capillaries for Open Tubular Ion Chromatography', *Anal. Chem.*, 88(24), 12013-12020.

[75] Connolly, D., Victory, D. and Paull, B. (2004) 'Rapid, low pressure, and simultaneous ion chromatography of common inorganic anions and cations on short permanently coated monolithic columns', *J. Sep. Sci.*, 27(10-11), 912-920.

[76] Pelletier, S. and Lucy, C. (2006) 'Achieving rapid low-pressure ion chromatography separations on short silica-based monolithic columns', *J. Chrom. A*, 1118(1), 12-18

[77] Li, J., Zhu, Y. and Guo, Y. (2006) 'Fast determination of anions on a short-coated column', *J. Chrom. A*, 1118(1), 46-50.

[78] Horioka, Y., Kusumoto, R., Yamane, K., Nomura, R., Hirokawa, T. and Ito, K. (2016), 'Determination of Inorganic Anions in Seawater Samples by Ion Chromatography with ultraviolet Detection Using Monolithic Octadecylsilyl Columns Coated with Dodecylammonium Cation', *Anal. Sci.*, 32(10), 1123-1128.

[79] Sharm, S., Plistil, A., Simpson, R.S., Liu, K., Farnsworth, P.B., Stearns, S.D., Lee, M.L. (2014) 'Instrumentation for hand-portable liquid chromatography', *J. Chrom. A*, 1327, 80-89.

[80] Axcend Corporation (2019) The Axcend Focus LC [online], available: https://www.axcendcorp.com/product [accessed 15 June 2019].

Chapter 2

A colorimetric method for use within portable test kits for nitrate determination in various water matrices

Eoin Murray [1, 2], Ekaterina P. Nesterenko [3], Margaret McCaul [3], Aoife Morrin [2, 3], Dermot Diamond [3], Breda Moore [1*]

1. *Research & Development, T.E. Laboratories Ltd. (TelLab), Tullow, Carlow, Ireland*
2. *School of Chemical Sciences Department, Dublin City University, Dublin 9, Ireland*
3. *Insight Centre for Data Analytics, National Centre for Sensor Research, Dublin City University, Dublin 9, Ireland*

Publication: Analytical Methods, 2017, DOI: 10.1039/C6AY03190K

Chapter Overview

This chapter describes the optimisation and validation of a colorimetric method for the determination of nitrate in various water media. The developed method is designed to be integrated into a simple, low-cost nitrate test kit (< €15). This test kit enables quick in-field nitrate analysis and exhibits a limit of detection and analytical range relevant to legislative concentration levels in environmental waters.

Abstract

A method using zinc powder in conjunction with the common Griess assay was developed for the detection of nitrate in water. This method is applicable to portable water test kits and allows for the accurate determination of nitrate in freshwater. The linear range for the method was shown to be 0.5–45 mg L^{-1} NO_3^- and the limit of detection (LOD) was 0.5 mg L^{-1} NO_3^-. The proposed method was validated over a five-day period and acceptable recovery and uncertainties were achieved when analysing freshwater matrices. The performance of the developed method was compared to an ISO-accredited ion chromatographic (IC) method by carrying out blind sample analysis. A good agreement between the two methods was achieved as comparable concentrations were determined using each method. In addition, the Zn method was compared to the performance of a novel solid-phase reagent method, previously developed within the group. The most accurate performance was demonstrated by the Zn powder method when analysing freshwater samples. The novel solid-phase reagent method demonstrated the greater accuracy when analysing seawater samples.

2.1 Introduction

Nitrate concentrations vary widely within natural and waste water samples. Nitrate concentrations can range from below 0.20 mg L^{-1} NO_3^- in deep seawater to 85 mg L^{-1} NO_3^- in shallow groundwater and surface streams depending on soil type and land use practices [1]. Natural sources of nitrate in the environment include gaseous nitrogen fixation through microorganisms such as *Azotobacter* and cyanobacteria, soil degradation and the deposition of animal and plant residues. Although nitrate is found within a multiplicity of natural processes, contamination in water systems is most typically associated with anthropogenic activities.

Anthropogenic sources of nitrate include fertilisation of agricultural crops using chemical nitrogenous fertilisers, plant and animal waste, municipal and industrial wastewater discharges, sewage disposal systems, and the food industry [2]. In addition, atmospheric deposition of nitrogen-containing compounds also plays a role in contributing to nitrate contamination within water systems [3].

Elevated concentrations of nitrate in water systems pose a significant risk to both the environment and to human health when considering the utilisation of water for drinking purposes. High nitrate levels in water systems contribute significantly to eutrophication, especially within lakes and saline waters [4]. Eutrophication leads to the overproduction of aquatic plants and algae which in turn results in dissolved oxygen depletion; odorous waters and the stimulation of bacteria proliferation as algae and macrophytes die [5]. When freshwater is used for drinking, nitrate contamination can negatively impact human health. The most important health effect associated with nitrate ingestion arises through the reduction of nitrate to nitrite in the digestive system. Nitrite oxidizes iron in the haemoglobin of red blood cells forming a molecule called methemoglobin. This molecule hinders oxygen transport and can result in a condition called methemoglobinemia or 'blue baby syndrome' [6]. Nitrate which has been reduced to nitrite has also been shown to react with nitrosatable compounds in the human stomach to form carcinogenic N-nitroso compounds [7].

Under EU regulation, nitrate concentrations within all fresh and marine water bodies must be monitored. According to legislation, nitrate levels must not exceed 50 mg L^{-1} NO_3^- in surface waters [8]. Many analytical methods are available for the determination of nitrate in water matrices. Suppressed ion chromatography (IC) is regarded as the standard for the analysis of nitrate in water, and is in fact the proposed method by the environmental protection agency [9]. However, sample matrix complexity, in particular high salinity waters, can have a significant impact on IC performance. In addition, samples must be transported to a lab to be analysed using IC. Due to good limits of detection and simple assay-type protocols, colorimetric methods are an effective alternative to IC and are readily employed for nitrate determination.

When considering colorimetric detection of NO_3^-, the simplest and most frequently applied assay involves the reduction of nitrate to nitrite and its subsequent detection using the Griess reaction [10, 11]. A range of methods can be used to reduce NO_3^- to NO_2^-. Enzymatic reduction using nitrate reductase or photochemical reduction through the use of UV light can be used, however these methods typically offer poor reproducibility [12]. Most commonly, copperised cadmium is used for nitrate reduction to nitrite and reduction efficiencies of over 90% are possible [12]. Despite this fact, the use of cadmium may be seen as undesirable due to its highly toxic nature. Therefore, the use of a less toxic reductant is desirable. Zinc represents an example of a less toxic solid-state reductant which can be used to reduce nitrate to nitrite. Metallic zinc has previously been used in other studies as a reducing agent, but is rarely used in favour of cadmium due to lower reduction efficiencies [13]. Merino (2009) successfully employed zinc reduction for nitrate determination in foodstuffs and water, achieving an analytical range of 0-1.62 mg L^{-1} NO_3^- [14]. Ellis *et al.* (2011) then successfully developed a simple spectrophotometric flow analysis method using granular Zn for NO_3^- determination in water. This flow analysis method demonstrated an analytical range of 0.01 – 3.1 mg L^{-1} NO_3^- [15]. In addition, other successful nitrate colorimetric determination methods which move away from the use of cadmium have also recently been developed. However, these methods employ harsh corrosive reagents and are not well suited for use in test kits [16,

17]. Despite these recent developments, the cadmium reduction method is still the leading nitrate determination methodology.

Within this study, an optimised zinc reduction method in combination with the Griess assay for water analysis is validated and assessed. Through blind sample analysis, the performance of the developed method is compared to that of an accredited IC according to ISO/IEC 17025:2005. For the blind sample analysis, a range of freshwater samples were analysed along with a selection of various effluents. The performance of the Zn powder method was also compared to that of a solid-based colorimetric nitrate determination method. The solid-based method was a novel non-toxic solid phase colorimetric method, developed by Nesterenko *et al.* (2016), which uses azo and diazo components, solid organic acid acidifier, catalyst, masking agent and zinc as the reducing agent [11]. The performance of the two methods was assessed following blind sample analysis of various water matrices.

2.2 Experimental

2.2.1 Materials and reagents

All chemicals used within this work were of analytical grade purity. Sulphanilamide, hydrochloric acid (37 %) and N-(1-naphtyl)-ethylenediamine dihydrochloride (NED) used to prepare Griess reagent were purchased from Sigma-Aldrich (Gillingham, UK). Zinc (99.99 %) in powder form with a particle size of 150 μm was purchased from VWR International. Chromotropic acid, *p*-nitroaniline, potassium chloride, malonic acid, potassium bromide and EDTA disodium salt were all purchased from Sigma-Aldrich. All solutions and dilutions were prepared using high-purity deionised water (18 MΩ cm). TelLab's certified 1000 mg L^{-1} nitrate standard and 100 mg L^{-1} nitrite standard were used as the stock solutions, from which working nitrate and nitrite standards were prepared via serial dilutions. A range of environmental samples were provided by the Environmental Department within TelLab. Six drinking water samples from various customer wells, effluent samples from a pump manufacturing facility, a water treatment facility and a hospital, a river water sample and seawater samples from Wexford harbour were investigated.

2.2.2 Instrumentation

Spectroscopic measurements were performed on a Unicam UV500 spectrophotometer using a 1 cm path length Hellma far-UV quartz cuvette applicable to the range 200-2500 nm. The wavelength range of the spectrophotometer was 190-1100 nm. The bandwidth was 1.5 nm, and an integration time of 2 s was used. IC determination of nitrate was carried out using an isocratic Dionex DX-120 Ion Chromatograph (Dionex, Sunnyvale, USA), equipped with autosampler and a Dionex AERS 500 anion self-regenerating suppressor for suppressed conductivity detection.

2.2.3 Methods

Proposed nitrate determination method using Zn reduction

Proposed nitrate determination method using Zn reduction. The Griess reagent which was used was prepared as described by Robledo *et al.* (2014) [10]. Sulphanilamide reagent was prepared by adding 10 mL of concentrated hydrochloric acid (37%) to 60 mL of deionised water and 1.0 g of sulphanilamide was then added to the solution. This solution was then diluted to 100 mL with deionised water. The NED reagent was prepared by dissolving 0.1 g of NED in 100 mL of deionised water. Both reagents were then mixed in equal proportions to produce Griess reagent. To a 10 mL volume of sample solution, 1 mL of Griess reagent was added. A 25 mg quantity of Zn powder, particle size 150 μm, was then added. The sample container was shaken 20 times in an up down motion and the solution was allowed to stand for 10 min. Following this, a 2 mL portion of this solution was immediately transferred into a cuvette and analysed spectrophotometrically using UV-Vis at a wavelength of 540 nm. The reaction mechanisms for the reduction of nitrate to nitrite using zinc, and the subsequent detection of nitrite employing the Griess assay are highlighted in eqn (1) and (2) respectively.

$$NO_3^- + Zn_{(s)} + 2H^+ \rightarrow NO_2^- + Zn^{2+} + H_2O \quad (1)$$

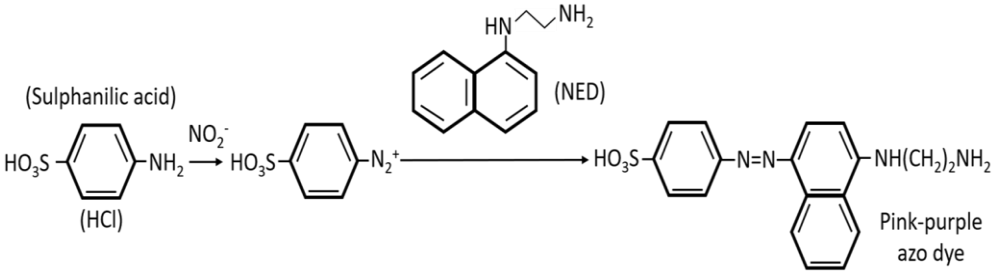

(2)

Ion-chromatographic analysis

The IC system which was used was accredited by the Irish National Accreditation Board (INAB) according to ISO 17025:2005. Prior to analysis all samples were filtered using a 0.2 µm pore size membrane filter to remove debris. An eluent comprised of 3.5 mM Na_2CO_3 / 1.0 mM $NaHCO_3$ solution was used at a flowrate of 1.2 mL min^{-1}. An IonPac AS14 (250 X 4 mm I.D.) anion exchange column along with an AERS 500 anionic suppressor (Dionex, Sunnyvale, USA) was used.

Solid-phase test reagent

The solid-phase reagent was comprised of p-nitroaniline (2 mass %), chromotropic acid (2 mass %), potassium chloride (4 mass %), potassium bromide (12 mass %), EDTA disodium salt (0.4 mass %) and malonic acid (79.6 mass %). To this 1.5 % Zn powder was added relative to the amount of solid reagent. For the determination of nitrate, a 5 mL volume of sample was added to a 100 ± 1 mg portion of the powdered reagent and allowed to react. When a sample containing nitrate was added to the powder, the reagent powder dissolved within 10 – 15 sec and colour formation began within 1 min. At low nitrate concentrations (0.5 mg/L), the colour change which was observed was from pale hay-yellow to ochroid-yellow. At higher concentrations of nitrate (up to 100 mg/L), the colour transitioned to a ripe cherry red. The intermediate hues which were observed were orange-yellow, orange, orange-red and red. A wavelength of 515 nm was determined to be the λ_{max} and was used to determine sample nitrate concentrations.

2.3 Results and Discussion

2.3.1 Determination of optimum working conditions for the Zn powder method

In order to determine the optimum quantity of Zn powder to be used, quantities of Zn powder ranging from 10 – 250 mg were added to a sample container containing 10 mL of 10 mg/L NO_3^- standard solution and 1 mL Griess reagent. Each sample container was shaken 10 times and allowed to stand for 5 min. The average absorbance (*n*=3) for each quantity was calculated and plotted against the quantity of Zn powder added as shown in Figure 2.1A. The highest absorbance was routinely observed when 25 mg of Zn powder was added. Thus, the quantity of 25 mg of Zn was determined to be optimal. The decrease in absorbance readings when higher quantities of Zn is used is likely attributed to the over reduction of nitrogen to lower oxidation states such as ammonia. Furthermore, when higher quantities of Zn powder are added, this leads to an increased turbidity and consequently a drop in absorbance values.

The effect of mixing on NO_3^- reduction using Zn powder was then established. A sample container containing 1 mL of Griess reagent, 10 mL of 10 mg/L NO_3^- standard and 25 mg of Zn powder was shaken a specific number of times (1 – 60 times) in an up-down motion at a rate of 1 shake per second. Each solution was allowed to stand for 5 min and the absorbance was measured. As illustrated in Figure 2.1B, by shaking the solution 20 times the greatest reduction efficiency is achieved as an absorbance of 0.699 was obtained. The decrease in absorbance resulted due to the fact, the more the sample is shaken, the greater the contact time between the reductant and the sample. Thus, an over reduction of nitrogen to lower oxidation states most likely occurs. Kinetic studies were then carried out. In order to establish whether or not different kinetic profiles are observed for different nitrate concentrations, both a 5 mg/L NO_3^- solution and a 45 mg/L NO_3^- solution were assessed. As demonstrated in Figure 2.1C, the absorbance readings increased for both solutions until 5 min and then declined. Although the highest absorbance was observed at 5 min, a considerable standard deviation was also present. As the lowest standard deviation was observed at 10 min, a standing time of 10 min was selected as optimal. According to Nollet *et al.* (2013),

reduction using metallic zinc requires a strict control of standing time in order to avoid reduction of nitrogen to lower oxidation states [12]. The results obtained in this experiment are in agreement with this statement as absorbance readings fluctuate with varying standing times.

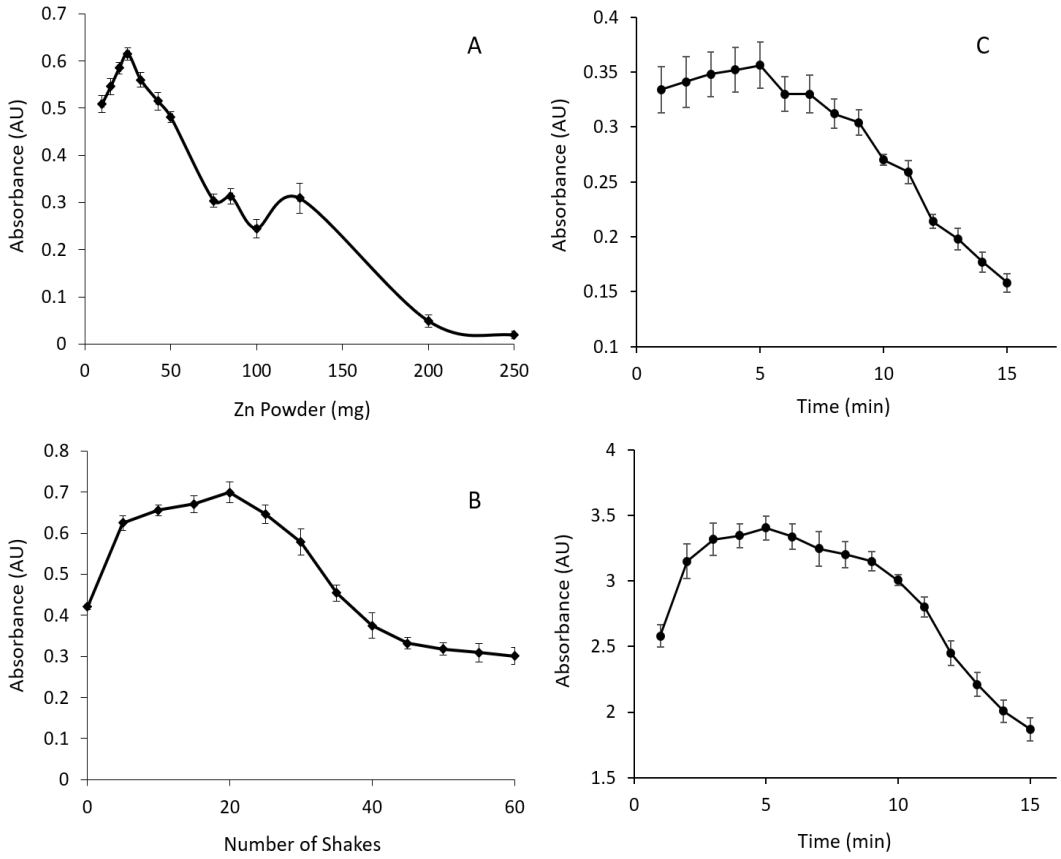

Figure 2.1: (A) Quantity of Zn powder used and resulting absorbance values when analysing a 10 mg/L NO_3^- standard; (B) Effect of mixing on reduction of nitrate analysing a 10 mg/L NO_3^- standard; (C) Kinetic study for NO_3^- standard solutions using Zn powder to reduce nitrate to nitrite (n=3). The top graph was obtained when analysing a 5 mg/L NO_3^- standard and the bottom graph was obtained when analysing a 45 mg/L NO_3^- standard.

2.3.2 Method Validation

Calibration Curves

Firstly, a calibration curve for nitrite (Figure 2.2A) was generated by analysing fresh nitrite standards using the standard Griess assay (*n*=5). The linear range was determined to be between 0.025-4.0 mg/L NO_2^-. Following this, nitrate standards were analysed using the optimised Zn powder method and a nitrate calibration curve was generated (*n*=5). This calibration curve is shown in Figure

2.2B. The linear range was 0.5 – 45 mg/L NO_3^-. Due to the low standard deviation which was observed, error bars are not clearly visible despite being present on both graphs. The upper detection limit of the method was determined to be 45 mg/L NO_3^-. At concentrations above this point, the detectable difference in colour and absorbance values decreased.

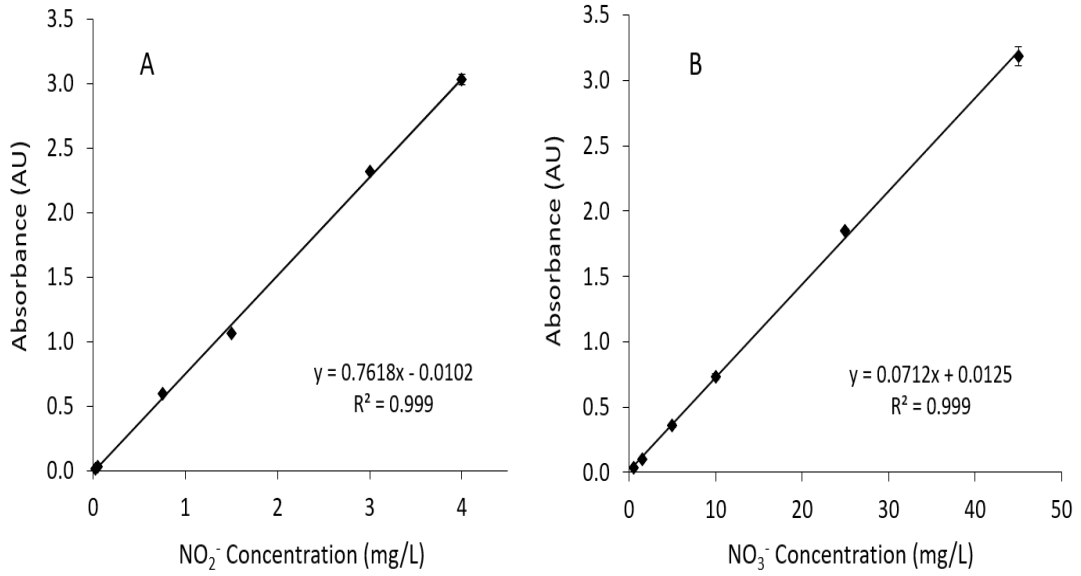

Figure 2.2: (A) Nitrite calibration curve using Griess Assay; (B) Nitrate calibration curve using Zn powder method (n=5)

Sample Analysis

All water samples were analysed in triplicate over a five-day validation period (i.e. *n*=15). The four sample matrices were firstly analysed using Griess reagent to establish whether or not nitrite was present. An average absorbance of 0.058 AU was observed for the seawater sample, which correlated to a nitrite concentration of 0.0895 mg/L NO_2^-. While no absorbance was obtained for the other matrices meaning no nitrite was present. The nitrite content (expressed as 0.027 mg/L NO_2^--N) present within the seawater sample was subtracted from the concentration (mg/L NO_3^--N) obtained when analysing the seawater for nitrate. Using the equation of the line from the calibration curve shown in Figure 2.2B, the concentrations of nitrate in the sample solutions were determined based on the average absorbance obtained. The actual nitrate concentrations present in each of the samples determined using IC, the average nitrate concentrations determined using the Zn powder method, the standard deviation

and the RSD values are shown in Table 2.1. The actual nitrate concentrations present in the seawater samples were determined using standard Hach spectrophotometric methods. The low range cadmium reduction method (method 8192) was used for the unspiked sample and the high range cadmium reduction method (method 8171) was used for the spiked sample.

Table 2.1: Actual nitrate concentrations in samples and determined concentrations within samples (*n*=15). The QC20 sample was a quality control 20 mg/L NO_3^- standard, LOD 1 was a 0.5 mg/L NO_3^- standard and LOD 2 was a 1 mg/L NO_3^- standard. These samples were used for validation calculations.

Sample	Actual NO_3^- Conc. (mg/L)	Average NO_3^- Conc. (mg/L) Determined using Zn Powder Method	Standard Deviation (n=15)	RSD (%, n=15)
QC20	20.40	21.26	1.05	4.93
LOD 1	0.51	0.33	0.08	24.24
LOD 2	1.02	0.76	0.08	10.52
Potable Water Unspiked	14.23	15.68	0.42	2.68
Potable Spiked	24.15	24.02	0.76	3.16
Effluent Unspiked	18.07	18.47	0.40	2.16
Effluent Spiked	28.05	28.49	0.78	2.74
Stream Water Unspiked	25.02	26.89	0.85	3.16
Stream Water Spiked	35.03	36.26	1.85	5.10
Sea Water Unspiked*	0.12	< 0.5	/	/
Sea Water Spiked**	10.04	6.41	0.57	8.89

* Hach LR cadmium reduction method (method 8192) used to determine NO_3^- concentration

** Hach HR cadmium reduction method (method 8171) used to determine NO_3^- concentration

From the information obtained from the analysis of the spiked and unspiked samples over the five-day period, the recovery, uncertainty and limit of detection of the method were calculated. The calculations were carried out using equations recommended by the Water Research Centre's (WRC) guide to analytical quality control for water analysis, document CEN/TC 230 N 180 section 8, and 'standard methods for the examination of water and wastewater' [18].

Recovery

Recoveries were calculated for each of the sample matrices and are represented as a percentage. Recoveries were calculated using equations as recommended by Eaton *et al.* (2005) [18].

$$\text{Recovery} = \text{Spiked Conc.} - \left(\left(\text{Unspiked Conc.}/250\ \text{mL}\right) \times 247.5\ \text{mL}\right)$$

$$\text{Recovery \%} = \text{Recovery}/10\ \text{mg/L} \times 100\ \%$$

The nitrate concentration determined within the unspiked samples were divided by 250 mL, then multiplied by 247.5 mL to account for dilution. This was due to the fact that the spiked samples were prepared by pipetting 2.5 mL of 1000 mg/L NO_3^- standard into a 250 mL volumetric flask which was filled to the mark with the specific sample matrix. The calculated recovery was then divided by 10 mg/L, as 10 mg/L was the concentration of the spike. By multiplying this value by 100, recovery as a percentage is obtained. From the calculated recoveries, average recoveries were determined and these recoveries as percentages are illustrated in Table 2.2 below.

Table 2.2: Recoveries observed for each sample matrix and associated standard deviation for nitrate analysis using Zn powder method

Sample	Average Recovery	Standard Deviation (%, n=15)
Drinking Water	85.06%	0.507
Effluent Water	102.06%	0.508
Surface Water	96.34%	1.453
Sea Water	64.09%	0.523

According to the WRC, a recovery value observed within the range 85–115 % is seen as a suitable recovery in terms of validation [18]. The average recovery obtained for drinking, effluent and surface water matrices were within this accreditation range and thus demonstrated suitable accuracy. However, the recovery observed for the seawater matrix was 64.09 % and was therefore outside of the desired range. Based on this result, the developed Zn powder method would not be applicable for nitrate determination within seawater. This observation is in agreement with an interference study which was recently carried out by Jayawardane *et al.* (2014) when analysing for nitrate using zinc in combination with the Griess assay. Following the assessment of a wide range of potential interfering ions, it was shown that Na^+ had the greatest interfering effect. When analysing nitrate in solutions containing 1150 mg L^{-1} Na^+ and above, a percentage recovery of 58.9 ± 10.4 % was observed [22]. Ellis *et al.* (2011) overcame these interferences through the use of granular zinc and citrate buffer, as ions such as Na^+, Mg^{2+} Ca^{2+} Fe^{2+} and Cu^{2+} had no significant interfering effect on nitrate determination [15]. However, this method only achieved an analytical range up to 3.1 mg L^{-1} NO_3^-, well below the nitrate levels which are readily observed in freshwater samples.

Limit of Detection

Two samples were analysed to determine the limit of detection of the Zn powder method. LOD 1 was a 0.5 mg/L NO_3^- standard and LOD 2 was a 1 mg/L NO_3^- standard. The concentrations determined over the five-day validation period and standard deviations for the two LOD samples are shown in Table 2.3 which follows.

Table 2.3: Concentrations and standard deviation for LOD 1 and LOD 2

Day	LOD 1 (mg/L NO_3^-)	LOD 2 (mg/L NO_3^-)
1	0.33	0.68
	0.27	0.78
	0.24	0.71
2	0.22	0.63
	0.23	0.60
	0.25	0.70
3	0.45	0.78
	0.44	0.80
	0.38	0.80
4	0.32	0.76
	0.30	0.81
	0.30	0.77
5	0.39	0.84
	0.40	0.85
	0.42	0.91
Average Concentration	0.33	0.76
Standard Deviation	0.08	0.08

According to Eaton *et al.* (2005), the average concentration obtained for the NO_3^- standard must > 4 times the standard deviation of the pooled results for a concentration to be accepted as the limit of detection [18]. In this case, results indicated that 0.5 mg/L NO_3^- was an acceptable limit of detection for accreditation.

Uncertainty

The uncertainties associated with each sample matrix were calculated using equations as recommended by Eaton *et al.* (2005) [18].

$$\% \text{ Uncertainty} = (2(P_R)^2 + 2(W_R)^2)^{½}$$

Where:

P_R (Precision) = $\sqrt{}$ Sum of square difference/(n-1)

W_R (Bias) = $\sqrt{}$ Sum of square difference/n

Difference = Recovery - 10 (As sample was spiked with 10 mg/L NO_3^-)

The expanded uncertainties associated with each matrix were also calculated. The expanded uncertainty (U) for each matrix was calculated using the following equation;

$$U = (k)(u)$$

Where *k* was the coverage factor and *u* was standard uncertainty. In this case a coverage factor of 2 was used, defining an interval with a confidence level of approximately 95 %. The % uncertainty and expanded uncertainties determined for each sample matrix are illustrated in Table 2.4. Each sample was analysed in triplicate over the five-day validation period. Uncertainty was lowest for the effluent water matrix. The effluent sample was taken from a pump manufacturing plant following treatment of the raw effluent in the complexes water treatment facility. This treatment of the effluent most likely enabled the low uncertainty value to be achieved. The uncertainty determined for the drinking and surface water matrices were also at low levels. The highest uncertainty was observed for the seawater matrix, as an expanded uncertainty of ± 1.471 mg/L NO_3^- was obtained. This again highlights the image that this Zn powder method is not applicable for seawater analysis.

Table 2.4: Calculated uncertainties associated with each sample matrix (*n*=15)

Sample	% Uncertainty	Expanded Uncertainty
Drinking Water	3.234	± 0.65 mg/L
Effluent Water	0.983	± 0.19 mg/L
Surface Water	2.597	± 0.52 mg/L
Sea Water	7.353	± 1.47 mg/L

2.3.3 Comparison of Zn powder method against accredited IC analysis

Blind sample analysis was carried out for this comparison study. The samples were analysed using the Zn powder method and an accredited IC method. Samples were analysed for nitrite first by adding Griess reagent only to the sample solution. The nitrite concentration was determined using the calibration curve in Figure 2.2A. The samples were then analysed for nitrate using the optimised Zn powder method. The nitrite concentration (mg/L NO_2^--N) present in the sample was subtracted from the nitrate concentration (mg/L NO_3^--N)

determined using the Zn powder method. The nitrate concentrations determined within each sample using the Zn powder method in comparison to the nitrate concentrations determined using an accredited IC are shown in Table 2.5 below.

Table 2.5: Nitrate concentrations observed following nitrate analysis using Zn powder method and a comparison against an accredited IC system (*n*=5)

Sample	Characteristics	Zn Powder Method (mg/L NO_3^-)	Accredited IC (mg/L NO_3^-)	Percentage Difference (%)
A	Potable Water	37.06	37.51	1.20
B	Stream Water	19.75	19.16	3.08
C	Effluent	13.54	11.71	15.63
D	Potable Water	**51.51***	50.93	1.14
E	Effluent	**46.52***	49.45	5.93
H	Blank	< 0.5	0.49	-
I	10 mg/L Standard	10.07	9.27	8.63

* Concentrations which were above the upper limit of the Zn powder method

On evaluation of the NO_3^- concentrations determined for each sample using IC and the developed Zn method, it is evident that the NO_3^- concentrations determined are comparable. The largest percentage difference was observed for the effluent sample as a difference of 15.63 % was obtained. This comparability highlights the effectiveness of the Zn powder method in terms of NO_3^- determination in various water matrices.

2.3.4 Comparison against alternative colorimetric method

Blind sample analysis was again carried out using a different range of water samples containing nitrate. Samples were analysed using IC, the developed Zn powder method and a novel solid-based reagent method. The nitrate concentrations obtained using each methodology are illustrated in Table 2.6. Again, a good correlation is observed between the developed Zn powder method and the accredited IC when analysing freshwater samples. The solid-phased method exhibited good accuracy when analysing samples containing higher NO_3^-

concentrations, but in general was less accurate compared to the Zn powder method. The solid-phased method demonstrated accurate analysis of the seawater sample, whereas the Zn powder method demonstrated poor accuracy when analysing the seawater matrix.

Table 2.6: Nitrate concentrations of blind samples determined using IC, the developed Zn method and a novel solid-phased reagent method (*n*=5)

Sample Reference	Sample Characteristics	IC (mg/L NO_3^-)	Zn Powder Method (mg/L NO_3^-)	Solid-Phased test reagent (mg/L NO_3^-)
A	Drinking water	37.87	38.51±0.15	38.99±0.09
B	Borehole	3.95	3.44±0.21	1.76±1.41
C	Standard (2 mg/L NO_3^-)	2.17	1.95±0.07	4.59±0.09
D	Process Water	11.82	12.63±0.11	14.43±0.51
E	Standard (4 mg/L NO_3^-)	3.89	3.12±0.31	6.26±0.18
F	Borehole	0.55	<0.5	3.48±0.16
G	Seawater* (10 mg/L NO_3^-)	9.79	6.35±1.39	9.5±1.05

* Hach HR cadmium reduction method (method 8171) used to determine NO_3^- in seawater sample

2.4 Conclusions

A nitrate determination method for use within portable, field water test kits based on nitrate reduction using zinc and the Griess assay was developed. When using Zn as a reducing agent for nitrate it was shown that Zn quantity, the extent of mixing and standing time had a significant effect on nitrate reduction efficiency. Following validation and investigation of performance characteristics it was shown that the developed method is capable of determining nitrate in various water matrices including drinking, river, effluent and groundwater. However, the method was not applicable to marine water. When compared to a novel non-toxic solid-based reagent method the Zn powder method

demonstrated greater accuracy when analysing freshwater. The developed Zn method allows for ease of use at fast analysis times and the method is now being employed within TelLab's Hydromonitrix water test kits for NO_3^- analysis [19]. In comparison to leading freshwater test kits [20, 21], the Hydromonitrix NO_3^- test kit offers the potential for greater analytical accuracy than test strip kits and is less toxic than cadmium-based nitrate test kits. In addition, the Zn method also offers the potential to be coupled with a portable spectrophotometer, providing the opportunity to achieve higher sensitivity and reproducibility in comparison to using visual test kits [23].

2.5 Acknowledgements

The authors would like to acknowledge financial support from the Irish Research Council, Grant No. EBPPG/2015/127 and Science Foundation Ireland (SFI) under the INSIGHT Centre award, Grant No. SFI/12/RC/2289. In addition, support was also provided by the COMMON SENSE project funded through the European Union's Seventh Framework Programme, Grant No. 614155.

2.6 References

[1] A. Jang, Z. Zou, K. Kug Lee, C. H. Ahn and P. Bishop, *Meas. Sci. Technol.*, 2011, 22(3), 18–33.

[2] Y. Zhang, L. Fadong, Z. Qiuying, L. Jing and L. Qiang, *Sci. Total Environ.*, 2014, 213–222.

[3] S. Cornell, A. Randell and T. Jickells, *Nature*, 1995, 376, 243–246.

[4] L. Nollet and L. De Gelder, *Handbook of Water Analysis*, Marcel Dekker, New York, 2000.

[5] M. Allaby, *Dictionary of the Environment*, New York University Press, New York, 3rd edn, 1989.

[6] C. J. Johnson and B. C. Kross, *Am. J. Ind. Med.*, 1990, 18(4), 449–456.

[7] D. Forman, S. Al-Dabbagh, T. Knight and R. Doll, *Ann. N.Y. Acad. Sci.*, 1988, 534, 597–603.

[8] European Commission, *The Nitrates Directive*, 2016, online, available, http://www.ec.europa.eu/environment/water/waternitrates/index_en.html, 17 Sept 2016.

[9] EPA, *Method 300.0: Determination of Inorganic Anions by Ion Chromatography*, Environmental Protection Agency, Cincinnati, 1993.

[10] E. Garcia-Robledo, A. Corzo and S. Papaspyrou, *Mar. Chem.*, 2014, 162, 30–36.

[11] E. P. Nesterenko, B. Murphy, E. Murray, B. Moore and D. Diamond, *Anal. Methods*, 2016, 8, 6520–6528.

[12] L. Nollet and L. De Gelder, *Handbook of Water Analysis*, CRC Press, Florida, 3rd edn, 2013.

[13] EPA, *Methods for the Chemical Analysis of Water and Wastes*, Environmental Protection Agency, Washington DC, 1974.

[14] L. Merino, *Food Anal. Methods*, 2009, 2, 212–220.

[15] P. Ellis, A. Shabani, B. Gentle and I. Mckelvie, *Talanta*, 2011, 84(1), 98–103.

[16] D. Cogan, J. Cleary, T. Phelan, E. McNamara, M. Bowkett and D. Diamond, *Anal. Methods*, 2013, 5, 4798–4804.

[17] D. Cogan, C. Fay, D. Boyle, C. Osborne, N. Kent, J. Cleary and D. Diamond, *Anal. Methods*, 2015, 7, 5396–5405.

[18] A. D. Eaton, L. S. Clesceri, E. W. Rice and A. E. Greenberg, *Standard methods for the examination of water and wastewater*, Port City Press, Baltimore, 21st edn, 2005.

[19] TelLab, *Hydromonitrix*, 2016, online, available, http://www.tellab.ie/hydromonitirx.pdf, 13 Oct 2016.

[20] *Hach nitrite and nitrate test strips*, available, https://www.hach.com/nitrate-and-nitrite-test-strips/product-details?id=7640211606, 9 Oct 2016.

[21] *Hach nitrate-nitrite test kit model NI-12*, available, https://www.hach.com/nitrate-nitrite-test-kit-model-ni-12/product?id=7640220989, 9 Oct 2016.

[22] B. M. Jayawardane, S. Wei, I. D. Mckelvie and S. D. Kolev, *Anal. Chem*., 2014, 86, 7274–7279.

[23] *Hanna nitrate-nitrogen portable photometer*, available, http://www.hannainst.com/hi96728-nitrate-portable-photometer.html, 02 Jan 2017.

Chapter 3

Miniaturised capillary ion chromatograph with indirect UV LED based detection for anion analysis in potable and environmental waters

Eoin Murray [1, 2], Yan Li [3], Sinead A. Currivan [3], Breda Moore [1], Aoife Morrin [2], Dermot Diamond [2], Mirek Macka [3], Brett Paull [3]

1. *Research & Development, T.E. Laboratories Ltd. (TelLab), Tullow, Carlow, Ireland*
2. *Insight Centre for Data Analytics, National Centre for Sensor Research, School of Chemical Sciences, Dublin City University, Dublin 9, Ireland*
3. *Australian Centre for Research on Separation Science (ACROSS), School of Physical Sciences, University of Tasmania, Sandy Bay, Hobart 7001, Australia*

Publication: Journal of Separation Science, 2018, 10.1002/jssc.201800495

Chapter Overview

This chapter moves beyond the simplistic manual in-field test kit described in chapter 2 and investigates a chromatographic approach towards automated, *in-situ* nutrient analysis in waters. Chapter 3 describes the design, development and testing of a novel miniaturised capillary IC which incorporates indirect UV LED based detection for anion analysis in environmental waters. The IC has a modular design and is low-cost, costing < €5000, in comparison to state-of-the-art bench top IC systems. A basic bench top anion IC, such as a Dionex Aquion costs ~ €40,000, while a high-pressure dual ion bench top IC, such as a Dionex ICS5000 costs ~ €110,000. The miniaturised IC system allows for the analysis of nitrate, nitrite and other small inorganic anions over broad concentration ranges with limits of detection applicable to water legislation compliances.

Journal Front Cover

Abstract

A miniaturised, flexible and low-cost capillary ion chromatography system has been developed for anion analysis in water. The ion chromatograph has an open platform, modular design and allows for ease of modification. The assembled platform weighs ca. 0.6 kg and is 25 x 25 cm in size. Isocratic separation of common anions (F^-, Cl^-, NO_2^-, Br^- and NO_3^-) could be achieved in under 15 min using sodium benzoate eluent at a flow rate of 3 μL/min, a packed capillary column (0.150 x 150 mm) containing Waters IC-Pak 10 μm anion exchange resin, and light emitting diode based indirect UV detection. Several low UV LEDs were assessed in terms of detection sensitivity, including a new 235 nm LED, however the highest sensitivity was demonstrated using a 255 nm LED. Linear calibration ranges applicable to typical natural water analysis were obtained. For retention time and peak area repeatability, relative standard deviation values ranged from 0.60 – 0.95 % and 1.95 – 3.53 %, respectively. Several water samples were analysed and accuracy (recovery) was demonstrated through analysis of a prepared mixed anion standard. Relative errors of - 0.36, - 1.25, - 0.80 and - 0.76 % were obtained for fluoride, chloride, nitrite and nitrate respectively.

3.1. Introduction

As human populations expand and industrial and agricultural activities grow, declining water quality has become an increasing global concern. Globally, a broad range of legislation exists which is in place to help protect water quality [1-3]. As a result of such legislation, monitoring of water quality from numerous water sources is required. Drinking water, municipal wastewaters and environmental waters (groundwater and surface waters both fresh and marine) all must be monitored according to legislation [4]. At present, water monitoring is primarily based on manual grab sampling. Discrete samples are collected from specific locations at certain times and are transported to a laboratory for analysis. For stable anions such as Cl^- and F^-, when carried out correctly, this approach yields high quality qualitative and quantitative data. However, for those less stable anion species (e.g. NO_2^-), changes to sample composition and integrity during collection and transportation is a concern. In addition, high costs are associated with this 'grab and lab' approach, due to personnel requirements for sample collection, transportation and analysis. In the field of environmental monitoring, this results in limited temporal and spatial data, affecting the accuracy of large-scale pollution profiles. To address such challenges, there has been, and continues to be, great interest in the development of portable and/or miniaturised analytical systems, capable of performing analytical measurements *in-situ* [5].

When considering the analysis of ionic species in water, ion chromatography (IC) is regarded as the standard analytical technique. However, traditional bench-top IC systems are far from portable due to their physical size, weight, eluent requirements and power consumption. As a result, it is not practical or cost-effective to attempt to use bench-top systems for *in-situ* water monitoring [6]. Over the years, several attempts at producing portable IC systems have been reported, primarily aimed at monitoring inorganic and organic ions in natural waters. For example, in the 1990s, Baram *et al.* [7] reported a portable LC system capable of ion analysis, albeit weighing ca. 15 kg, for use in a mobile laboratory. Boringa *et al.* [8] also described a portable IC, in this case reduced to 10 kg in weight, which used capillary columns and conductometric detection. Soon after,

Tanaka *et al.* [9] employed a commercially available IC, powered for remote use by a car battery. The weight of the instrument without the battery was again 15 kg. In the early 2000s, Kalyakina *et al.* [10] also produced a portable IC with conductivity detection, with a system weight of 10 kg. More recently, Kiplagat *et al.* [11] presented a lightweight IC system (< 2.5 kg) for cation analysis based on gravity flow eluent delivery and open tubular capillaries, and most recently, Elkin [12] has demonstrated an autonomous IC for on-site analysis. The system used standard components and weighted 13 kg excluding the batteries and solar cells.

In this current work, we explore a different approach towards the development of a portable, miniaturised, lightweight and low-cost IC system, than all those previously reported. Building on work recently reported by Li *et al.* [13], we have developed a simple capillary IC system, assembled on a small footprint modular platform with an interchangeable design, comprised predominantly of off-the-shelf miniature and lightweight components. This design approach allowed for a light, flexible and low-cost system, in comparison to the previous 'portable' systems described above. In this paper, the characterisation and application of the miniaturised capillary IC is described. The analytical capillary column was fabricated and packed in-house using a commercial anion exchange resin. An indirect UV absorbance detection method was employed using a capillary scale UV LED – photodiode based detector, for the analysis of fluoride, chloride, nitrite and nitrate in various water samples. The analytical performance and repeatability of the system was assessed for the anions of interest. Water samples and standard solutions were analysed using the miniaturised IC and the results obtained are presented.

3.2. Materials and methods

3.2.1 Reagents and materials

All chemicals used within this work were of analytical or higher grade. All dilutions and solutions were prepared using high-purity deionised water (Milli-Q). Sodium benzoate used as the eluent was purchased from Ajax Chemicals (Auburn, NSW, AU). The quaternary amine functionalised polymethacrylate particulate stationary phase used herein (10 μm particles) was obtained from a

Waters IC-Pak anion column (4.6 x 50 mm). D-Gluconic acid solution (49 – 53 wt. % in H_2O) and boric acid used within the column packing procedure were purchased from Sigma Aldrich (St. Louis, MO). Fluoride, chloride, nitrite and nitrate stock solutions were prepared in-house using NaF, NaCl, $NaNO_2$ and KNO_3 salts respectively (Sigma-Aldrich Co., St. Louis, MO). Anion standard solutions of varying concentrations were prepared by dilution of the stock solutions.

3.2.2 Packing of capillary anion exchange column

For column packing, a capillary column packing kit from Trajan Medical and Scientific was used (Trajan Medical and Scientific, Melbourne, Australia). The Waters IC-Pak anion phase was used to prepare a 500 µL slurry in 1.3 mM gluconic acid and boric acid (buffer A). Using the column packing kit, an aliquot of 175 µL of the slurry was placed in the packing reservoir, by means of a 1.27 mm diameter syringe (18 gauge), until the reservoir was full. The PEEKsil capillary column was connected to the slurry column and a fritted ferrule was added as a retaining frit. The column was connected to a Thermo Scientific Ultimate 3000 Rapid Separation LC system. Using a flow rate of 10 µL/min, buffer A was used to flush particles from the packing reservoir to the 0.150 x 150 mm PEEKsil column. The column was left packing overnight, with an observed pressure drop of approximately 240 bar. The column was then equilibrated with a sodium benzoate eluent and used for anion separations on the portable IC system.

3.2.3 Capillary ion chromatography platform

Before the integration of the indirect method onto the miniaturised IC platform, the method was first demonstrated and optimised in terms of wavelength selection and eluent concentration using a standard benchtop IC. The miniature IC platform design was an adapted variation of the medium pressure LC system previously reported by Li *et al.* [13]. The IC system was fabricated using a LabSmith uProcess™ microfluidic system with other off-the-shelf components integrated into the system [14]. The microfluidic, automated pumping system was comprised of four SPS01 microsyringe pumps (100 x 25 x 21 mm) with 20 µL SPS01 glass syringes. Three pumps were used for eluent delivery and one

pump was used for automatic sample injection. Three AV201-C360 four port, two position microfluidic switching valves (LabSmith, Livermore, CA, USA) were used for eluent delivery and a fourth microfluidic switching valve was used for automated sample injection. An AV303 automated 6-port injection valve was used for sample introduction into the system [15]. A sample loop volume of 300 nL was used for analysis. All LabSmith system components were driven and operated using uProcess™ (LabSmith) software. Anion separation was achieved using the in-house packed 150 µm i.d. PEEKSil capillary column, 150 mm in length. The eluent used for sample analysis was 1.5 mM sodium benzoate. System components were connected using PEEK capillary (150 µm i.d., 360 µm o.d.; LabSmith). Capillaries and system components were connected using PEEK fittings (150 µm i.d.; LabSmith). The capillary IC system configuration and design is illustrated both schematically and as a photograph within Figure 3.1.

Indirect UV-absorption detection within the platform was achieved using an LED-based capillary scale photometric detection system, employing a z-shaped flow cell obtained from Knauer 2600 UV detector (Knauer, Berlin, Germany) and LED-photodiode holder, the optical performance of which is described in detail by Li *et al.* (2018) [16]. The LED light source was connected to a fibre optic cable, which was then connected to a holder attached to the z-flow cell. The photodiode was fixed into a holder on the opposite side of the z-flow cell, allowing optical alignment of the LED and the photodiode. To control and record the LED current and detector signal, an in-house fabricated controlling unit was used [17]. The detector signal generated by the controlling unit was absorbance, which was obtained through digital log conversion. The output absorbance generated by the controlling unit was fed into an EDAQ (Denistone East, NSW, Australia) PowerChrom 280 System (Model ER280)) interface unit which interfaced the LED detection system with the eChart software used to generate chromatograms. The LEDs which were used within this work were purchased from Crystal IS (Green Island, NY, USA). LEDs with emission wavelengths of 235, 255 and 280 nm were used. A broadband SiC based UV photodiode (TOCON ABC2) purchased from Sglux SolGel Technologies GmbH (Berlin, Germany) was used for detection for all wavelengths investigated.

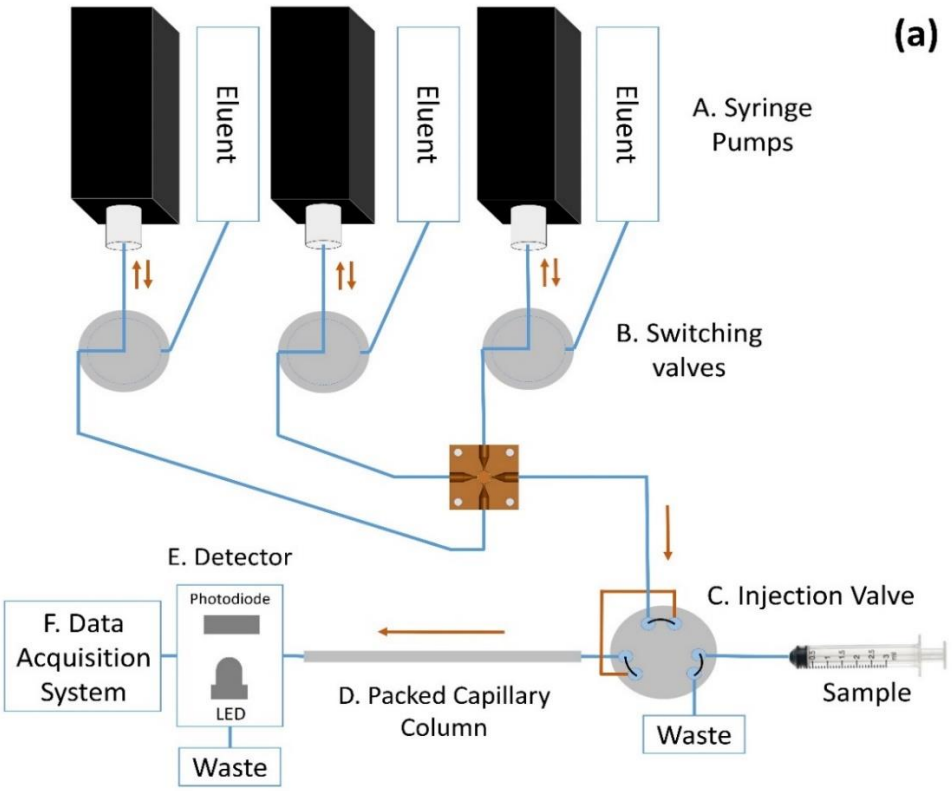

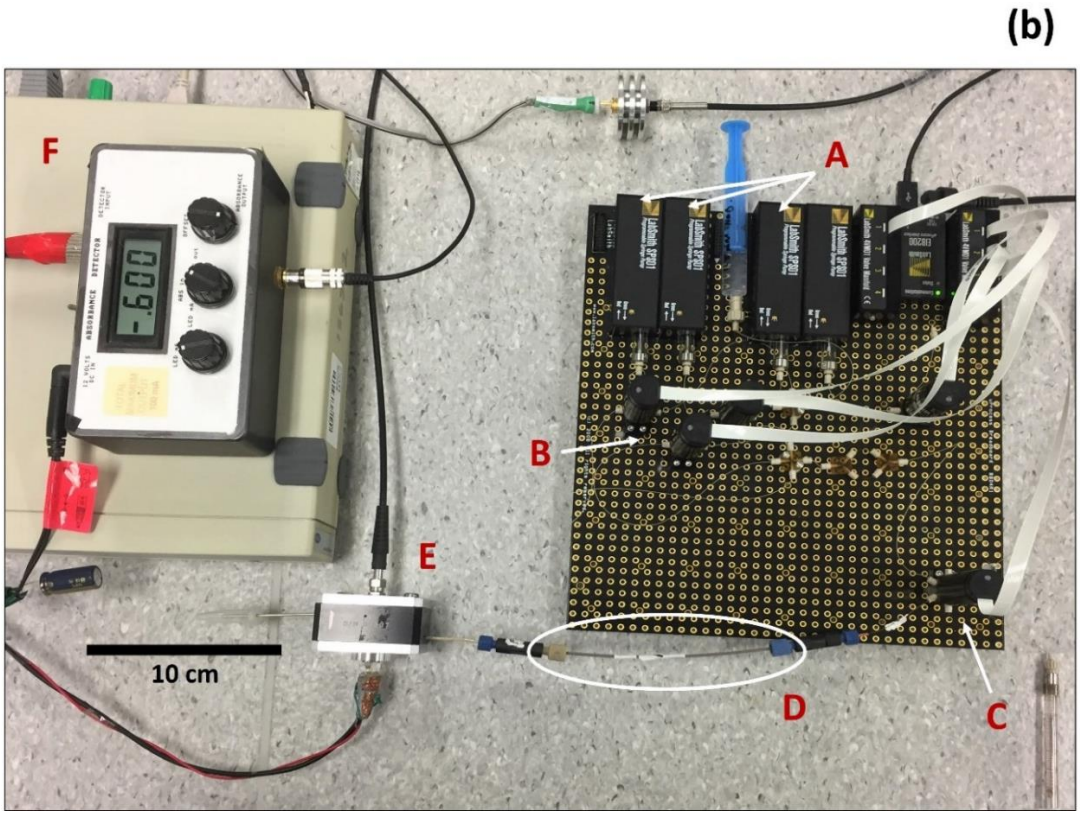

Figure 3.1 (a) Schematic of miniaturised IC system. (b) Photograph of IC platform with system components labelled as follows: A - syringe pumps attached to eluent reservoir, B - switching valves, C - injection valve, D - capillary column, E - optical detection z-cell, F - data acquisition units. The IC platform itself is 25 x 25 cm and weighs < 600 g.

3.3. Results and discussions

3.3.1 LED comparison and assessment

Deep UV LEDs emitting at 255 and 280 nm have previously been coupled with standard HPLC systems for direct optical detection [18], and more recently, a 235 nm LED has been demonstrated for on-capillary direct UV detection [19]. Herein, three UVC range LEDs (235 nm, 255 nm and 280 nm) were assessed as light sources and compared in terms of overall detector sensitivity and performance when applied in indirect UV detection mode, using the benzoate eluent, for the common inorganic anions of interest. These UVC range LEDs were selected to provide sufficient light, at or close to, the λmax of the absorbance spectrum of the sodium benzoate eluent, which lies within the region ~ 230 nm. Typical chromatograms of a four-anion standard obtained using the capillary platform and the capillary absorbance detector, fitted with each of the above LEDs are shown in Figure 3.2. The output parameters, including energy efficiency (calculated by dividing optical energy out by electrical energy in), of each UVC LED used and performance in terms of measured signal-to-noise ratio (S/N) for each anion of interest can be found within Table 3.1 [20]. The S/N for each LED was determined through the analysis of a four-anion standard containing 5 mg L^{-1} F^- and Cl^-, 10 mg L^{-1} NO_2^- and 15 mg L^{-1} NO_3^-. The level of signal resulting from the presence of each analyte was compared to the background noise level. Background noise results from a combination of electrical noise associated with the LED, pumping of the eluent and the amount of light which passes through the detection cell which is a function of LED optical output. As can be seen from Figure 3.2, each LED was successful in providing sufficient UV light to enable indirect UV absorbance detection, but each vary in terms of signal intensity. Therefore, although all three LEDs can be used in this mode, as can be seen from Table 3.1, under the conditions applied, the highest signal-to-noise ratio with indirect absorbance mode was obtained using the 255 nm LED. As a result, the 255 nm LED was selected as the detector of choice for more detailed evaluation within the miniaturised IC system.

Table 3.1: UVC LED parameters and S/N ratios obtained analysing a four-anion standard containing 5 mg L^{-1} F^- and Cl^-, 10 mg L^{-1} NO_2^- and 15 mg L^{-1} NO_3^-

LED	Peak Wavelength (nm)	Optical Power (mW)	Electrical Power (mW)	Energy Conversion Rate (%)	S/N for each anion			
					F^-	Cl^-	NO_2^-	NO_3^-
280	279	1.48	812	0.183	10.8	4.8	7.3	2.8
235	236	0.05	1030	0.005	9.5	5.5	5.3	4.1
255	257	0.79	902	0.097	51.7	27.7	35.2	27.7

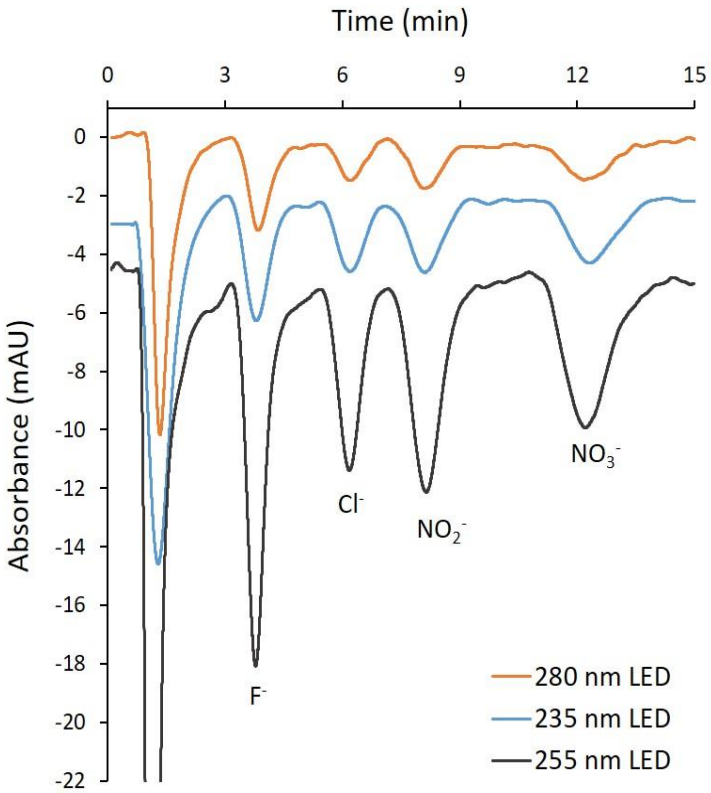

Figure 3.2: Performance comparison when using a 280 nm LED (orange chromatogram), 235 nm LED (blue chromatogram) and a 255 nm LED (black chromatogram). Each chromatogram represents a 300 nL injection volume of 4-anion standard containing 5 mg L^{-1} F^- and Cl^-, 10 mg L^{-1} NO_2^- and 15 mg L^{-1} NO_3^-. Eluent was 1.5 mM $NaC_7H_5O_2$ at a flow rate of 3 µL min^{-1} using the in-house packed capillary column.

3.3.2 Chromatographic repeatability

Measurement repeatability is an important factor when considering any IC system as it can be seen as a measure of instrument stability. Repeatability is also of distinct importance in relation to potential portability of the IC, particularly when applied for *in-situ*, or automated analysis [12]. Eleven chromatograms were generated for a four-anion standard solution. Prior to the first injection, the system was equilibrated with the eluent for approximately 25 min. Automatic injection was configured using an additional syringe pump. The four-anion standard solution was injected every 20 min. The overlaid ion chromatograms for six sequential injections are shown in Figure 3.3. The repeatability of the retention times and peak areas are presented in Table 3.2. The RSDs of peak areas and retention times for the 11 runs ranged from 1.95 – 3.53 % and 0.60 – 0.95 % respectively, and are comparable to the small-scale IC system reported by Elkin [12] over the same number of runs. Given the simple design of the micro-syringe pumps used herein, the relatively low back-pressure of the capillary column (<14 bar), together with the simple LED based detection, the repeatability data generated were satisfactory and comparable to typical commercial IC systems.

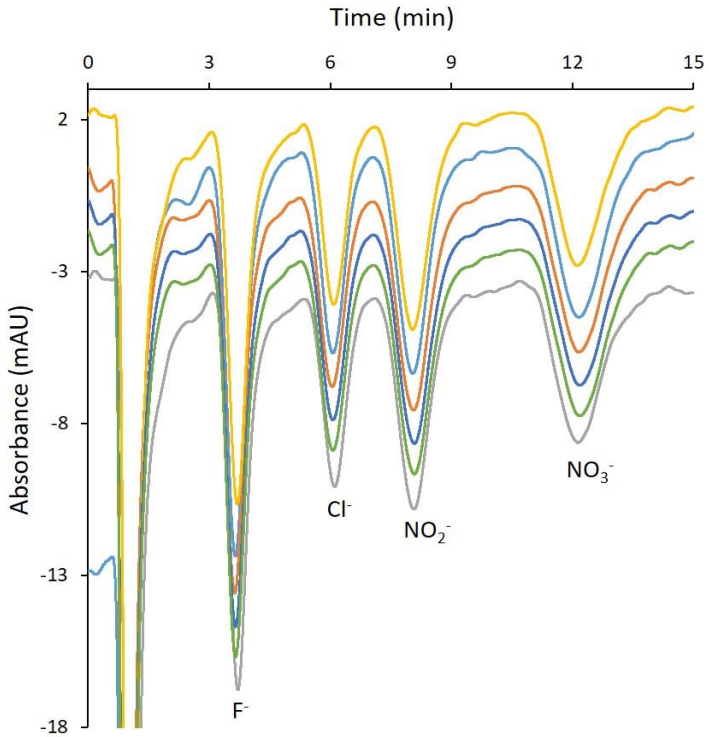

Figure 3.3: Repeatability of six sequential chromatograms (offset 1.2 mAU). Chromatographic conditions as above, each chromatogram represents 300 nL injection of the 4-anion standard.

Table 3.2: Repeatability study analysing a 300 nL injection volume of 4-anion standard containing 5 mg L^{-1} F^- and Cl^-, 10 mg L^{-1} NO_2^- and 15 mg L^{-1} NO_3^-. The eluent was 1.5 mM $NaC_7H_5O_2$ at a flow rate of 3 µL min^{-1} using the in-house packed capillary column and 255 nm LED with optical cell.

Analyte	Average Retention Time (min)	Retention Time RSD (*n* = 11)	Average Peak Area (mAU*s)	Peak Area RSD (*n* = 11)
Fluoride	3.84	0.78%	440.15	2.46%
Chloride	6.31	0.95%	257.51	3.53%
Nitrite	8.29	0.60%	376.15	1.95%
Nitrate	12.43	0.72%	439.98	2.99%

3.3.3 Capillary IC analytical performance

The developed basic method and capillary IC platform allowed for the simultaneous separation and detection of two important nitrogen nutrients, namely nitrite and nitrate, along with other small inorganic anions such as fluoride and chloride. Under the applied conditions the capillary IC delivered a run time of under 15 min, allowing for a sampling rate of four samples per hour. Satisfactory resolution was observed and the calibration plots obtained for the selected anions were linear over sufficiently wide concentration ranges. Linear ranges of 0.30 – 33.28, 0.30 – 51.20, 0.50 – 89.60 and 0.90 – 154.00 mg L^{-1} were obtained for F^-, Cl^-, NO_2^- and NO_3^-, respectively. Calibration plots for each analyte are graphically represented in Figure B1 – B4 of the supplementary information. The analytical parameters of the miniaturised IC system for the selected anions are summarised in Table 3.3. The limit of detection (LOD) for each analyte anion was calculated, using a signal-to-noise ratio (S/N) = 3 and the limit of quantification (LOQ) was calculated using S/N = 10 [12]. The sub-mg L^{-1} LODs obtained are comparable to those reported by others using standard instrumentation and indirect UV based methods [21-23], which given the capillary format applied herein, is also highly encouraging. The analytical performance demonstrated by the system, as listed within Table 3.3, confirms the suitability of the miniaturised IC platform for the analysis of a range of natural and potable waters.

Table 3.3: Assessment of performance of capillary IC for selected anions

Analyte	Linear Range (mg L^{-1})	R^2	Relative LOD (mg L^{-1})	Absolute LOD (pg)	LOQ (mg L^{-1})
Fluoride	0.30 - 33.28	0.999	0.17	51	0.56
Chloride	0.30 - 51.20	0.999	0.21	63	0.71
Nitrite	0.50 - 89.60	0.999	0.28	84	0.94
Nitrate	0.90 - 154.00	0.999	0.54	162	1.80

3.3.4 Water sample analysis

Local tap water (Hobart), spring water (Mount Wellington Park) and a mixed standard solution of known concentration of anions was analysed by the system using prepared calibration curves to evaluate recovery and precision. Prior to analysis, all samples were filtered using 0.45 µm nylon filters to remove suspended particles. For anion quantitation, samples were analysed in triplicate. Table 3.4 shows the anion concentrations determined within each sample using the capillary IC system. The generated sample chromatograms are shown in Figure 3.4 (a). Additionally, the isocratic separation of another anion mixed standard, with bromide also included, is shown in Figure 3.4 (b).

In terms of recovery data for the prepared mixed anion standard, acceptable relative errors were observed. Relative errors of - 0.36, - 1.25, - 0.80 and - 0.76 % were obtained for fluoride, chloride, nitrite and nitrate respectively, indicating the accuracy of the miniaturised system. In relation to the water samples which were analysed by the system, the anion concentrations were as expected. According to the Department of Health and Human Services Tasmania, the fluoride concentration in municipal water supplies is 1 mg L^{-1} F^- [24]. The fluoride concentration found in the tap water using the system of 1.06 mg ± 0.06 L^{-1} F^- is closely in agreement with this value. The chloride concentration determined within the tap water sample was in-line with typical chloride concentrations found in Tasmanian tap water and Southern Australian tap water as concentrations typically lie between 5 – 15 mg L^{-1} Cl^- [25]. Chloride was the only anion of interest detected within the spring water sample (5.24 ± 0.18 mg L^{-1} Cl^-).

Table 3.4: Analysis of samples using capillary IC platform (*n*=3)

Sample	Fluoride (mg L^{-1} F^-)	Chloride (mg L^{-1} Cl^-)	Nitrite (mg L^{-1} NO_2^-)	Nitrate (mg L^{-1} NO_3^-)
Tap Water	1.06 ± 0.06	9.92 ± 0.18	-	-
Spring Water	-	5.24 ± 0.18	-	-
Mixed Standard*	8.27 ± 0.14	12.64 ± 0.30	22.22 ± 0.32	38.11 ± 0.44

*Anion concentrations in standard: 8.30 mg L^{-1} F^-, 12.80 mg L^{-1} Cl^-, 22.40 mg L^{-1} NO_2^-, 38.40 mg L^{-1} NO_3^-

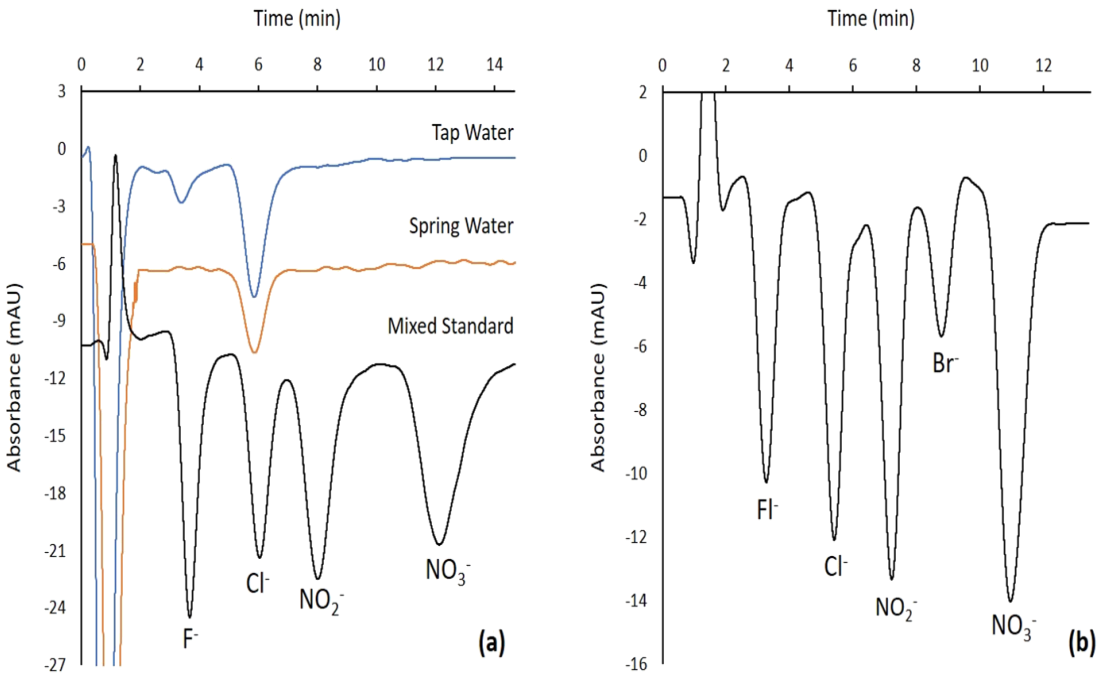

Figure 3.4: (a) Chromatograms of each analysed sample. Tap water sample (blue chromatogram), spring water sample (orange chromatogram), mixed standard sample (black chromatogram). For each sample, a 300 nL injection volume was used. The eluent was 1.5 mM $NaC_7H_5O_2$ at a flow rate of 3 µL min^{-1} using the in-house packed capillary column. (b) Chromatogram demonstrating the potential of the system to detect bromide with other anions. This chromatogram represents a 300 nL injection volume of 5-anion standard containing 4 mg L^{-1} F^-, 8 mg L^{-1} Cl^-, 16 mg L^{-1} NO_2^-, 8 mg L^{-1} Br- and 30 mg L^{-1} NO_3^-. The eluent was 1.8 mM $NaC_7H_5O_2$, flow rate 2.8 µL min^{-1}.

3.4 Conclusions

A miniaturised, lightweight capillary IC system for the analysis of anions in water has been developed and demonstrated in a laboratory setting. The IC uses off-the-shelf low-cost, miniaturised components, compared to standard IC systems, and through a modular design enables flexible system modification. The analytical column used within the system was an in-house packed capillary containing Waters IC-Pak anion exchange resin which enabled sufficient separation of small inorganic anions. Indirect absorbance detection on a capillary scale was explored for the first time using low UV LEDs and photodiodes housed within a capillary z-cell type detector. The miniaturised IC demonstrated good performance in terms of repeatability and precision, and delivered a wide linear detection range for F^-, Cl^-, NO_2^- and NO_3^-. Several LEDs in the UVC wavelength range, including a new 235 nm LED, were tested within the system. Detection was possible with all LEDs, however the 255 nm LED demonstrated the highest sensitivity and was selected for use within the system. Water samples were analysed using the miniaturised IC system and anion concentrations determined were within expected concentration levels. The accuracy of the developed system was demonstrated through the analysis of a prepared mixed anion standard, relative errors of no greater than 1.25 % were observed for each anion of interest.

Future work and further development of the system will focus on further reducing cost, achieving portability for direct analysis in the environment and assessing the robustness of the system in the field. Rapid prototyping techniques to achieve the manufacture of low cost z-cell optical detection and a custom interface unit and communications system will be investigated with the system along with battery power towards autonomous deployment of the IC.

3.5 Acknowledgements

The authors would like to acknowledge financial support from the Irish Research Council, Grant No. EBPPG/2015/127 and the Australian Research Council, Grant IC140100022.

3.6 References

[1] EU Water Framework Directive (WFD) (2000/60/EC)

[2] Clean Water Act (CWA) 33 U.S.C. §1251 et seq.

[3] Bourdeau K. S., Fulton C. S., Fraker R. N., China announces new comprehensive water pollution control plan. Beveridge & Diamond, Washington D.C. 2015.

[4] Mukhopadhyay S. C., Mason A., Smart Sensors for Real-Time Water Quality Monitoring. Springer-Verlag, Berlin 2013.

[5] Diamond D., Internet Scale Sensing. *Anal. Chem.* 2004, 87, 278 A-286 A.

[6] Beaton A. D., Sieben V. J., Floquet C. F. A., Waugh E. M., Abi Kaed Bey S., Ogilivie I. R. G., Mowlem M. C., Morgan H., An automated microfluidic colorimetric sensor applied in situ to determine nitrite concentration. *Sens. Actuator B Chem.* 2011, 156, 1009.

[7] Baram G.I., Portable liquid chromatograph for mobile laboratories: I. Aims. *J. Chromatogr. A* 728 (1996) 387-399.

[8] Boring C.B., Dasgupta P.K., Sjogren A., Compact, field-portable capillary ion chromatograph. *J. Chromatogr. A* 1998, 804, 45-54.

[9] Tanaka K., Ohta K., Haddad P. R., Fritz J. S., Lee K. P., Hasebe K., Ieuji A., Miyanaga A., Acid-rain monitoring in East Asia with a portable-type ion-exclusion–cation-exchange chromatographic analyser. *J. Chromatogr. A* 1999, 850, 311-317.

[10] Kalyakina O. P., Dolgonosov A. M., Ion-Chromatographic Determination of Fluoride Ions in Atmospheric Precipitates and Natural Waters. *Journal of Analytical Chemistry* 2003, 58, 951-953.

[11] Kiplagat I. K., Kubáňˇ P., Pelcováa P., Kubáňˇ V., Portable, lightweight, low power, ion chromatographic system with open tubular capillary columns. *J. Chromatogr. A* 2010, 1217, 5116–512.

[12] Elkin K. R., Portable, fully autonomous, ion chromatography system for on-site analyses. *J. Chromatogr. A* 2014, 1352, 38-45.

[13] Li Y., Dvořák M., Nesterenko P. N., Stanley R., Nuchtavorn N., Krčmová L. K., Aufartová J., Macka M., Miniaturised medium pressure capillary liquid chromatography system flexible open platform design using off-the-shelf microfluidic components. *Anal. Chim. Acta* 2015, 896, 166-176.

[14] http://products.labsmith.com/fluid-control-and-connectors/#.VdJ3Nfmqqko (accessed May 20, 2017).

[15] Li, Y., Pace, K., Nesterenko, P. N., Paull, B., Stanley, R., Macka, M., Miniaturised electrically actuated high pressure injection valve for portable capillary liquid chromatography. *Talanta* 2018, 180, 32-35.

[16] Li Y., Nesterenko P. N., Stanley R., Paull B., Macka M., Deep-UV LED based photometric detection integrated with capillary Z-type flow cell for capillary LC. *Anal. Chim. Acta.* 2018.

[17] Johns C., Macka M., Haddad P. R., Design and performance of a light-emitting diode detector compatible with a commercial capillary electrophoresis instrument. *Electrophoresis* 2004, 25, 3145 - 3152.

[18] Anh Bui, D., Bomastyk, B., Hauser, P.C., Absorbance detector based on a deep UV light emitting diode for narrow-column HPLC. *J. Sep. Sci* 2013, 36, 3152-3157.

[19] Li Y., Nesterenko P. N., Paull B., Stanley R., Macka M., Performance of a new 235 nm UV-LED based on-capillary photometric detector. *Anal. Chem.* 2016, 88, 12116–12121.

[20] Li Y., Dvořák M., Nesterenko P. N., Nuchtavorn N., Macka M., High power deep UV-LEDs for analytical optical instrumentation. *Sens. Actuator B Chem.* 2018, 255, 1238-1243.

[21] Shen X., Tomellini S. A., Indirect Photometric and Fluorometric Detection in High-Performance Liquid Chromatography: A Tutorial Review. *Crit. Rev. Anal. Chem.* 2007, 37, 107–126.

[22] El Haddad M., Mamouni R., Ridaoui M., Lazar S., Rapid simultaneous analysis of oxyhalides and inorganic anions in aqueous media by ion exchange chromatography with indirect UV detection. *J. Saudi Chem. Soc.* 2015, 19, 108–111.

[23] Hiissa T., Siren H., Kotiaho T., Snellman M., Hautojarvi A., Quantification of anions and cations in environmental water samples Measurements with capillary electrophoresis and indirect-UV detection. *J. Chromatogr. A* 1999, 853, 403–411.

[24] Department of Health and Human Services, Tasmania, Annual Report - Drinking Water Quality of Public Water Supplies in Tasmania July 1 2011 – July 30 2012.

[25] https://www.melbournewater.com.au/waterdata/drinkingwaterquality data/pages/drinking-water-quality.aspx (accessed June 1, 2017).

Chapter 4:

Low cost 235 nm UV-LED based absorbance detector for application in a portable ion chromatography system for nitrite and nitrate monitoring

Eoin Murray [1, 2], Patrick Roche [1], Kevin Harrington [1], Margaret McCaul [2], Breda Moore [1], Aoife Morrin [2], Dermot Diamond [2], Brett Paull [3, 4]

1. *Research & Development, T.E. Laboratories Ltd. (TelLab), Tullow, Carlow, Ireland*
2. *Insight Centre for Data Analytics, National Centre for Sensor Research, School of Chemical Sciences, Dublin City University, Dublin 9, Ireland*
3. *Australian Centre for Research on Separation Science (ACROSS), School of Physical Sciences, University of Tasmania, Sandy Bay, Hobart 7001, Australia*
4. *ARC Training Centre for Portable Analytical Separation Technologies (ASTech), School of Physical Sciences, University of Tasmania, Sandy Bay, Hobart 7001, Australia*

Publication: Journal of Chromatography A, 2019, DOI: J.ChromA.2019.05.036

Chapter Overview

This chapter builds on the work described in chapter 3. The miniaturised capillary IC demonstrated in the previous chapter represents a significant step towards cost-effective portable IC. However, the indirect UV detection method detects not only nutrient anions, but also other inorganic and organic analytes. This could result in coelution when analysing challenging matrices such as effluent or brackish waters. In addition, the flow cell used for detection was adapted from a UV-Vis instrument which presents challenges in terms of cost, but also in terms of component sourcing when considering mass manufacture. Chapter 4 describes the work carried out to overcome these issues. A new, low-cost optical z-cell was designed and manufactured. A deep-UV 235 nm LED was also sourced and integrated into the optical cell to enable selective, direct UV detection of nitrate and nitrite.

Abstract

A low cost, UV absorbance detector incorporating a 235 nm light emitting diode (LED) for portable ion chromatography has been designed and fabricated to achieve rapid, selective detection of nitrite and nitrate in natural waters. The optical cell was fabricated through micromilling and solvent vapour bonding of two layers of poly (methyl methacrylate) (PMMA). The cell was fitted within a 3D printed housing and the LED and photodiode were aligned using 3D printed holders. Isocratic separation and selective detection of nitrite and nitrate was achieved in under 2.5 min using the 235 nm LED based detector and custom electronics. The design of the new detector assembly allowed for effective and sustained operation of the deep UV LED source at a low current (< 10 mA), maintaining consistent and low LED temperatures during operation, eliminating the need for a heat sink. The detector cell was produced at a fraction of the cost of commercial optical cells and demonstrated very low stray light (0.01 %). For retention time and peak area repeatability, RSD values ranged from 0.75 – 1.10 % and 3.06 – 4.19 %, respectively. Broad analytical ranges were obtained for nitrite and nitrate, with limits of detection at ppb levels. The analytical performance of the IC set up with optical cell was compared to that of an ISO-accredited IC through the analysis of five various water samples. Relative errors not exceeding 6.86 % were obtained for all samples. The detector was also coupled to a low pressure, low cost syringe pump to assess the potential for use within a portable analytical system. RSD values for retention time and peak area using this simple configuration were < 1.15 % and < 3.57 % respectively, highlighting repeatability values comparable to those in which a commercial HPLC pump was used.

4.1. Introduction

Nitrogen in the form of nitrite (NO_2^-) and nitrate (NO_3^-) is naturally found in environmental waters. These anions play an integral role in facilitating the growth of algae and flora essential for aquatic ecosystems. Despite their intrinsic nature within environmental waters, excessive levels of nitrate and nitrite, as a consequence of point and nonpoint pollution sources derived from anthropogenic activities, present a notable risk to both environmental and human health [1]. Both nitrite and nitrate contribute to eutrophication which results in the overproduction of algae and aquatic plants. Algal blooms readily produce toxins and bacteria which are harmful to human health. These blooms can also severely reduce oxygen levels in water which has a detrimental impact on aquatic life. In addition to environmental impacts, nutrient pollution also has a significant economic impact. In the U.S. alone, nutrient pollution costs $2.2 billion dollars per year [2] and this economic impact is reflected on a global scale [3].

A broad range of standard analytical techniques exist for the analysis of nitrite and nitrate in water samples [4, 5], the most common of which being colorimetry and suppressed ion chromatography (IC) [6-8]. Under global legislation, such as the Water Framework Directive (WFD) within Europe and the U.S. Clean Water Act, the concentrations of nitrate and nitrite within environmental waters must be monitored. In order to achieve truly effective water quality management, deployable *in-situ* sensor systems capable of achieving high frequency and spatial data are required. With the advent of rapid prototyping technologies, such as 3D printing and micro-milling, a number of *in-situ* nitrite and nitrate analysers have been reported [9, 10]. Yet these technologies remain poorly implemented and have not seen widespread adoption for aquatic nutrient monitoring [11]. Leading *in-situ* analysers for nitrate and nitrite employ colorimetric chemistries coupled with visible LED based optical detection [9, 12]. These analysers require multiple reagents which can be affected by temperature and for nitrate detection require a reducing agent such as cadmium or vanadium chloride adding further complexity. A number of *in-situ* analysers which perform direct UV detection of nitrate are also commercially available, however these systems remain at a

significant price point and have high power consumption requirements due to the use of a UV lamp [13, 14]. Current technological limitations and prohibitive costs have hampered robust *in-situ* systems from becoming routinely used and adopted. [11].

Over the past decade, light emitting diodes (LEDs) have seen increasing use within optical detectors across a broad range of applications within analytical chemistry [15]. Their low-cost (relative to traditional lamps), low power consumption, small size, robustness and narrow emission bandwidth, make them ideal for use within portable, miniature and deployable analytical systems. As mentioned above, until now, most nutrient analysis systems and approaches, which employ LED based detection, do so in conjunction with colorimetric chemistries in the visible or near UV spectrum, typically focused on nitrate, nitrite and phosphate detection [16, 17]. However, LEDs emitting in the deep-UV range (< 280 nm) have recently become more readily available [18] and have now been applied for absorbance detection in combination with a range of analytical techniques, e.g. HPLC, IC and CZE, for the detection of organic and inorganic analytes [19-22]. Given that nitrite and nitrate have maximum absorption wavelength values (λ_{max}) of 209 and 200 nm respectively [23], a deep-UVC LED of < 240 nm is required to enable direct absorbance-based detection of these species. Recently, Li *et al.* 2016 [24] demonstrated for the first time the use of a 235 nm LED for chemical analysis, performing direct absorbance detection of nitrate and nitrite using standard capillary IC coupled with a modified on-capillary detector, comprising of a commercial optical interface. Within this detector set up, the LED required relatively high currents to generate sufficient light intensity for operation on a capillary scale. This high current saw increased LED temperatures, and as LED performance, lifetime and emission wavelength are negatively affected with increasing temperature, a heat sink for heat dissipation was required [25]. Similarly, Silveira Petruci *et al.* 2017 [26] demonstrated the use of a 235 nm LED for direct detection of organic analytes with standard commercial HPLC and again a heat sink was required for analysis. For portable low-cost instruments this additional requirement, albeit passive or active, adds unwanted complexity to the detector cell, which potentially could be avoided.

In this work, we describe an alternative deep-UV low-cost detector design, and demonstrate its simplicity and performance when applied as the optical detector with a portable IC configuration for nitrite and nitrate monitoring. The detector itself was fabricated using rapid prototyping techniques, including micromilling and 3D printing, and it incorporates a 235 nm deep-UV LED with UV photodiode for the direct detection of nitrite and nitrate. Rapid separation of the analytes is achieved using a low backpressure (< 12 bar) ion chromatography approach. The new design of the optical cell eliminates the need for heat sinks or heat dissipation and this is demonstrated through a thermal study of the LED within the optical detector during one hour of continuous operation. Without the need for a heat sink, complexity and manufacturing time associated with the optical detector is reduced. Custom electronics were used with the detector facilitating portability and again enabling a reduction in system cost. The stray light and effective path length of the fabricated optical cell was determined, along with the analytical performance and chromatographic repeatability. Environmental samples and blind standards were also analysed using the prototype instrument to establish the analytical accuracy when using the direct UV absorbance approach. Finally, low cost eluent syringe pumps were fabricated and tested with the developed method and detector to demonstrate the potential for implementation within a portable format.

4.2. Experimental

4.2.1. Chemicals and Reagents

All chemicals employed within this work were of analytical or higher grade. All solutions and dilutions were prepared using high-purity deionised water (Milli-Q). Potassium hydroxide used as the eluent was purchased from Sigma-Aldrich (St. Louis, MO). Nitrite and nitrate stock solutions were prepared using $NaNO_2$ and KNO_3 salts respectively (Sigma-Aldrich, St. Louis, MO). For the interference study, fluoride, chloride, iodide, iodate, bromide, phosphate, sulphate and carbonate stock solutions were prepared using NaF, NaCl, KI, KIO_3, KBr, KH_2PO_4, K_2SO_4 and K_2CO_3 salts respectively (Sigma-Aldrich Co., St. Louis, MO). Orange G used within the optical study of the detector cell was obtained from Fluka (Buchs, Switzerland). Working standards were prepared through dilution of stock

solutions. The environmental samples, along with the Environmental Protection Agency (EPA) intercalibration standard, were provided by the Environmental Department within TelLab (Carlow, Ireland).

4.2.2. Instrumentation

A Thermo Fisher Scientific Ultimate 3000 HPLC pump was used to deliver 100 mM KOH eluent at a rate of 0.8 mL min^{-1}. The pump was coupled to a manual 6 port 2-position high pressure injection valve provided by VICI AG (Schenkon, Switzerland). Rapid separation was achieved using a 4 × 50 mm Dionex AG15 guard column from Thermo Fisher Scientific (Sunnyvale, CA). The 235 nm deep UV-LED used for absorbance detection was provided by Crystal IS (Green Island, NY, USA). A UVC photodiode (TOCON_C1) with integrated amplifier employed for photodetection was purchased from Sglux GmbH (Berlin, Germany). For the analytical comparison study, nitrate and nitrite concentrations in environmental and blind samples were determined using an accredited Dionex DX-120 Ion Chromatograph (Dionex, Sunnyvale, USA), equipped with autosampler and a Dionex AERS 500 anion self-regenerating suppressor for suppressed conductivity detection. The low-pressure eluent syringe pumps which were coupled with the developed method and detector were designed using Fusion 360 computer aided design software (Autodesk Inc., California, USA). Syringe pump drive plates and back plates were made using Onyx filament sourced from Markforged, Inc. (Massachusetts, USA) and were printed using a Markforged Mark Two printer. The syringes used were 1 mL gas tight luer lock glass syringes sourced from Sigma-Aldrich (Wicklow, Ireland). Flushing of syringes was achieved through the use of 12 V brushed geared DC motors (Pololu, Las Vegas, USA) connected to an Aim-TTi EL303R power supply (RS Radionics, Dublin, Ireland). Rod collars and motor couplings were also provided by RS Radionics.

Operation of the LED and photodiode along with data acquisition was achieved using in-house customised electronics, comprised of electronic components sourced from Mouser Electronics (Texas, USA). Functionality was enabled through the use of an 8-bit Arduino microcontroller (ATMEGA2560). The LED was powered using a constant current driver (AL8805) with a PWM (pulse width

modulation) signal used to control light intensity. The resultant analogue signal from the photodiode was sent to a 16-bit analogue to digital converter (ADS1115). Raw bit values produced by the converter were filtered with a 15-point running average and data was then sampled at a frequency of 20 Hz. Chromatogram data were transmitted *via* serial port to a PC for real-time visualisation of the data using Arduino serial plotter. Data generated for each sample were arranged into a comma separated value (CSV) format and were stored on a microSD card in a CSV file for post processing. Absorbance (AU) values were obtained using the equation of $AU = -\text{Log}_{10}(V_S)/(V_B)$, where V_S was the voltage signal generated by the photodiode following sample injection and V_B was the baseline voltage signal. Origin data software was used for processing of chromatograms and peak area integration (OriginLab Corportaion, USA).

4.2.3. UV Optical Detector

The custom designed optical detector (Figure 4.1), based on a z-shape format, was fabricated using two layers of poly (methyl methacrylate) (PMMA) and was 50 x 25 x 12 mm in size. On the bottom PMMA layer a microfluidic z-shaped channel with a diameter of 500 μm and optical path of 2.15 cm was micro-milled. The internal volume of the z-cell channel was 11 μL. On the top PMMA layer two threaded openings were milled. One opening was used as an inlet and the second opening as the cell outlet. Micromilling of the PMMA was carried out by EFJ Engineering (Dublin, Ireland). The two PMMA layers were bonded through solvent vapour bonding, as described by Ogilvie et al. [27]. The bonding process involved solvent exposure of the micromilled PMMA substrates. Chloroform was the solvent used within this process. Following this, the PMMA layers were pressed together by hand and then finally bonded through the use of a hot press machine. Following the solvent bonding of the two PMMA layers, UV-transparent fused silica glass windows (Edmund Optics Inc., Barrington, NJ) were positioned and bonded at each side of the detector optical channel using epoxy putty obtained from J-B Weld (Sulphur Springs, TX). The detection cell was assembled within a 3D printed housing. The LED and photodiode were positioned and aligned at each window of the cell using custom 3D printed holders adapted from Donohoe *et al.* [28]. All 3D printing of components was carried out using a

Markforged Mark Two printer. The total component cost for the UV optical detector, including LED, photodiode and electronics for data acquisition and operation was < €430.

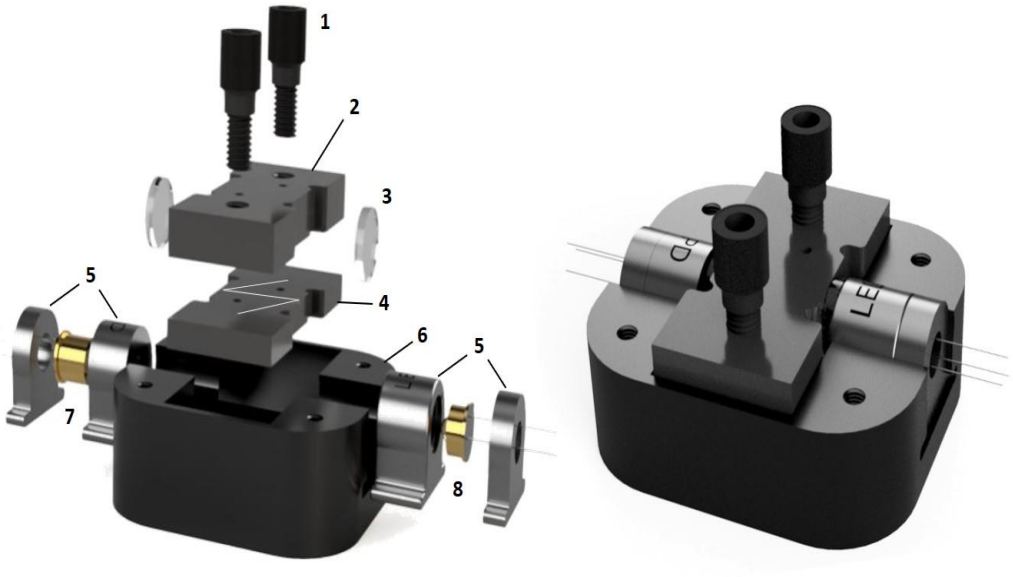

Figure 4.1. Design of the low-cost UV absorbance detector (left) and illustration of assembled detector (right). Legend: (1) flangeless nut fittings; (2) top PMMA layer with milled, threaded holes for cell inlet and outlet; (3) fused silica glass UV-transparent windows (12.5 x 2 mm); (4) bottom PMMA layer with milled z-shape fluidic channel; (5) 3D printed holders for LED and photodiode; (6) 3D printed optical cell holder; (7) photodiode; (8) 235 nm LED.

4.2.4. Stray Light and Effective Path Length Determination

The procedure employed within this study was similar to that described by Li *et al.* 2016 [24]. The dye Orange G was used to demonstrate the detector linearity as an absorbance to concentration relationship. A sensitivity versus absorbance plot was generated with sensitivity being determined by dividing absorbance by concentration [29, 24]. An Orange G stock solution was prepared and working standards were then made through serial dilution of the stock using DI water. Orange G standards, of concentrations ranging from 0.5 – 1000 μM, were analysed. Analysis was performed by flushing 5 mL of standard solution through the cell, the flow was then stopped and the absorbance was measured using the 235 nm LED under static flow conditions. Analysis of each standard solution was carried out in triplicate and in order of increasing concentration. Between each analysis of Orange G solution, the cell was flushed with 5 mL of DI water to

prevent carry over. Percentage of stray light and effective path length of the detector were calculated using the sensitivity versus absorbance plot as specified by Macka *et al.* [29].

4.3. Results and Discussions

4.3.1. Thermal Study of LED and Detector

It has been established that thermal management of deep-UV LEDs is an important consideration when employed for analytical operations. High currents are most typically applied for analysis using these LEDs and electrical power not converted into light is converted into heat. With increasing LED temperature, luminous efficiency decreases, emission wavelengths shift and LED lifetime is reduced [15]. In recent works in which the 235 nm LED was used for optical detection with chromatographic analysis, the use of a heat sink for heat dissipation was essential to achieve analytical performance as currents of 100 mA [24] and 66 mA [26] were used to operate the LED. Due to the 500 µm channel dimensions within the current cell and alignment of the LED and photodiode which was achieved by the 3D printed holders and housing, it was found that effective analyte detection could be achieved when operating the LED within the detector at a constant current of just 9 mA. Under these conditions, the background noise, determined by monitoring baseline signal for 60 s and recording maximum fluctuations, was 0.25 mAU. This was comparable to the 0.30 mAU noise reported by Silveira Petruci *et al.* [26]. By operating the LED at this low current, the issue of LED overheating was eliminated and in turn an LED heat sink was not required. Temperature measurements of the 235 nm LED within the detector over one hour of continuous operation are shown in Figure 4.2. The temperature reading was recorded from the point of the LED in which the highest temperature was observed. Thermal imagery of the LED and cell is shown in Figure C1 of the ESI. The average temperature of the hottest point of the LED during continuous operation was 27.29 ± 0.163°C.

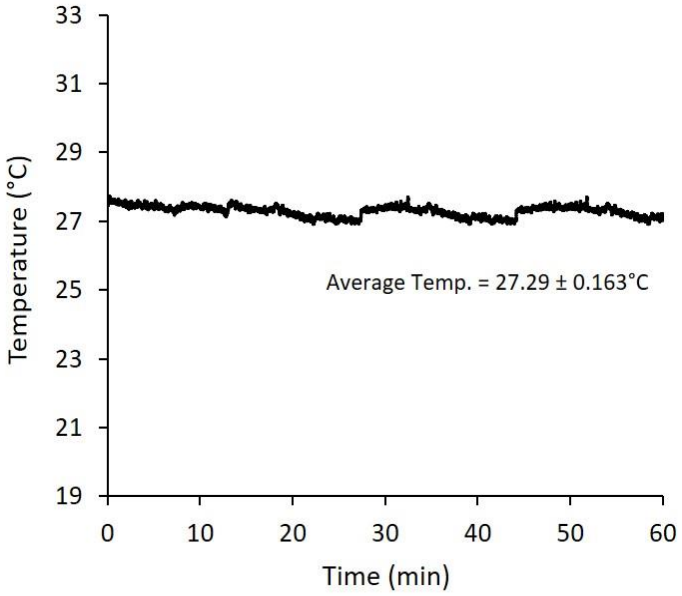

Figure 4.2. Temperature measurement of 235 nm UV-LED within optical cell over 1 hour of continuous operation, recorded using thermal camera. Temperature reading represents the temperature of the hottest point of the LED during operation.

4.3.2. Detector Stray Light and Effective Optical Path Length

The stray light and effective path length associated with the fabricated UV optical cell was determined through the use of the azo dye Orange G. The effective pathlength and stray light were determined using the same approach set out by Li *et al.* [24] and others [30], in which the theoretical model based on Beer's law reported by Macka *et al.* [29] is used. The equations associated with the theoretical model proposed by Macka *et al.* are highlighted in C2 of the supplementary information. The effective pathlength (L_{eff}) and stray light were calculated using the plot of detection sensitivity (AU/mol L^{-1}) versus absorbance (Figure 4.3). Extrapolation to the y-axis yielded a sensitivity value of 38000 AU/mol L^{-1}. Using this estimated value along with the molar absorptivity value of Orange G (18300 L mol^{-1} cm^{-1}), an effective pathlength of 2.07 cm was observed. This effective pathlength corresponded to 96.28 % of the actual optical channel length of the detector (2.15 cm). The upper limit of detector linearity, corresponding to a 5 % drop in sensitivity, was 3.162 AU. This observed upper linearity limit is higher than commercially available high sensitivity detection cells (detector linearity up to 2 AU), while at a fraction of the cost [31]. Following extrapolation to the x-axis, where sensitivity = 0, an

absorbance of 4.114 AU was observed which corresponds to a negligible stray light level of < 0.01 %. This very low stray light level is most likely associated with the large optical path length and the non-transparency of the PMMA to UV light. This stray light level is considerably lower in comparison to other detection cells employing deep UV LEDs, such as the LED-based detector reported by Sharma *et al.* in which a stray light of 3.6 % was observed [32]. Similarly, the lowest stray light reported by Li *et al.* for a high sensitivity UV LED-based detector incorporating commercial z-cells was 3 % [21].

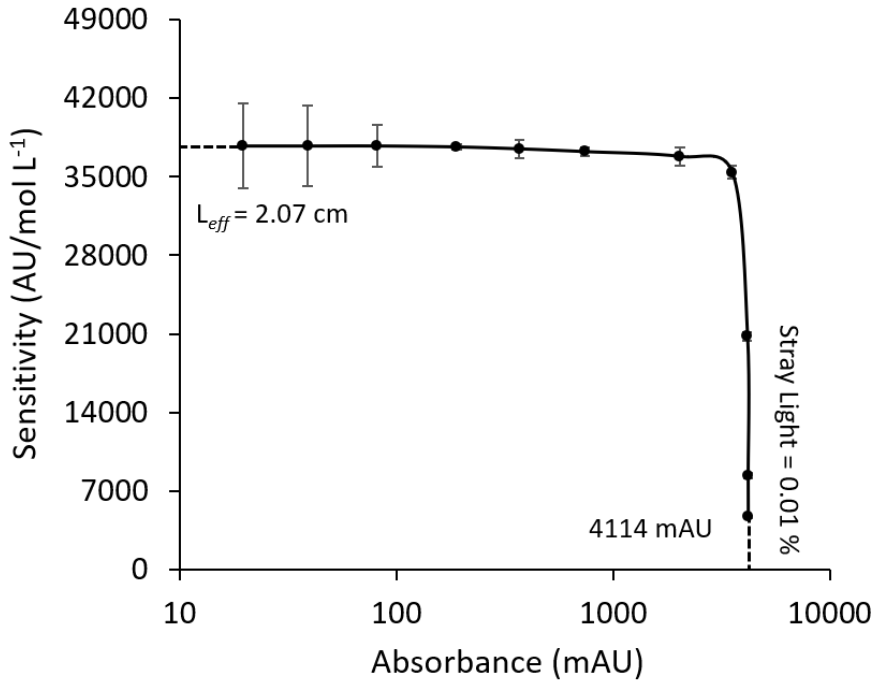

Figure 4.3. Linearity of 235 nm LED-based detector illustrated as sensitivity versus absorbance plot (error bars are standard deviations for *n*=3 replicates). A stray light value of 0.01 % was estimated for the detector and an effective pathlength of 2.07 cm was calculated.

4.3.3. Chromatography Repeatability

The measurement repeatability associated with the LED-based optical detector combined with the IC set up was established through the analysis of an anion standard solution containing 0.5 mg L^{-1} NO_2^- and 2.5 mg L^{-1} NO_3^-. The anion standard was injected 30 consecutive times. The retention time and peak area repeatability for both analytes are graphically presented in Figure 4.4. Relative standard deviations (RSD) of retention times and peak areas for the 30 runs ranged from 0.75 – 1.10 % and 3.06 – 4.19 %, respectively. Chromatographic

repeatability is also illustrated in Figure C3 of the supplementary information, as a selection of chromatograms from the 30 injections are overlaid. Despite the rapid separation, simple configuration and low-cost detection, these repeatability data are comparable to those typically observed within commercial standard IC systems and those reported for other IC set-ups aimed towards portability [33, 22].

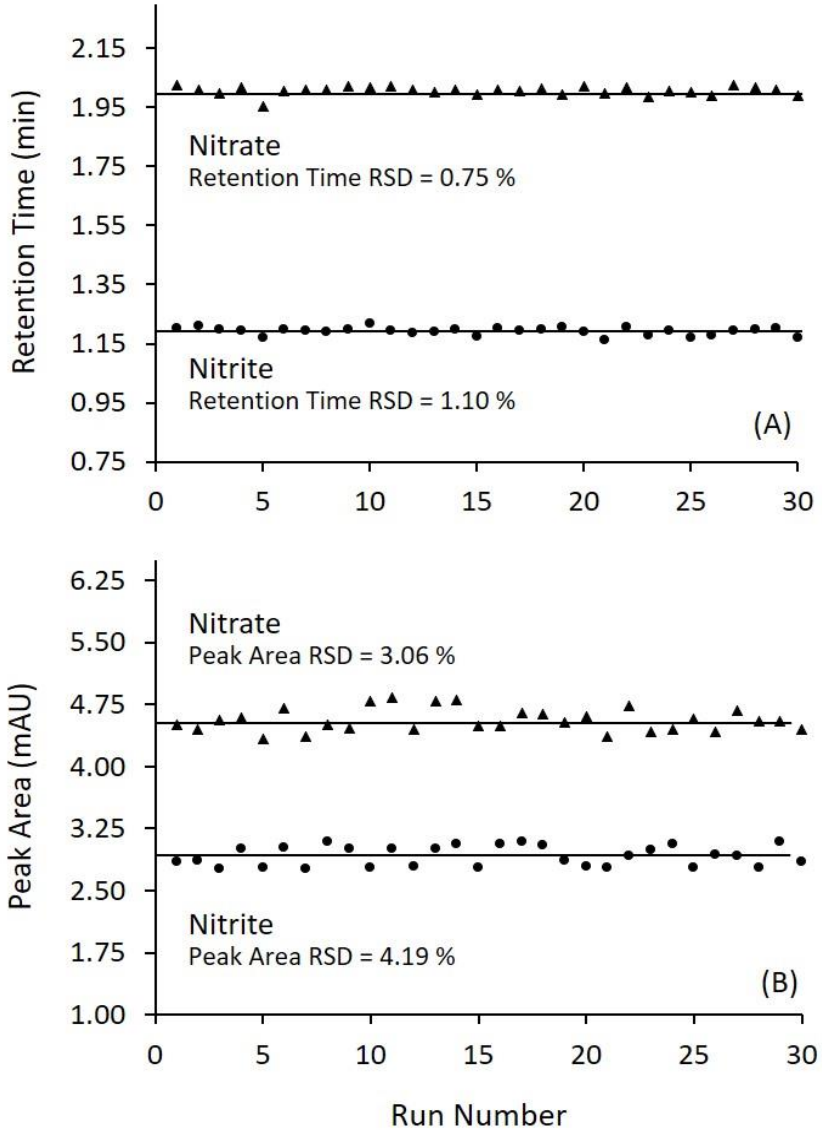

Figure 4.4. Repeatability study over 30 sequential runs, analysing 150 µL injection volume of standard containing 0.5 mg L^{-1} NO_2^- and 2.5 mg L^{-1} NO_3^-. Eluent used was 100 mM KOH at a flowrate of 0.8 mL min^{-1} with AG15 guard column for separation. (A) Repeatability of retention times for nitrite and nitrate over runs with associated RSD values. (B) Repeatability of peak area values determined for both analytes over 30 runs and associated RSD values.

4.3.4. Assessment of Interfering Anions

The interference of common anions was studied to ensure no coelution of nitrite and nitrate with other anions was observed when analysing environmental waters. The inorganic anions F^-, Cl^-, IO_3^-, I^-, CO_3^{2-}, SO_4^{2-}, Br^- and PO_4^{3-} were analysed as they are readily found within natural waters. Of these anions, iodide, iodate and bromide were potentially the most problematic as these anions have absorption spectra extending into the 230 nm region [34]. An anion mixture containing 10 mg L^{-1} of eight typical anions along with nitrite and nitrate was analysed using the simple IC set up coupled with the 235 nm LED detector and custom electronics. The generated chromatogram is shown in Figure 4.5. Detection of nitrite and nitrate was unaffected by the presence of other small inorganic anions. Iodate was the only analyte observed within the 2.5 min elution time, however resolution (R_s) between iodate and nitrite remained sufficient as a R_s value of 2.45 was observed.

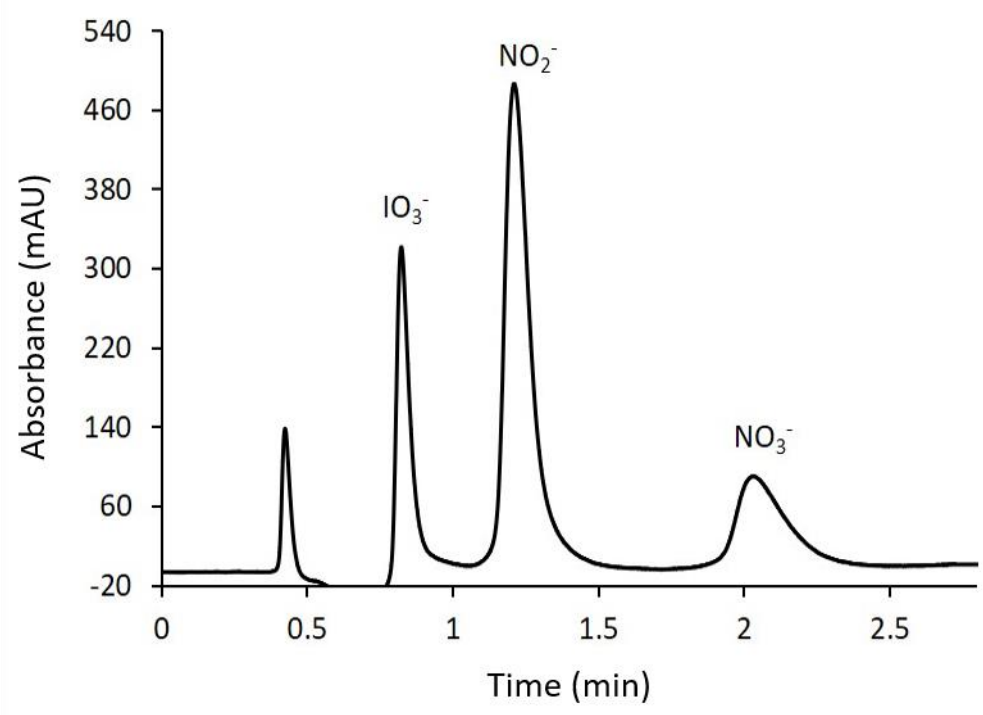

Figure 4.5. Chromatogram representing a 150 µL injection volume of 10-anion standard containing 10 mg L^{-1} F^-, Cl^-, NO_2^-, NO_3^-, IO_3^-, I^-, CO_3^{2-}, SO_4^{2-}, Br^- and PO_4^{3-}. The eluent was 100 mM KOH at a flow rate of 0.8 mL min^{-1} using the AG15 guard column as the separator column and 235 nm LED with fabricated optical detection cell.

4.3.5. Analytical performance and sample analysis

The relative error obtained for the analysis of the EPA intercalibration solution was < 2 %. Under isocratic conditions using 100 mM KOH eluent, an AG15 column and a sample injection volume of 150 μL combined with the 235 nm optical detector with custom electronics both nitrite and nitrate are detected in under 2.5 minutes. A low backpressure of 11.5 bar is generated by the system, which implies that a lower cost, portable pump could be used. Analytical ranges, using calibration curves based on peak area values and a polynomial fit, ranged from 0.010 – 15 mg L^{-1} for nitrite and 0.070 – 75 mg L^{-1} for nitrate. Calibration plots for each analyte are graphically represented in Figure C4 – C5 of the supplementary information. A limit of detection (LOD) of 0.007 mg L^{-1} for NO_2^- and 0.040 mg L^{-1} for NO_3^- was observed, using a signal-to-noise ratio (S/N) of 3 as the threshold [33]. This analytical performance is comparable to those typically reported for commercial benchtop IC systems [35, 36].

A combination of blind standard solutions and environmental samples comprising one river water sample (Environmental A) and one treated effluent water sample from a sugar processing plant (Environmental B) were analysed. The detailed composition of these samples is tabulated in Table C6 of the ESI. In addition, an EPA intercalibration solution was also analysed. The intercalibration standard was provided by TelLab and was a standard which is used within the Irish EPA Environmental Intercalibration Programme. This programme assesses analytical performance to ensure validity and comparability of environmental data for laboratories which submit data to the EPA. All samples were first passed through 0.45 μm nylon filters to remove suspended particles. Nitrite and nitrate concentrations determined within each sample using the IC with 235 nm LED detector in comparison to concentrations determined using the accredited IC method are shown in Table 4.1. The highest relative error for nitrite determination was 6.86 % and for nitrate was 5.40 %. The relative error obtained for the analysis of the EPA intercalibration solution was -1.90 %. Although relative errors not exceeding 8.80 % were observed when linear calibrations were employed for nitrite and nitrate estimation, by replacing linear curves with a polynomial fit, total error in terms of the sum of squared residuals (SSR) is

reduced by 38.5%. Concentration results obtained using linear calibration curves compared to concentrations obtained by the accredited IC is reported in Table C7 of the ESI.

Table 4.1 Concentrations obtained by IC with UV detector versus accredited IC (*n*=3)

Sample	Analyte	IC Set-up (mg L^{-1})	Accredited IC (mg L^{-1})	Relative Error (%)
A	Nitrite	1.09 ± 0.01	1.02 ± 0.01	6.86
B	Nitrate	5.14 ± 0.05	5.07 ± 0.05	1.38
Environmental A	Nitrite	0.52 ± 0.01	0.50 ± 0.01	4.00
	Nitrate	4.99 ± 0.05	5.03 ± 0.04	-0.79
Environmental B	Nitrite	0.16 ± 0.01	0.15 ± 0.01	6.67
	Nitrate	61.13 ± 0.40	58.00 ± 0.54	5.40
EPA	Nitrate	53.63 ± 1.08	54.67 ± 0.89	-1.90

4.3.6. Integration of detector with low pressure syringe pump

In order to achieve low-cost, portable IC analysis using the developed UV detector and the proposed method, a cost-effective lightweight pumping solution for eluent delivery is required. As a consequence of the low backpressure (11.5 bar) generated by the system, the use of a low-pressure eluent pump is enabled. As a step towards low-cost portable IC analysis using the proposed method, automated syringe pumps were designed, fabricated and coupled with the microinjection valve, AG15 column and the 235 nm LED detection system as shown in Figure 4.6. The automated syringe pumps provided eluent delivery and were based on three 1 mL glass syringes housed within 3D printed holders fitted with three brushed DC motors. The design of the eluent syringe pumps is highlighted in Figure C8 of the supplementary information. A voltage of 4.5 V was applied to the motors, attached to the syringe drive plates, which enabled a flowrate of 0.7 mL min^{-1}. The dimensions of the syringe pump configuration were 21 x 13 x 4 cm, with a total weight of < 900 g and a cost price of < €235. Selected chromatograms overlaid (offset by 15 mAU) following 12 sequential runs using the automated syringe pump and IC configuration with the 235 nm LED and optical detector are illustrated inset of Figure 4.6. RSD values for retention times and peak areas for the 12 runs ranged from 0.80 – 1.15 % and 2.41 – 3.57 %

respectively. This chromatographic repeatability achieved when using the low-cost, low pressure syringe pump was comparable to that demonstrated when using the 235 nm detector coupled with the commercial HPLC pump (Figure 4.4), highlighting the potential of the method and the detector for utilisation within a portable format.

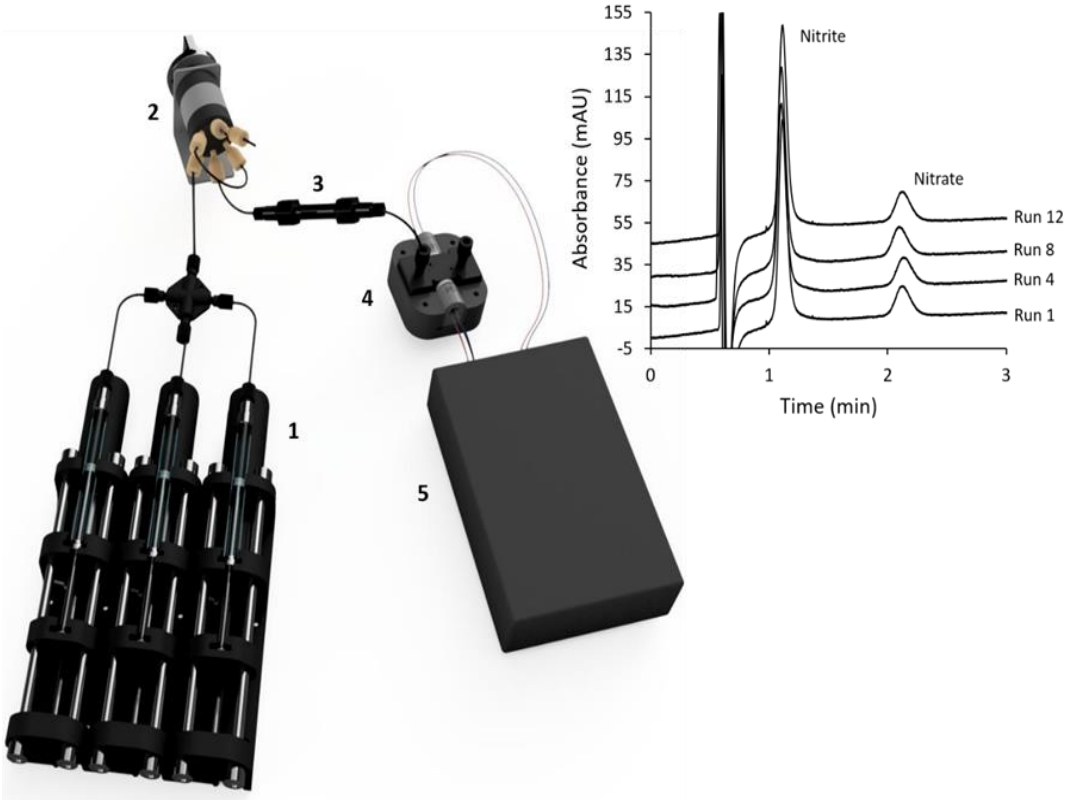

Figure 4.6: Illustration of detector, electronics and method coupled with low-pressure syringe pump configuration demonstrating the potential for integration into portable IC format. Legend: (1) Low pressure syringe pumps; (2) manual microinjection valve (3) AG15 guard column; (4) 235 nm LED based UV detector; (5) electronics for LED/PD operation and data acquisition. Selected chromatograms overlaid (offset by 15 mAU) following 12 sequential runs using IC set up with 235 nm LED absorbance detector shown inset. Each chromatogram represents 5 µL injection of standard containing 20 mg L^{-1} NO_2^- and NO_3^-. Eluent was 100 mM KOH at a flowrate of 0.7 mL min^{-1} with AG15 guard column.

4.4. Conclusion

A compact, low-cost UV optical detector has been designed and fabricated. Rapid, high sensitivity detection of nitrite and nitrate was achieved by integrating a 235 nm LED with the detector and coupling this detector with a simple, low backpressure IC set up with in-house built electronics for detector control and data acquisition. The detection cell was based on a z-type design and was fabricated through micromilling and solvent vapour bonding of PMMA. The housings for the optical cell and the LED and photodiode were 3D printed, facilitating optical alignment as the holders were fitted into the cell housing. Direct absorbance detection of NO_2^- and NO_3^- was achieved in under 2.5 min under isocratic conditions using 100 mM KOH eluent, an AG15 guard column for separation and the 235 nm LED-based optical detector. The power demand of the LED during analysis was 0.108 W, while a UV deuterium lamp typically employed for direct nitrate and nitrite absorbance detection can have a power demand of 30 W [37]. In addition, as a guard column was used as the separator column, separation was achieved at the low backpressure of 11.5 bar. Both the low power demand demonstrated by the 235 nm LED based detector, along with this low backpressure highlight the potential of the method for implementation within a portable IC analyser.

The need for heat dissipation of the 235 nm LED was eliminated when used with this detector as the LED was operated at a low current (< 10 mA), enabling stable LED temperatures while analytical performance was maintained. Despite the low-cost nature of the detector, very low stray light and high upper limit of detector linearity was observed. On assessment of chromatographic repeatability, precision comparable to commercial detectors was observed and selective detection for nitrite and nitrate in the presence of other typical small inorganic anions was achieved. The LOD of 0.007 mg L^{-1} for NO_2^- and 0.040 mg L^{-1} for NO_3^- obtained using the low-cost UV detector were comparable to those reported by commercial IC, and analytical ranges suitable for the analysis of almost all-natural freshwaters were demonstrated. When compared to an ISO-accredited IC, suitable accuracy was observed as low relative errors (< 8.80 %) were obtained. The detector and method were also coupled to a low pressure,

low cost syringe pump to demonstrate the potential of the system for portable analysis. This simple configuration demonstrated comparable chromatographic repeatability to that achieved when using a commercial HPLC pump.

Future work and development will focus on the design and fabrication of a sample intake system to be coupled with the IC method and detector. An embedded system will also be developed for integration with the IC method and components to enable system automation and communications towards achieving a low-cost, fully automated *in-situ* nitrate and nitrite analyser for environmental water monitoring.

4.5. Acknowledgements

The authors would like to acknowledge financial support from the Irish Research Council, Grant No. EBPPG/2015/127 and the Australia Awards - Endeavour Research Fellowship, Grant No. 6389_2018. Science Foundation Ireland INSIGHT Centre award SFI/12/RC/2289 is also acknowledged.

4.6. References

[1] J.A. Camargo, A. Alonso, Ecological and toxicological effects of inorganic nitrogen pollution in aquatic ecosystems: A global assessment, Environ. Int. 32 (2006) 831-849.

[2] Integrated Ocean Observing System, ACT Nutrient Sensor Challenge. https://ioos.noaa.gov/news/act-nutrient-sensor-challenge-winners-announced/, 2017 (accessed 10 October 2018).

[3] A. Moxey, Agriculture and Water Quality: Monetary Costs and Benefits across OECD Countries, Pareto Consulting, Edinburgh, 2012

[4] M.J. Moorcroft, J. Davis, R.G. Compton, Detection and determination of nitrate and nitrite: a review, Talanta 54 (2001) 785–803.

[5] Q.H. Wang, L.J. Yu, Y. Liu, L. Lin, R.G. Lu, J.P. Zhu, L. He, Z.L. Lu, Methods for the detection and determination of nitrite and nitrate: A review, Talanta 165 (2017) 709–720.

[6] J.W. O'Dell, Method 353.2: Determination of nitrate-nitrite nitrogen by automated colorimetry, U.S. Environmental Protection Agency, Cincinnati, 1993.

[7] J. Zhang, P. B. Ortner, C. J. Fischer, Method 353.4: Determination of Nitrate and Nitrite in Estuarine and Coastal Waters by Gas Segmented Continuous Flow Colorimetric Analysis, U.S. Environmental Protection Agency, Washington, 1997.

[8] D.P. Hautman, D.J. Munch, Method 300.1: Determination of Inorganic Anions by Ion Chromatography, U.S. Environmental Protection Agency, Cincinnati, 1997.

[9] A.D. Beaton, C.L. Cardwell, R.S. Thomas, V.J. Sieben, F.E Legiret, E.M. Waugh, P.J. Statham, M.C. Mowlem, H. Morgan, Lab-on-Chip Measurement of Nitrate and Nitrite for In Situ Analysis of Natural Waters, Environ. Sci. Technol. 46 (2012) 9548-9556.

[10] H. Hwang, Y. Kim, J. Cho, J. Lee, M. Choi, Y. Cho, Lab-on-a-Disc for Simultaneous Determination of Nutrients in Water, Anal. Chem. 85 (2013) 2954-2960.

[11] T.M. Schierenbeck, M.C. Smith, Path to Impact for Autonomous Field Deployable Chemical Sensors: A Case Study of in Situ Nitrite Sensors, Environ. Sci. Technol. 51 (2017) 4755–4771.

[12] Systea S.p.A Analytical Technologies, WIZ Portable In-situ Probe For Water Analysis http://www.systea.it/index.php?option=com_k2&view=item&id=383:wiz-news&lang=en, 2015 (accessed 13 October 2018).

[13] s::can Messtechnik GmbH, spectro::lyser spectrometer probe https://www.s- can.at/products/spectrometer-probes, 2018 (accessed 13 October 2018).

[14] Sea Bird Scientific, SUNA V2 Nitrate Sensor https://www.seabird.com/nutrient-sensors/suna-v2-nitrate-sensor/family?productCategoryId=54627869922, 2018 (accessed 13 October 2018).

[15] M. Macka, T. Piasecki, P.K. Dasgupta, Light-emitting diodes for analytical chemistry, Annu. Rev. Anal. Chem. 7 (2014) 183-207.

[16] C.M. McGraw, S.E. Stitzel, J. Cleary, C. Slater, D. Diamond, Autonomous microfluidic system for phosphate detection, Talanta 71 (2007) 1180–1185.

[17] M. Sequeira, M. Bowden, E. Minogue, D. Diamond, Towards autonomous environmental monitoring systems, Talanta 56 (2002) 355–363.

[18] S. Schmid, M. Macka, P.C. Hauser, UV-absorbance detector for HPLC based on a light-emitting diode, Analyst 133 (2008) 465-469.

[19] D.A. Bui, B. Bomastyk, P.C. Hauser, Absorbance detector based on a deep UV light emitting diode for narrow-column HPLC, J. Sep. Sci 36 (2013), 3152-3157.

[20] L. Krčmová, A. Stjernlof, S. Mehlen, P.C. Hauser, S. Abele, B. Paull, M. Macka, Deep-UV-LEDs in photometric detection: A 255 nm LED on-capillary detector in capillary electrophoresis, Analyst 134 (2009), 2394–2396.

[21] Y. Li., P. N. Nesterenko, R. Stanley, B. Paull, M. Macka, High sensitivity deep-UV LED-based z-cell photometric detector for capillary liquid chromatography, Anal. Chim. Acta 1032 (2018) 197-202.

[22] E. Murray, Y. Li, S.A. Currivan, B. Moore, A. Morrin, D. Diamond, M. Macka, B. Paull, Miniaturized capillary ion chromatograph with UV light-emitting diode based indirect absorbance detection for anion analysis in potable and environmental waters, J. Sep. Sci. 16 (2018) 3224-3231.

[23] J. Mack, J.R. Bolton, Photochemistry of nitrite and nitrate in aqueous solution: a review, J. Photochem. Photobiol. A 128 (1999) 1–13.

[24] Y. Li., P. N. Nesterenko, B. Paull, R. Stanley, M. Macka, Performance of a new 235 nm UV LED based on-capillary photometric detector, Anal. Chem. 88 (2016) 12116–12121.

[25] M.S Shur, R. Gaska, Deep-Ultraviolet Light-Emitting Diodes, IEEE Trans. Electron Devices 57 (2010), 12–25.

[26] J.F.S. Petruci, M.G. Liebetanz, A.A. Cardoso, P.C. Hauser, Absorbance detector for high performance liquid chromatography based on a deep-UV light-emitting diode at 235 nm, J. Chromatogr. A 1512 (2017) 143-146.

[27] I.R.G. Ogilvie, V.J. Sieben, C.F. Floquet, R. Zmijan, M.C Mowlem, H. Morgan, Reduction of surface roughness for optical quality microfluidic devices in PMMA and COC, J. Micromech. Microeng. 20 (2010) 065016.

[28] A. Donohoe, G. Lacour, P. McCluskey, D. Diamond, M. McCaul, Development of a Cost-Effective Sensing Platform for Monitoring Phosphate in Natural Waters, Chemosensors 6 (2018) 57.

[29] M. Macka, P. Andersson, P.R. Haddad, Linearity evaluation in absorbance detection: the use of light-emitting diodes for on-capillary detection in capillary electrophoresis, Electrophoresis 17 (1996) 1898-1905.

[30] C. Johns, M. Macka, P.R. Haddad, M. King, B. Paull, Practical method for evaluation of linearity and effective pathlength of on-capillary photometric detectors in capillary electrophoresis, J. Chromatogr. A 927 (2001) 237-241.

[31] Agilent Technologies, Incorporated, High Sensitivity Detection Cell https://www.agilent.com/en/products/capillary-electrophoresis-ce-ms/ce-ce-ms-supplies/tools-kits-standards/high-sensitivity-detection-cell#productdetails, 2019 (accessed 03 January 2019).

[32] S. Sharma, D. Tolley, P.B. Farnsworth, M.L. Lee, LED-Based UV Absorption Detector with Low Detection Limits for Capillary Liquid Chromatography, Anal. Chem. 87 (2015) 1381−1386.

[33] K.R. Elkin, Portable, fully autonomous, ion chromatography system for on-site analyses, J. Chromatogr. A 1352 (2014) 38-45.

[34] Dionex Thermo Scientific, Determination of nitrite and nitrate in drinking water using ion chromatography with direct UV detection https://assets.thermofisher.com/TFS-Assets/CMD/Application-Notes/4189-AU132_Apr91_LPN034527.pdf, 1991 (accessed 12 November 2018).

[35] P. Jackson, Determination of Inorganic Anions in Drinking Water by Ion Chromatography https://assets.thermofisher.com/TFS-Assets/CMD/Application-Notes/AN-133-IC-Inorganic-Anions-Drinking-Water-AN71691-EN.pdf, 2015 (accessed 15 April 2019).

[36] S.N. Ronkart, Quantification of Trace and Major Anions in Water by Ion Chromatography in a High-Throughput Laboratory https://assets.thermofisher.com/TFS-Assets/CMD/Application-Notes/CAN-114-High-Throughput-IC-Anions-Bromate-LPN3023-EN.pdf, 2012 (accessed 14 April 2019).

[37] Thorlabs, Incorporated, Stabilized Deuterium UV Light Source https://www.thorlabs.com/newgrouppage9.cfm?objectgroup_id=11783&pn=SLS204, 2019 (accessed 05 January 2019).

Chapter 5:

Integrated 3D printed heaters for microfluidic applications: ammonium analysis within environmental water

Elisenda Fornells [1, 2*], Eoin Murray [3, 4*], Sidra Waheed [1], Aoife Morrin [4], Dermot Diamond [4], Brett Paull [1, 2], Michael Breadmore [1, 2]

1. ARC Training Centre for Portable Analytical Separation Technologies (ASTech), School of Physical Sciences, University of Tasmania, Sandy Bay, Hobart 7001, Australia
2. Australian Centre for Research on Separation Science (ACROSS), School of Physical Sciences, University of Tasmania, Sandy Bay, Hobart 7001, Australia
3. Research & Development, T.E. Laboratories Ltd. (TelLab), Tullow, Carlow, Ireland
4. Insight Centre for Data Analytics, National Centre for Sensor Research, School of Chemical Sciences, Dublin City University, Dublin 9, Ireland

* Both authors contributed equally to this work.

Publication: Analytica Chimica Acta, 2019

Chapter Overview

This chapter is aimed at generating a fast ammonium analysis method which could potentially be integrated with the direct UV detection method for nitrate and nitrite set out in Chapter 4. By working towards such a combination of methods, a portable and low-cost total nitrogen analysis system could potentially be developed. A 3D printed microfluidic heated reactor was designed and fabricated using a variety of printing materials including a new diamond infilled polymer. Using this reactor along with a colorimetric procedure for ammonium analysis and LED-based optical detection, fast determination of ammonium in water using a simple FIA set up is described.

Abstract

A multi-material 3D printed microfluidic reactor with integrated heating is presented, which was applied within a manifold for the colorimetric determination of ammonium in natural waters. Graphene doped polymer was used to provide localised heating when connected to a power source, achieving temperatures of up to 120°C at 12 V, 0.7 A. An electrically insulating layer of Acrylonitrile butadiene styrene (ABS) polymer or a new microdiamond-ABS polymer composite was used as a heater coating. The microdiamond polymer composite provided higher thermal conductivity and uniform heating of the serpentine microreactor which resulted in greater temperature control and accuracy in comparison to pure ABS polymer. The developed heater was then applied and demonstrated using a modified Berthelot reaction for ammonium analysis, in which the microreactor was configured at a predetermined optimised temperature. A 5-fold increase in reaction speed was observed compared to previously reported reaction rates. A simple flow injection analysis set up, comprising the microfluidic heater along with an LED-photodiode based optical detector, was assembled for ammonium analysis. Two river water samples and two blind ammonium standards were analysed and estimated concentrations were compared to concentrations determined using benchtop IC. The highest relative error observed following the analysis of the environmental samples was 11 % and for the blind standards was 5 %.

5.1. Introduction

The development of microfluidic devices demands the integration of numerous functions within a compact platform, among them temperature control. Constant temperature is of key importance in order to obtain efficient and robust operation of microfluidic devices, as reaction kinetics, and therefore reproducibility of reaction chemistry within the fluidic chip, are dependent on temperature. Some well-known chemical and biological applications frequently employed within deployable and microfluidic systems, in which temperature control is essential, are DNA amplification by polymerase chain reaction (PCR) [1,2], protein crystallization [3], membrane permeability studies [4] and colorimetric reactions and analysis [5,6].

Efficient micro-reactors transfer heat homogenously to the fluid contained within the reactor based upon large surface area to volume ratios, while simultaneously mixing reagents and providing optimal reaction conditions [7]. Integration of temperature control functionality within the compact platform is required to fully optimise their performance. A number of strategies to integrate precision heating and cooling capability within such micro-reactors have been presented and comprehensively reviewed [8], including the integration of micro-Peltier components [9], the application of Joule heating [10,11], the use of microwaves [12,13] and lasers [14].

Rapid prototyping strategies such as 3D printing, or additive manufacturing, represent a versatile and cost-effective approach towards the fabrication of microdevices and prototype devices. Among all of the 3D printing technologies, fused deposition modelling (FDM) is the most common technology currently applied, mainly due to its simplicity, cost, and the availability of a wide variety of base print materials, along with the option of multi-material printing [15]. In multi-material FDM various thermoplastic materials are alternately extruded through a high temperature nozzle to build the 3D model layer-by-layer [16]. To achieve an improved integration of functionalities, such as electronic components into microreactors, either multi-material 3D printing or a print-pause-print (PpP) approach can be used. PpP refers to pausing the printing to insert additional parts which are embedded in the device when printing resumes

[17]. Examples of microchemical devices manufactured using either functionalised polymeric filaments and/or embedded components include membranes, electrodes and integrated reagents [18, 19, 20], among many others. As a consequence of these multiple advantages, 3D printing is a potentially useful tool for manufacturing microfluidic and micro analytical devices. However, before the technique can be firmly adopted, a number of challenges need to be addressed [21]. One of the main challenges is that 3D printing systems rely on a relatively narrow range of commercial materials, thus limiting the physical and chemical properties of final 3D printed objects [22]. Accordingly, there has been increasing interest in the improvement and diversification of properties of generic printing materials by inclusion of micro/nano fillers with particular focus on generating distinct physio-chemical properties into resultant 3D printable material [23]. An example of which are carbon polymer composites, using carbon nanotubes (CNT) [24], carbon blacks [25, 26], or graphene [27, 28], which have allowed for the creation of devices with improved electrical conductivity, electromechanical/chemical sensitivity and mechanical strength [29]. In relation to heating devices, the first reported 3D printed heaters were manufactured using viscous graphene oxide to fabricate nanostructures, which were then subject to freeze-drying and thermal treatment [11] before Joule heating was induced. Of the various carbonaceous fillers available, synthetic high temperature and high pressure (HTHP) micro-diamond possesses several attractive features, especially with regard to printable heating devices [30, 31]. These include thermal stability and conductivity, electrical insulation and the low-cost nature of the material. [32, 33]. Recently the production of 3D print compatible HTHP-ABS composite fibres have been reported and characterised for their unique post-print thermal properties [34].

The capabilities enabled through the use of 3D printing have facilitated the development of portable analytical systems across a broad range of applications within analytical chemistry [35-38]. Of these applications, considerable focus has been directed towards environmental water monitoring, and several *in-situ* water analysers have been developed through the use of rapid prototyping techniques [39-41]. When considering the monitoring of natural waters, the levels of specific chemicals within various waters must be monitored according

to global legislation, key examples being the EU Water Framework Directive (WFD) and the U.S Clean Water Act (CWA). Ammonia is one of several forms of nitrogen found in environmental waters, and represents an important pollutant which must be monitored within water systems due to the toxic effect it has on aquatic life. A range of analytical approaches and methodologies exist for the analysis of ammonia in water such as ammonium-selective electrodes, titrimetry, fluorimetry and ion chromatography (IC) [42-46]. Colorimetry in the form of the Berthelot and Nessler methods are common methods, frequently used in environmental laboratories [47, 48]. When considering portable *in-situ* analysis systems for ammonia monitoring, ion-selective electrodes (ISE) are commonly employed [49]. ISEs are relatively easy to use and not particularly expensive, but often experience high drift, ionic interferences and can be significantly affected by biofouling in continuous monitoring as they are directly exposed to the sample during use [50]. As an alternative, wet chemical colorimetry has also been applied within automated analysers for ammonia detection [51].

In this work we describe the development of a multi-material 3D printed microfluidic heated reactor, and demonstrate this reactor by integrating it with a simple flow injection analysis (FIA) system for fast ammonium determination in water using a modified (less toxic) Berthelot reaction, previously described by Cogan *et al.* [52]. The use of the salicylate variant of the Berthelot method has been applied for ammonium analysis in a range of water samples in the past and the reaction mechanism is well established [53, 54, 52]. Within a NaOH medium, ammonium ions react with the Berthelot reagents, in which salicylate is present, producing a green colour solution which absorbs strongly at 660 nm. In order to integrate the heating platform into the microfluidic device, multi-material printing was employed. A graphene filled polymeric surface was printed in close contact to the microfluidic printed channel, but remained electrically isolated. Joule heating was then induced to generate homogeneous heating at temperatures below the polymers melting point. To increase heat transfer and temperature homogeneity, a thermally conductive diamond composite material was employed. The thermal characteristics of the 3D printed heater along with mixing within the chip were assessed. The impact of the temperature of the heated mixing cell on the rate of reaction for the colorimetric method was

examined and optimum temperature for analysis was selected. The analytical performance of the simple FIA configuration coupled with the 3D printed heating cell for the analysis of ammonium was established. Two environmental water samples and two blind standards were analysed using the system and the results compared to those determined using IC.

5.2. Experimental

5.2.1. Chemicals and Reagents

Chemicals used within this work were of analytical or higher grade. All solutions and dilutions were prepared using high-purity deionised water (Milli-Q). Colorimetric reagents were made according to the procedure highlighted in Cogan *et al.* [52]. Sodium salicylate, sodium nitroprusside and sodium hydroxide used to prepare reagent 1 (R1), along with sodium hypochlorite (10-15 % available chlorine) used within reagent 2 (R2) were obtained from Sigma-Aldrich (St. Louis, MO). Ammonium stock solution was prepared using ammonium chloride (Sigma-Aldrich, St. Louis, MO). Working standard solutions were prepared through dilution of the ammonium stock. Samples were taken from two urban rivulets (Hobart, Tasmania), approx. 600 m upstream from their mouth. They were filtered through a 0.22 µm nylon syringe filter to remove particles and were analysed using both the FIA and IC methods. IC analysis was performed using a Dionex IonPac CS16 3.0 x 250 mm column and 3.0 x 50 mm guard column. The mobile phase was 35 mM methanesulfonic acid at 0.50 mL/min and a sample injection volume of 75 µL was used.

5.2.2. Heating chip design and printing

Heating devices were produced using various 3D printing filaments. The electrically conductive material used was a graphene PLA (polylactic acid) based filament (Black Magic 3D Calverton, NY USA), which has a reported volume resistivity of 0.6 Ohm cm^{-1}. The electrically insulating materials were either clear ABS (acrylonitrile butadiene styrene) (Auraurum, Keysborough VIC, Australia), or a diamond-ABS (D-ABS) composite. Extruding temperatures were set to 215, 255 and 255 °C for PLA, ABS and D-ABS respectively. D-ABS filament was manufactured on site according to the procedure set out by Waheed *et al.* [34].

An Original Prusa i3 3D printer equipped with MK2/S Multi Material kit was used to print PLA and ABS filaments. A 2 nozzle Felix 3D printer was used to print D-ABS, equipped with titanium alloy corrugated gears to avoid abrasion when driving the filament into the nozzle. In all cases, the base layer was 200 μm thick and subsequent layers were 150 μm thick. Copper tape was used to integrate electrodes and devices were designed using SolidWorks software. A 0-30 V, 2.5 A regulated power supply with variable current limit was used for heating of the cell. A FLIR E40 thermal imaging camera was used to measure chip temperatures and was connected to FLIR Tools software for data recording purposes. A XH-W1601 PID temperature control module was used to regulate temperature in the heating device.

5.2.3. System configuration and measurement procedures

Mixing within the 3D printed chips was assessed by observing dye mixing at the channel inlet using a DinoLite microscope. For ammonium determination, a 3-channel syringe pump configuration using automated syringe pumps (Harvard Apparatus PHD 2000) with standard 5 mL luer lock syringes was assembled. Under FIA conditions, 2 syringes were used for reagent delivery, while the third syringe contained DI water as a carrier. A delivery ratio of 1:1:2, reagent 1 (R1), reagent 2 (R2) and carrier was used. Sample injection was enabled using a 6 port 2-position micro-injection valve from VICI AG (Schenkon, Switzerland). The FIA system is illustrated in Figure 5.1. R1 and R2 merged into one channel before being combined with the carrier phase. The combined reaction media was then introduced into the 3D printed heated reactor and subsequently into a custom-built optical detection cell, previously reported by Murray *et al.* [55] for UV-LED based optical detection. In this case, a 660 nm LED (L-53SRC-C) and photodiode (TSL257), obtained from RS components (Dublin, Ireland), were fitted within the 3D printed holders and inserted into the detector housing. The detector was then placed within a small box to prevent ambient light from having an effect on photodiode readings. Data acquisition and LED operation were achieved using the previously reported electronic prototype board [55].

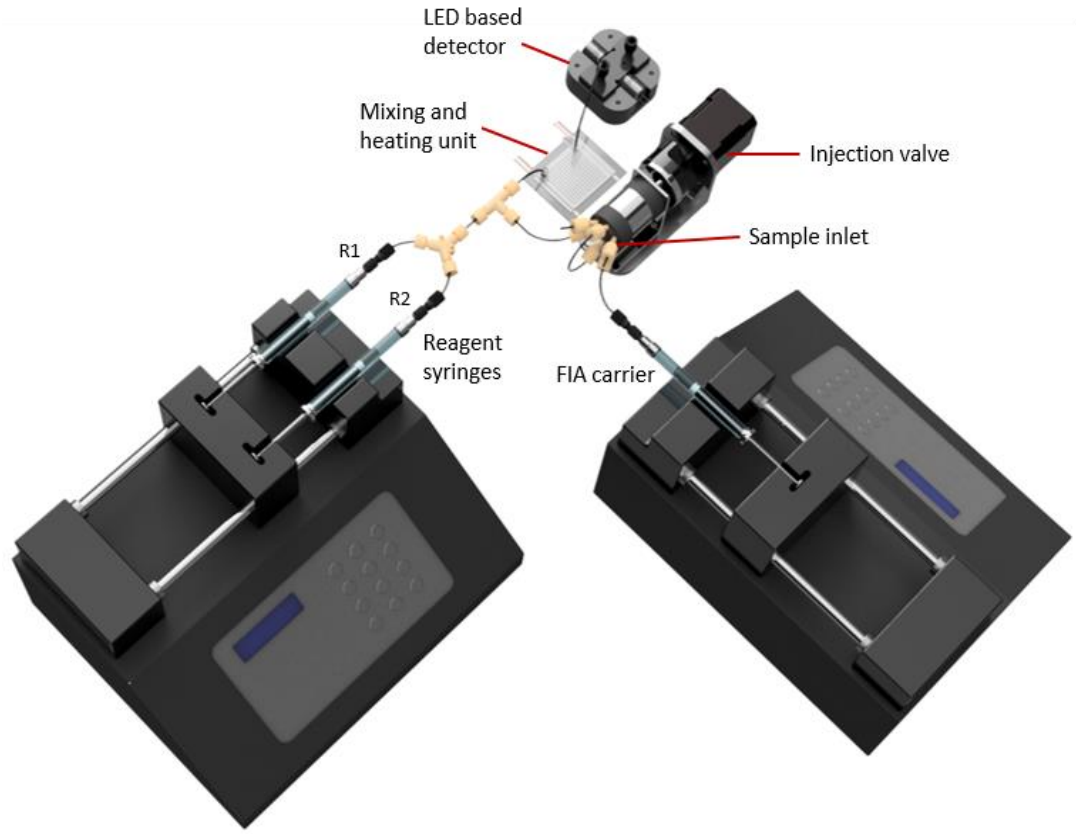

Figure 5.1: Illustration of flow injection analysis system incorporating the 3D printed heated mixing cell and the LED-based optical detector employing a 660 nm LED. The simplified Berthelot method which employs two reagents was utilised. Reagent 1 was comprised of sodium salicylate and sodium nitroprusside, while reagent 2 was a sodium hypochlorite-based solution.

5.2.4. Thermal study for ammonium analysis

The effect of the increasing temperature of the 3D printed mixing cell on ammonium detection using the simplified Berthelot method was studied under continuous flow conditions. Reagent syringe pump 1 was filled with R1 reagent, syringe pump 2 was filled with R2 reagent and the third syringe pump was filled with a 5 mg L^{-1} NH_4^+ standard prepared from ammonium chloride stock solution. A range of reaction times were assessed by changing the flow rate to 160, 120, 60 and 24 µL min^{-1} which corresponded to reaction times of 1.2, 1.6, 3.3 and 8.0 min, respectively. The mixing cell was set at various temperatures ranging from room temperature to 60 °C and the effect on analyte detection was assessed.

5.3. Results and Discussions

5.3.1. Heater fabrication and thermal characterisation

The manufacturing process (Figure 5.2) for the 3D printed heating cell consisted of printing a single material base layer of insulating material followed by multi-material layers where the geometry of the heating zone was defined using graphene PLA. ABS was used as insulating material, as well D-ABS tested as the thermally conductive polymer. D-ABS is a microdiamond infilled ABS polymer recently reported in literature [37], showing improved thermal conductivity from 0.17 to 0.37 W./m.K, for a 37.5% (wt) diamond-ABS composite. To integrate the electrodes, a 2 mm wide slot was created within the bottom layer, the printing process was then paused and copper tape strips were manually placed into the slots. When resuming printing on top of the copper tape electrodes, the graphene PLA material was printed horizontally from electrode to electrode. Finally, ABS/D-ABS was used to cover the electric circuit leaving part of the electrodes exposed. The heating cell was designed to have a minimal insulating (ABS/D-ABS) layer to protect the electric circuit, while providing maximum proximity between the heating source and the object being heated. The total thickness of graphene filled material was 750 μm, accounting for a total of 5 layers, while the electrodes were placed midway at 300 μm.

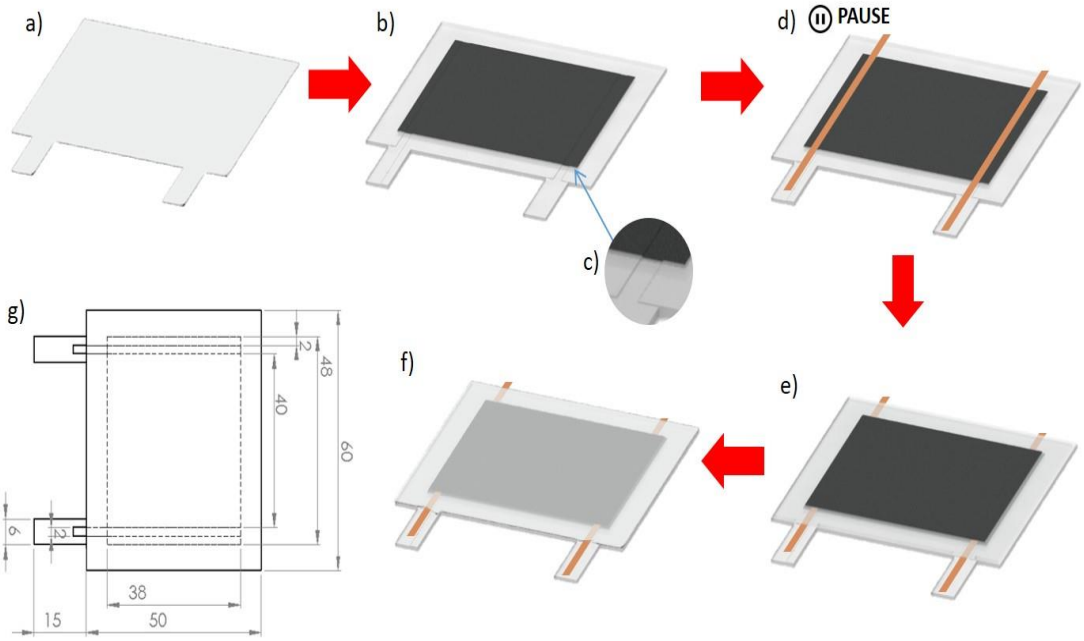

Figure 5.2: Multimaterial FDM step-by-step fabrication process of 3D printed heater. a) Deposition of a base layer of electrically insulating material (ABS based). b) Printing of 3 layers of electrically conductive material creating a 150 µm deep slot (c). d) Positioning of copper tape 2 mm wide electrodes on the existing slots after pausing the printing process. e) Coverage of the electrodes with electrically conductive material in the heating zone. f) Coverage of the electric circuit and heater with electrically insulating material (ABS based). g) Design and sizes (mm) of the heating device.

Heat was generated when voltage was applied between the two electrodes and current distributed evenly throughout the graphene filled layer. The temperature on the ABS surface was measured in real time with an infrared camera. Higher temperatures were associated with increased voltages, as expected. Figure 5.3A shows a photograph of heaters printed within ABS (left) and D-ABS (right). To compare the performance of ABS and D-ABS heating devices, the temperature was monitored for a period of 10 minutes at several voltages. A period of 10 minutes was selected for assessment as temperatures stabilised at 10 minutes. The average temperature as well as minimum and maximum temperatures were recorded in the centre of the heating square, excluding the electrodes. The area was defined in the software as shown in the thermal image Figure 5.3B. In addition, the maximum temperature observed within the image was also monitored corresponding to the electrode hotspot, labelled as a cross in Figure 5.3B. The data were plotted in Figure 5.3C and show the measured temperatures

for heaters using ABS (left column) and D-ABS (right column). ABS heaters showed a consistent hotspot throughout the analysis. However, when using the D-ABS device, the hotspot dissipated in approximately 2 minutes. The hotspot was up to 10 °C hotter than the maximum temperature in the central square of the thermal image for ABS. In the case of D-ABS, overheating was practically halved, meaning the difference between the hotspot and the maximum temperature in the heating zone was reduced by a factor of 1.89 ± 0.04, averaging results at the 4 tested voltages. D-ABS presented more stable heating and lower temperature gradients in terms of the difference between maximum and minimum temperatures in the heating zone. Such difference was statistically insignificant at 5V, but between 8 and 12 V the temperature gradient was nearly 5 °C lower.

The average temperatures of the heating zones of the heaters, recorded at 10 min as temperatures reached stabilisation at this time, increased linearly with increasing voltage (5 – 12 V) for both ABS and D-ABS heaters. Similar slopes of 10.06 and 11.51 and an R^2 of 0.990 and 0.998 were observed for ABS and D-ABS heaters, respectively, as shown in Figure D1 of the electronic supplementary information (ESI). Measured current ranged between 0.3 A at 5 V and 0.7 A at 12 V. The average temperature at a voltage of 12 V stabilized at 120 °C, with higher voltages leading to melting of the PLA based material and a decrease in current and temperature over the 10-minute period. PID control (proportional-integral-derivative) was utilised to maintain consistent heating at a targeted set temperature. This was achieved by attaching a thermocouple below the heater and using a PID stand-alone microcontroller which switched the 12 V power supply so as to maintain the set temperature. A Temperature vs. Voltage plot is shown in Figure D2 of the ESI, where it can be observed that the temperature is stabilised after 5 minutes.

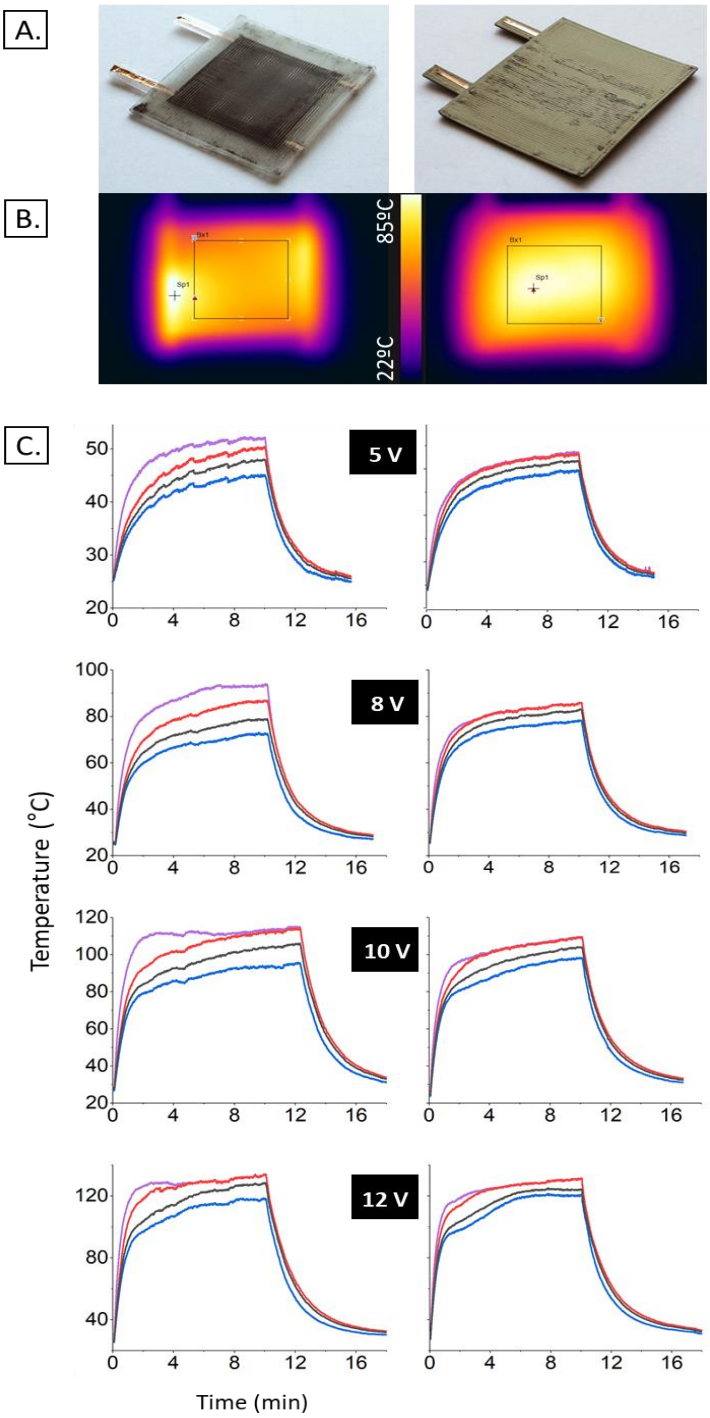

Figure 5.3: (A) Photograph of heaters printed within ABS (left) and D-ABS (right). (B) Thermal image of heating for 5 min at 8 V, showing the defined central heating area (square) and the whole image maximum temperature spot or hotspot (cross). Using D-ABS the hotspot is recorded inside the central square. Scale bar between 22 and 85 °C. (C) Temperatures measured at several voltages using ABS embedded heater (left column) and D-ABS embedded heater (right column). Colours correspond to the electrode hotspot (purple) and to temperatures in the central heating square corresponding to the coldest point (blue), average temperature (black) and hottest point (red).

5.3.2. Assessment of mixing on chip

The fluidic channels were printed on top of the 3D printed heaters, through the use of the heaters the temperature in the channels within the microfluidic platform could be controlled. The channels could be printed up to one printing layer, or 150 μm, from the heating source. In this study, channels were placed two printed layers (i.e. 300 μm) from the graphene material to ensure a robust leak free system was produced. The design and configuration of the fluidic platform is shown in Figure 5.4. Due to the polymer hardening process, shrinking of the channels occurs. To study this effect, several channel cross sections were obtained under the microscope and their sizes measured (Figure 5.4C). The average width and depth were calculated at 576 ± 16 μm and 254 ± 21 μm (n=6). Mixing in the channel inlet was then assessed at different flow rates, which were employed to provide different residence times inside the device. To maximise mixing, the printing orientation of the channel base and cover layers were set at a 45° angle as suggested in literature [56]. To assess mixing, blue and yellow dyes were used in place of reagents and carrier, and mixing was observed under a microscope. Images of the device inlet during this mixing study were captured and are demonstrated in Figure D3 of the ESI. During this study, the mixing of the blue and yellow dyes to generate a green colour was observed. At a flow rate of 160 μL min^{-1}, blue and yellow colours are visible at the beginning of the channel and after 10 mm the dyes begin to merge into a green colour. At slower flowrates, the blue and yellow dyes mix into a green colour in a shorter distance along the fluidic channel. The mixing was deemed satisfactory to proceed with the temperature study at several reaction times.

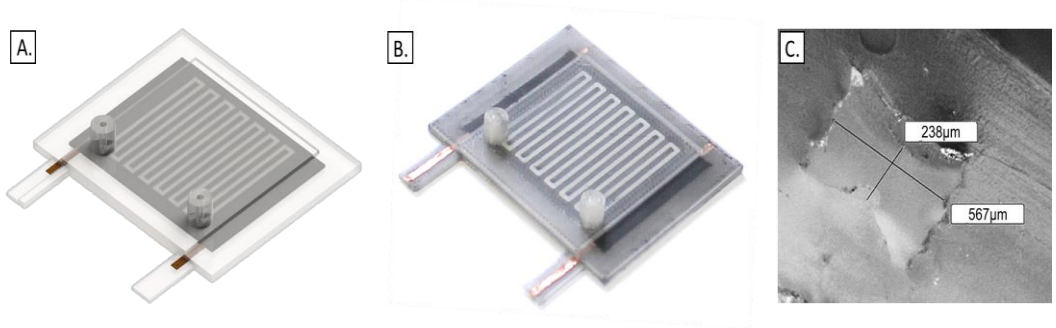

Figure 5.4: (A.) CAD design of 3D printed heater with serpentine mixing. (B.) Photograph of 3D printed heater (C.) Microscope photograph of microfluidic channel at inlet of mixing chip, highlighting channel cross section and sizes.

5.3.3. Temperature study with simplified Berthelot method

Continuous flow conditions were used for this assessment. Absorbance values resulting from increasing temperatures at varying reaction rates are plotted in Figure 5.5. At room temperature, higher absorbance values were observed at longer reaction times which is in agreement with Cogan *et al.* [52]. At higher temperatures, absorbance also increased until a steady-state condition was established. At lower temperatures, longer reaction times were required to reach the maximum absorbance, however a reaction time of 1.2 min was not long enough for the reaction to reach maximum absorbance at the highest tested temperature of 60 °C. The selected optimum conditions were deemed to be at 60 °C and a reaction time of just 1.6 min (flow rate of 120 µL min^{-1}). These conditions allowed for a complete reaction, where the maximum absorbance was obtained at the fastest possible time. This was significantly faster compared to the 8-minute reaction time reported previously [52].

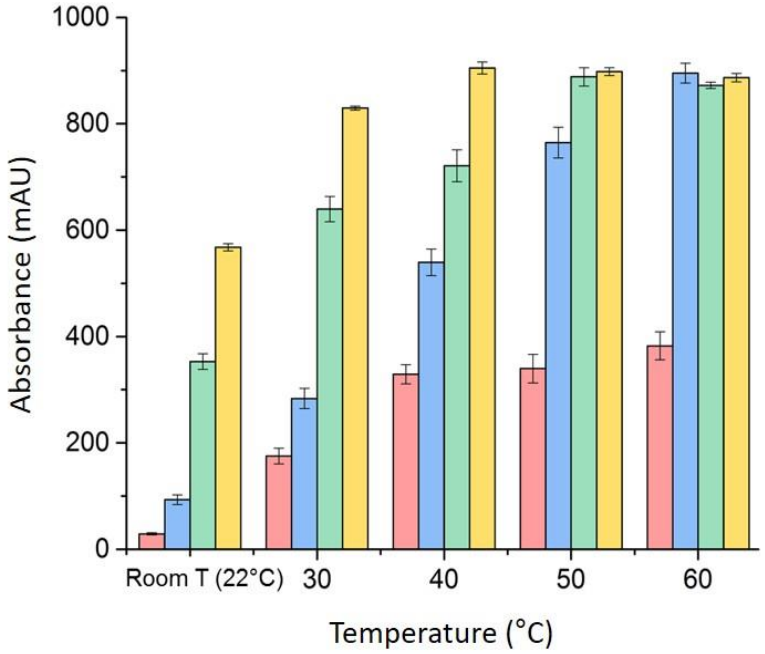

Figure 5.5: Absorbance values obtained using modified Berthelot reaction for a 5 mg L^{-1} NH_4^+ standard after different reaction times of 1.2 (pink), 1.6 (blue), 3.3 (green) and 8 (yellow) minutes. Experimentation was carried out at increasing temperatures.

5.3.4. Sample Analysis

Using the optimised conditions determined above, FIA analysis of ammonium standards and water samples was carried out. Firstly, calibration was performed between 0.5 and 5 mg L^{-1} NH_4^+. The FIA response curves obtained for each of the ammonium standards are overlaid and illustrated in Figure 5.6. Acceptable linearity was obtained with a R^2 value of 0.996, while a limit of detection (LOD) of 0.15 mg L^{-1} NH_4^+ was calculated using a signal-noise-ratio (S/N) = 3. The linear curve of peak area versus concentration is provided within the supplementary information (Figure D4). Two waters samples from local rivulets were then analysed. As a comparison, these samples were also analysed using IC. In addition, two blind ammonium standards were analysed using the FIA set up. Concentrations observed following sample analysis with standard deviations (n=3) and relative concentrations are shown in Table 5.1. The ion chromatogram which was generated is shown in the supplementary information (Figure D5). For environmental sample 1, a difference of ~11% between the two methods was observed, while for environmental sample 2, an 8.5 % difference was recorded. Analysis of blind standard A (5 mg L^{-1} NH_4^+) yielded a concentration of 4.74 mg L^{-1} and for blind standard B (1 mg L^{-1} NH_4^+) a concentration of 0.96 mg L^{-1} was obtained, which corresponded to recoveries of 95 % and 96 %, respectively. Given the simple, low-cost and fast ammonium determination achieved using the FIA system with 3D printed heater, the results of the above comparison with IC were deemed acceptable.

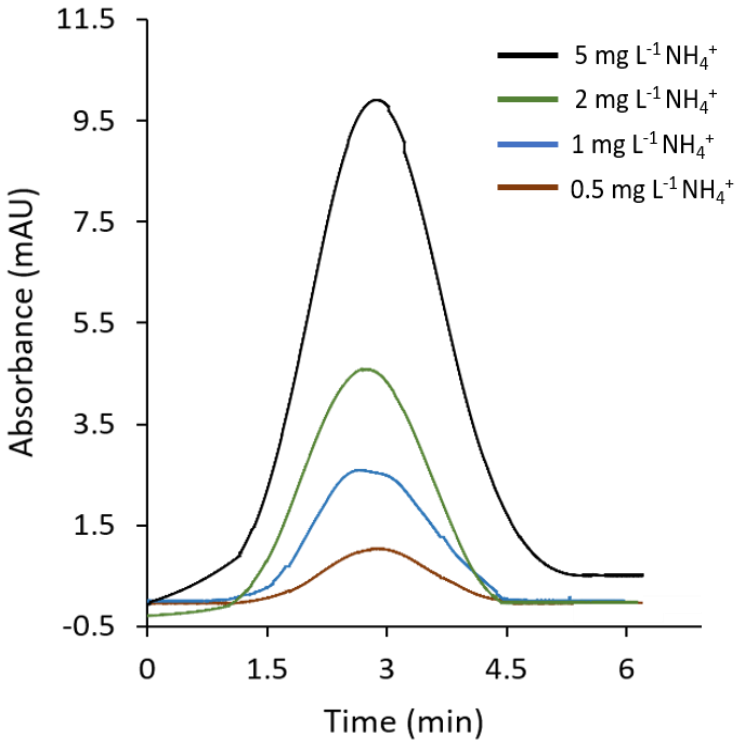

Figure 5.6: Overlaid FIA response curves observed following the analysis of standard solutions containing 0.5, 1, 2 and 5 mg L^{-1} NH_4^+ Using the simple FIA configuration and 3D printed heater. Conditions: Total flowrate of 120 µL min^{-1}, heater set at 60 °C and a sample injection volume of 100 µL.

Table 5.1 Ammonium concentrations determined using the FIA configuration in comparison to concentrations determined using benchtop IC (n=3)

Sample	FIA (NH_4^+ mg L^{-1})	IC (NH_4^+ mg L^{-1})	Relative Error (%)
Environmental 1	1.754 ± 0.232	1.579 ± 0.026	11.08
Environmental 2	0.547 ± 0.178	0.504 ± 0.009	8.53
Standard A*	4.740 ± 0.196	-	-5.02
Standard B*	0.959 ± 0.221	-	4.1

*Ammonium concentration in standard A was 5 mg L^{-1} NH_4^+, standard B was 1 mg L^{-1} NH_4^+

5.4. Conclusion

A multi-material 3D printed microfluidic reactor was developed and demonstrated when integrated into a simple FIA configuration for the determination of ammonium using a modified Berthelot reaction. FDM printing was used to construct the reactor using several thermoplastic materials, including a new diamond infilled ABS material. Graphene was used as the thermally conductive material within the heating cell and Joule heating was employed to achieve homogeneous heating across the heating cell. The reactors demonstrated effective heating along with satisfactory mixing within the 3D printed microfluidic channels. When integrated with a less-toxic, simplified Berthelot reaction for ammonium analysis, increasing temperature of the reactor was found to increase the rate of reaction. Using the heated mixing cell, the required reaction time for reaction completion was 5 times faster than the previous reported approach. Using an FIA configuration coupled with the 3D printed heating cell for ammonium analysis, an analytical range applicable to ammonium levels in natural waters was determined.

The developed heated microreactor may be used in a variety of colorimetric assays, and can be seen as a convenient tool for microreactions in which controlled heating is desirable. The temperature control apparatus is cost-effective and is easy to modify and implement within a microfluidic system. Future work will investigate the lifetime of the heater and the possibility of leaching from the polymeric materials into the reaction media at high temperatures and the impact this may have, if any.

5.5 Acknowledgements

The authors thank Bahador Dastorian Jamnani and Dr. Petr Smejkal for their support when operating various 3D printing systems. The authors would like to acknowledge financial support from the Irish Research Council, Grant No. EBPPG/2015/127, the Australia Awards - Endeavour Research Fellowship, Grant No. 6389_2018, the Australian Research Council (FT130100101) and Science Foundation Ireland through the INSIGHT Centre (grant number SFI/12/RC/2289).

5.6 References

[1] L. Cao, X. Cui, J. Hu, Z. Li, J.R. Choi, Q. Yang, M. Lin, L. Ying Hui, F. Xu, Advances in digital polymerase chain reaction (dPCR) and its emerging biomedical applications, Biosens. Bioelectron. 90 (2017) 459–474.

[2] N. Bae, S. Lim, Y. Song, S. Jeong, S. Shin, Y. Kim, T. Lee, K. Lee, S. Lee, Y.-J. Oh, Y. Park, N.H. Bae, S.Y. Lim, Y. Song, S.W. Jeong, S.Y. Shin, Y.T. Kim, T.J. Lee, K.G. Lee, S.J. Lee, Y.-J. Oh, Y.M. Park, A Disposable and Multi-Chamber Film-Based PCR Chip for Detection of Foodborne Pathogen, Sensors. 18 (2018) 3158.

[3] P. Laval, N. Lisai, J.B. Salmon, M. Joanicot, A microfluidic device based on droplet storage for screening solubility diagrams, Lab Chip, 7 (2007) 829–834.

[4] J. Peng, C. Fang, S. Ren, J. Pan, Y. Jia, Z. Shu, D. Gao, Development of a microfluidic device with precise on-chip temperature control by integrated cooling and heating components for single cell-based analysis, Int. J. Heat Mass Transf., 130 (2019) 660–667.

[5] K. Muramatsu, Direct Colorimetric Method for the Determination of Free Ammonia in Blood, Agr. Biol. Chem., 31 (1967) 301-308.

[6] W.T. Bolleter, C.J. Bushman, P.W. Tidwell, Spectrophotometric Determination of Ammonia as Indophenol, Anal. Chem., 33 (1961) 592–594.

[7] K.S. Elvira, X.C. I Solvas, R.C.R. Wootton, A.J. Demello, The past, present and potential for microfluidic reactor technology in chemical synthesis, Nat. Chem., 5 (2013) 905–915.

[8] V. Miralles, A. Huerre, F. Malloggi, M.-C. Jullien, A Review of Heating and Temperature Control in Microfluidic Systems: Techniques and Applications, Diagnostics. 3 (2013) 33–67.

[9] G. Maltezos, M. Johnston, A. Scherer, Thermal management in microfluidics using micro-Peltier junctions, Appl. Phys. Lett., 87 (2005) 154105.

[10] C. Fang, D. Lee, B. Stober, G.G. Fuller, A.Q. Shen, Integrated microfluidic platform for instantaneous flow and localized temperature control, RSC Adv. 5 (2015) 85620–85629.

[11] Y. Yao, K.K. Fu, C. Yan, J. Dai, Y. Chen, Y. Wang, B. Zhang, E. Hitz, L. Hu, Three-Dimensional Printable High-Temperature and High-Rate Heaters, ACS Nano., 10 (2016) 5272–5279.

[12] A.J.L. Morgan, J. Naylon, S. Gooding, C. John, O. Squires, J. Lees, D.A. Barrow, A. Porch, Efficient microwave heating of microfluidic systems, Sensors Actuators B Chem. 181 (2013) 904–909.

[13] T. Markovic, J. Bao, I. Ocket, D. Kil, L. Brancato, R. Puers, B. Nauwelaers, Uniplanar microwave heater for digital microfluidics, in: 2017 First IEEE MTT-S Int. Microw. Bio Conf., IEEE, 2017: pp. 1–4.

[14] T. Walsh, J. Lee, K. Park, Laser-assisted photothermal heating of a plasmonic nanoparticle-suspended droplet in a microchannel, Analyst, 140 (2015) 1535–1542.

[15] T.D. Ngo, A. Kashani, G. Imbalzano, K.T. Nguyen, D. Hui, Additive manufacturing (3D printing): A review of materials, methods, applications and challenges, Compos. Part-B Eng. 143 (2018) 172-196.

[16] S. Waheed, J.M. Cabot, N.P. Macdonald, T. Lewis, R.M. Guijt, B. Paull, M.C. Breadmore, 3D printed microfluidic devices: Enablers and barriers, Lab Chip. 16 (2016) 1993–2013.

[17] J.Y. Lee, J. An, C.K. Chua, Fundamentals and applications of 3D printing for novel materials. Appl. Mater. Today, 7 (2017) 120-133.

[18] C.W. Pinger, A.A. Heller, D.M. Spence, A Printed Equilibrium Dialysis Device with Integrated Membranes for Improved Binding Affinity Measurements, Anal. Chem., 89 (2017) 7302–7306.

[19] M.D. Symes, P.J. Kitson, J. Yan, C.J. Richmond, G.J.T. Cooper, R.W. Bowman, T. Vilbrandt, L. Cronin, Integrated 3D-printed reactionware for chemical synthesis and analysis, Nature Chemistry, 4 (2012) 349–354.

[20] F. Li, P. Smejkal, N.P. Macdonald, R.M. Guijt, M.C. Breadmore, One-Step Fabrication of a Microfluidic Device with an Integrated Membrane and Embedded Reagents by Multimaterial 3D Printing, Anal. Chem., 89 (2017) 4701–4707.

[21] Z.C. Kennedy, J.F. Christ, K.A. Evans, B.W. Arey, L.E. Sweet, M.G. Warner, R.L. Erikson, C.A. Barrett, 3D-Printed Poly (vinylidene fluoride)/Carbon nanotube Composites as a Tunable, Low-cost Chemical Vapour Sensing Platform, Nanoscale, 17 (2017) 5458-5466.

[22] U. Kalsoom, P.N. Nesterenko, B. Paull, Recent developments in 3D printable composite materials, RSC Adv. 6 (2016) 60355-60371.

[23] J. Zhang, B. Yang, F. Fu, F. You, X. Dong, M. Dai, Resistivity and Its Anisotropy Characterization of 3D-Printed Acrylonitrile Butadiene Styrene Copolymer (ABS)/Carbon Black (CB) Composites, Appl. Sci. 7 (2017) 20.

[24] S.J. Leigh, R.J. Bradley, C.P. Purssell, D.R. Billson, D.A. Hutchins, A simple, Low-cost Conductive Composite Material for 3D Printing of Electronic Sensors, PloS one, 7 (2012) 49365.

[25] A.E. Jakus, E.B. Secor, A.L. Rutz, S.W. Jordan, M.C. Hersam, R.N. Shah, Three-Dimensional Printing of High-Content Graphene Scaffolds for Electronic and Biomedical Applications, ACS Nano. 9 (2015) 4636-4648.

[26] X. Wei, D. Li, W. Jiang, Z. Gu, X. Wang, Z. Zhang, Z. Sun, 3D Printable Graphene Composite, Sci. Rep. 5 (2015) 11181.

[27] K. Fu, Y. Yao, J. Dai, L. Hu, Progress in 3D Printing of Carbon Materials for Energy-Related Applications, Adv. Mater. 29 (2017).

[28] A. Peristyy, A.N. Koreshkova, B. Paull, P.N. Nesterenko, Ion-Exchange Properties of High-Pressure High Temperature Synthetic Diamond, Diamond Rel. Mats. 75 (2017), 131-139.

[29] S. Waheed, J.M. Cabot, N.P. Macdonald, U. Kalsoom, S. Farajikhah, P.C. Innis, P.N. Nesterenko, T.W. Lewis, M.C. Breadmore, B. Paull, Enhanced Physicochemical Properties of Polydimethylsiloxane Based Microfluidic Devices and Thin Films by Incorporating Synthetic Micro-diamond, Sci. Rep. 7 (2017) 15109.

[30] M. Angjellari, E. Tamburri, L. Montaina, M. Natali, D. Passeri, M. Rossi, M.L. Terranova, Beyond the concepts of nanocomposite and 3D printing: PVA and Nanodiamonds for Layer-by-Layer Additive Manufacturing, Mater. Des. 119 (2017) 12-21

[31] U. Kalsoom, A. Peristyy, P. Nesterenko, B. Paull, A 3D Printable Diamond Polymer Composite: a novel Material for Fabrication of Low Cost Thermally Conducting Devices, RSC Adv. 6 (2016) 38140-38147.

[32] P. Parandoush, D. Lin, A review on Additive Manufacturing of Polymer-fiber Composites, Compos. Struct. 182 (2017) 36-53.

[33] F. Li, N.P. Macdonald, R.M. Guijt, M.C. Breadmore, Increasing the functionalities of 3D printed microchemical devices by single material, multimaterial, and print-pause-print 3D printing Lab on a Chip 19 (1), 35-49

[34] S. Waheed, J.M. Cabot, P. Smejkal, S. Farajikhah, S. Sayyar, P.C. Innis, S. Beirne, G. Barnsley, T.W. Lewis, M.C. Breadmore, B. Paull, Three-Dimensional Printing of Abrasive, Hard, and Thermally Conductive Synthetic Microdiamond–Polymer Composite Using Low-Cost Fused Deposition Modelling Printer, ACS Appl. Mater. Interfaces, (2019).

[35] U. Kalsoom, P.N. Nesterenko, B. Paull, Current and future impact of 3D printing on the separation sciences, Trends Anal. Chem. 105 (2018) 492-502.

[36] M. Banna, K. Bera, R. Sochol, L. Lin, H. Najjaran, R. Sadiq, M. Hoorfar, 3D Printing-Based Integrated Water Quality Sensing System, Sensors, 17 (2017) 1336-1353.

[37] C.M.B. Ho, S.H. Ng, K.H.H. Li, Y.J. Yoon, 3D Printed Microfluidics for Biological Applications, Lab Chip, 15 (2015) 3627-3637.

[38] V. C. Romao, S. A. M. Martins, J. Germano, F. A. Cardoso, S. Cardoso, P. P. Freitas, Lab-on-Chip devices: Gaining ground losing size, ACS Nano., 11 (2017) 10659-10664.

[39] A. Donohoe, G. Lacour, P. McCluskey, D. Diamond, M. McCaul, Development of a Cost-Effective Sensing Platform for Monitoring Phosphate in Natural Waters, Chemosensors, 6 (2018) 57-70.

[40] G.S. Clinton-Bailey, M.M. Grand, A.D. Beaton, A.M. Nightingale, D.R. Owsianka, G.J. Slavik, D.P. Connelly, C.L. Cardwell, M.C. Mowlem, A Lab-on-Chip Analyzer for *in Situ* Measurement of Soluble Reactive Phosphate: Improved Phosphate Blue Assay and Application to Fluvial Monitoring, Environ. Sci. Technol. 51 (2017) 9989–9995.

[41] M.F. Khanfar, W. Al-Faqheri, A. Al-Halhouli, Low Cost Lab on Chip for the Colorimetric Detection of Nitrate in Mineral Water Products, Sensors, 17 (2017) 2345-2354.

[42] D.H. Thomas, M. Rey, P.E. Jackson, Determination of inorganic cations and ammonium in environmental waters by ion chromatography with a high-capacity cation-exchange column, J. Chromatogr. A 956 (2002) 181-186.

[43] EPA Method 350.3: Nitrogen, Ammonia (Potentiometric, Ion Selective Electrode), U.S. Environmental Protection Agency, Cincinnati, 1974.

[44] EPA Method 350.2: Nitrogen, Ammonia (Colorimetric; Titrimetric; Potentiometric - Distillation Procedure), U.S. Environmental Protection Agency, Cincinnati, 1974.

[45] S.S. Goyal, D.W. Rains, R. C. Huffaker, Determination of ammonium ion by fluorometry or spectrophotometry after on-line derivatization with o-phthalaldehyde, Anal. Chem. 60 (1988) 175-179.

[46] R. Michalski, Ion Chromatography Applications in Wastewater Analysis, Separations, 5 (2018) 16.

[47] P.L. Searle, The Berthelot or indophenol reaction and its use in the analytical chemistry of nitrogen. A review, Analyst, 5 (1984) 549-568.

[48] N. T. Crosby, Determination of ammonia by the Nessler method in waters containing hydrazine, Analyst, 1107 (1968) 406-408.

[49] S. Capelo, F. Mira, A.M. de Bettencourt, In situ continuous monitoring of chloride, nitrate and ammonium in a temporary stream comparison with standard methods, Talanta, 71 (2007) 1166–1171.

[50] USGS, Continuous Monitoring for Nutrients: State of the Technology and State of the Science. https://acwi.gov/monitoring/webinars/national_monitoring_council_webinar_092414b_Pellerin.pdf (accessed 14 January 2019).

[51] Systea S.p.A Analytical Technologies, NPA Pro - Nutrients probe analyzer http://www.systea.it/index.php?option=com_k2&view=item&layout=item&id=221&Itemid=176&lang=en (accessed 20 Jan 2019).

[52] D. Cogan, J. Cleary, C. Fay, A. Rickard, K. Jankowski, T. Phelan, M. Bowkett, D. Diamond, The development of an autonomous sensing platform for the monitoring of ammonia in water using a simplified Berthelot method, Anal. Methods, 6 (2014) 7606–7614.

[53] H. Verdouw, C.J.A. Van Echteld, E.M.J. Dekkers, Ammonia determination based on indophenol formation with sodium salicylate, Water Research, 12 (1978) 399-402.

[54] FIAlab, Method for Ammonia Determination by Salicylate, Version 2.2, https://www.flowinjection.com/images/Methods/2018/FIA-010_Method-for-Ammonia-Determination-v2.1.pdf (accessed 02/10/2019)

[55] E. Murray, P. Roche, K. Harrington, M. McCaul, B. Moore, A. Morrin, D. Diamond, B. Paull, Low cost 235 nm UV-LED based absorbance detector for application in a portable ion chromatography system for nitrite and nitrate monitoring, J. Chrom. A., 1603 (2019) 8–14.

[56] F. Li, N.P. Macdonald, R.M. Guijt, M.C. Breadmore, Using Printing Orientation for Tuning Fluidic Behaviour in Microfluidic Chips Made by Fused Deposition Modelling 3D Printing, Anal. Chem. 89 (2017) 12805–12811.

Chapter 6:

Fully automated, low-cost ion chromatography system for *in-situ* analysis of nitrite and nitrate in natural waters

Eoin Murray [1, 2], Patrick Roche [1], Matthieu Briet [1], Breda Moore [1], Aoife Morrin [2], Dermot Diamond [2], Brett Paull [3, 4]

1. Research & Development, T.E. Laboratories Ltd. (TelLab), Tullow, Carlow, Ireland
2. Insight Centre for Data Analytics, National Centre for Sensor Research, School of Chemical Sciences, Dublin City University, Dublin 9, Ireland
3. Australian Centre for Research on Separation Science (ACROSS), School of Physical Sciences, University of Tasmania, Sandy Bay, Hobart 7001, Australia
4. ARC Training Centre for Portable Analytical Separation Technologies (ASTech), School of Physical Sciences, University of Tasmania, Sandy Bay, Hobart 7001, Australia

Publication: Submitted to Analytica Chimica Acta

Chapter Overview

This chapter presents a fully automated, low-cost portable IC system for nitrate and nitrite monitoring in a broad range of environmental waters. The system employs much of the know-how and knowledge which resulted from the development of the components and systems discussed in the preceding chapters. The developed portable IC was successfully deployed at various locations around the world and represents a significant step towards truly low-cost, *in-situ* nitrite and nitrate analysis.

Abstract

A low-cost, automated and portable IC has been developed for *in-situ* analysis of nitrite and nitrate in natural waters. The system employed 3D printed pumps for eluent delivery and a 235 nm LED based optical detector. Isocratic separation and selective detection of nitrite and nitrate was achieved in under 3 min. The total weight of the analyser was ~ 11 kg, and included electronics along with a sample intake system for automated analysis. Linear calibration ranges were generated using different sample injection loops. Using a 150 µL loop, an analytical range suitable for freshwater analysis was generated, while using a 10 µL loop an analytical range suitable for effluent and septic water was achieved. Chromatographic repeatability demonstrated by the system is graphically presented and RSD values of < 4% were obtained in terms of peak area and retention time over 82 sequential runs. The system was deployed *in-situ* at multiple sites for varying deployment periods analysing septic tank water, effluent from a waste water treatment plant and stream water. The data generated by the *in-situ* system were comparable to grab sample data generated by accredited lab instrumentation.

6.1. Introduction

The transition of analytical instrumentation from the laboratory to the field or *in-situ* offers significant benefits to a broad range of disciplines ranging from medical science to environmental monitoring. This transition was incited by the advent of micro total analysis systems (μTAS) in the 1990s, and has greatly progressed over the past two decades with the advancement of micromachining technologies and microelectronics [1, 2]. When considering environmental monitoring, water quality management represents an area in which portable, *in-situ* analysers are distinctly favourable and necessary. Traditional monitoring of water systems is carried out by manually collecting samples and transporting them to centralised laboratories for analyses. This approach is laborious and costly, and analyte speciation may be altered as a result of chemical or biological reactions within the sample prior to analysis. To eliminate these issues, and to achieve high spatial and temporal resolution monitoring, deployable automated analysers which perform *in-situ* analysis are required [3].

Nutrient pollution, in the form of nitrate, nitrite and phosphate, represents the most prevalent global water quality problem [4]. Yet despite this reality, nitrite and nitrate monitoring is still predominantly carried out using the antiquated and deficient 'grab and lab' approach. Over the years, a variety of strategies and analytical systems have been developed for near real-time *in-situ* nutrient analysis of aquatic environments [5-8]. However, use and application of these systems is restricted by power requirements, size, reagent usage and/or cost. Electrochemical sensors have also been extensively developed for the analysis of nitrate and nitrite in water. These sensors are cost effective, but when considering long term *in-situ* deployment are often hindered by electrode fouling and analytical drift over time [9-12]. To date, colorimetric based analysers, along with direct UV absorption systems have proven to be the dominant avenues towards achieving *in-situ* nitrate and nitrite analysers. Regarding the former, several *in-situ* analysers based on flow injection analysis (FIA) have been developed [8, 13], and a number of colorimetric based *in-situ* nitrate and nitrite analysers are commercially available [14-17]. Lab-on-a-chip (LOC) based systems which incorporate colorimetric reagents and LED-based

detection for nutrient monitoring have successfully been developed and deployed *in-situ* in a range of natural waters [3, 18-20]. These systems offer considerable advantages over FIA systems mainly in the form of reduced reagent consumption and power demands. Direct UV absorption-based systems have also been habitually employed for *in-situ* nitrate monitoring and several commercial systems are available [21-24].

Yet despite the commercial availability of numerous systems and the progress which has taken place in the field of *in-situ* nutrient analysers, technologies remain poorly implemented or adopted in environmental water monitoring [25]. Prohibitive costs and technological limitations have hampered these *in-situ* systems from routine use and adoption on a mass scale [26]. Direct UV systems remain at significant price points and have high power consumption requirements due to the use of UV lamps [27]. As for colorimetric based analysers, these systems are also of a high price point, but they have the added disadvantage of requiring multiple reagents which are often of a hazardous nature. LOC colorimetric based systems have demonstrated the greatest potential in terms of generating an *in-situ* nutrient analyser using low cost components. However, considerable costs and challenges arise in terms of mass manufacture of microfluidic components and assembly of LOC systems [25]. The need for low-cost *in-situ* nutrient analysers, at price points facilitating wide scale usage, is reflected in the recent challenges and competitions set out by the Alliance for Coastal Technologies (ACT) and the US EPA [28, 29]. The Nutrient Sensor Challenge was a market-based competition aimed at generating sensors for measuring nitrate and phosphate in natural waters with a purchase price of US $5000 [28]. The winning system was based on colorimetry and achieved the analytical targets, but the system purchase price was several times above the target price [30, 15]. Recently, the US EPA issued the Advanced Septic System Nitrogen Sensor Challenge which is aimed at generating *in-situ* nitrogen analysers at price points < $1500 for effluent and septic system water analysis [29].

In this work, we describe an alternative route to achieving a simple, low-cost analyser for *in-situ* nitrite and nitrate monitoring in natural waters, to those

previously reported. The analyser is based on rapid ion chromatography and UV detection employing a deep-UV LED. The low-cost portable IC uses 3D printed pumps in combination with a uniquely designed microfluidic optical detector cell. The system employs custom-built pumping, electronics and sample intake and has a simple configuration facilitating ease of assembly. The analytical performance of the system was established along with chromatographic repeatability. The system was tested and deployed *in-situ* within a septic water treatment unit in Massachusetts, USA as part of the Nitrogen sensor challenge and sensor results were compared to those generated by accredited instrumentation. Two additional portable IC systems were also built. One system was deployed and tested within an effluent treatment plant in Haapavesi, Finland and the other system was tested in a river, downstream of agricultural land in Wexford, Ireland.

6.2. Materials and methods

6.2.1. Chemicals and reagents

The chemicals used within this work were of analytical or higher grade. High-purity deionised water (Milli-Q) was used for preparation of all solutions. Potassium hydroxide used as the eluent was purchased from Sigma-Aldrich (St. Louis, MO). Nitrate and nitrite standard solutions were prepared using potassium nitrate and sodium nitrite salts, respectively (Sigma-Aldrich, St. Louis, MO). Working analyte standards were prepared through dilution of standard stock solutions.

6.2.2. Portable IC system

The automated portable nitrate and nitrite analyser described in this study was based on the IC method coupled with 235 nm LED based absorbance detection recently reported by Murray *et al.* [27]. A render of the IC system, depicting system components is shown in Figure 6.1. The syringe pumps were made of low cost, off-the-shelf components coupled with a 3D printed base and pusher block. The 3D printing was performed using Onyx filament sourced from Markforged, Inc. (Massachusetts, USA) and a Markforged Mark Two printer. The syringes used were 1 mL gas tight luer lock glass syringes sourced from Sigma-

Aldrich (Wicklow, Ireland). Flushing and filling of the syringes was achieved through the use of 12 V brushed geared DC motors (Pololu, Las Vegas, USA). Rod collars and motor couplings were provided by RS Radionics (Dublin, Ireland). A 6 port 2-position injection valve (VICI AG, Schenkon, Switzerland) which was automated using a hybrid stepper motor (Radionics, Dublin, Ireland) was used. Fast separation at low back pressures was achieved using a 4 × 50 mm Dionex AG15 guard column from Thermo Fisher Scientific (Sunnyvale, CA). The surface mount 235 nm deep UV-LED used for direct absorbance detection was provided by Crystal IS (Green Island, NY, USA). A UVC photodiode (TOCON_C1) with integrated amplifier for photodetection was purchased from Sglux GmbH (Berlin, Germany). The UV optical detection cell was based on the design previously reported [27]. All design work carried out for 3D printed components was performed using Fusion 360 computer aided design software (Autodesk Inc., California, USA). For eluent storage a 2 L fluid collection bag was used, sourced from Fannin Ltd. (Dublin, Ireland). Inline check valves and tubing connectors were provided by Kinesis (Altrincham, UK) and Sigma-Aldrich (St. Louis, MO). The system was housed within a 1510M Peli Case with exterior dimensions of 59.8 x 36.5 x 27 cm (Peli Products, Clare, Ireland). The total weight of the system including battery and full eluent was ~ 11 kg.

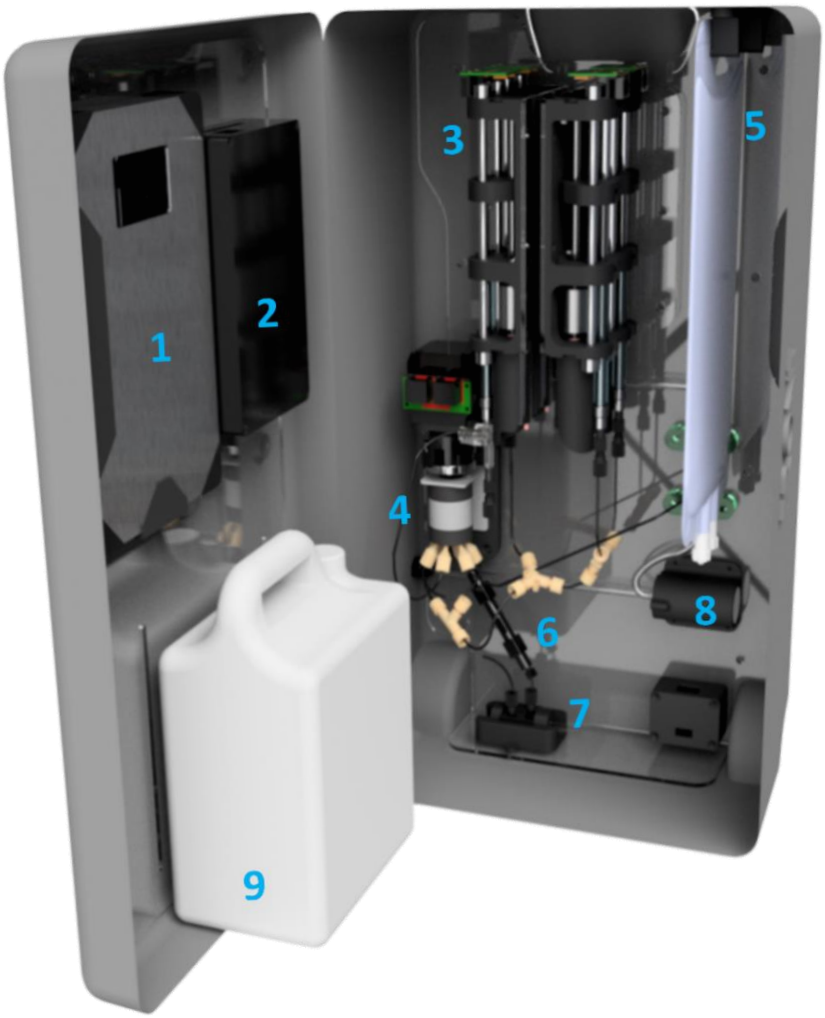

Figure 6.1: Render of portable IC system with components labelled. Legend: (1) battery; (2) electronics housing; (3) 3D printed syringe pumps; (4) six-way injection valve; (5) eluent storage bag; (6) AG15 column; (7) UV LED based optical detection; (8) 12 V sample intake pump; (9) waste container

6.2.3. Fluidic configuration

The fluidic operation of the system is schematically represented in Figure 6.2. The system was equipped with four low-cost 3D printed syringe pumps. Three pumps were used for eluent delivery, while the fourth pump was used for drawing sample from the sample reservoir through the sample loop, thereby loading the loop. During system operation, the three eluent syringe pumps operated in unison, each drawing 1.1 mL of eluent from the onboard eluent storage bag. Once the three syringes were full, parallel flushing of the eluent syringes commenced resulting in a flowrate of 0.8 mL min^{-1} through the 6-way

valve, column and detector. One-way valves were in place to ensure eluent was only drawn from the eluent storage during syringe fill and flow was directed through the column during syringe flushing. In parallel to the operation of the eluent syringe pumps filling with eluent, the sample syringe pump was filled, drawing 0.5 mL of sample from the reservoir. During flushing, the sample syringe pump was emptied into a waste container. As the eluent syringe pumps were flushing, the 6-way valve remained in the load position until 25 seconds had passed, after this time the valve automatically switched to inject, and the sample was injected. All syringe pumps were set to continue to empty until their home position was reached which was defined by the activation of limit switches.

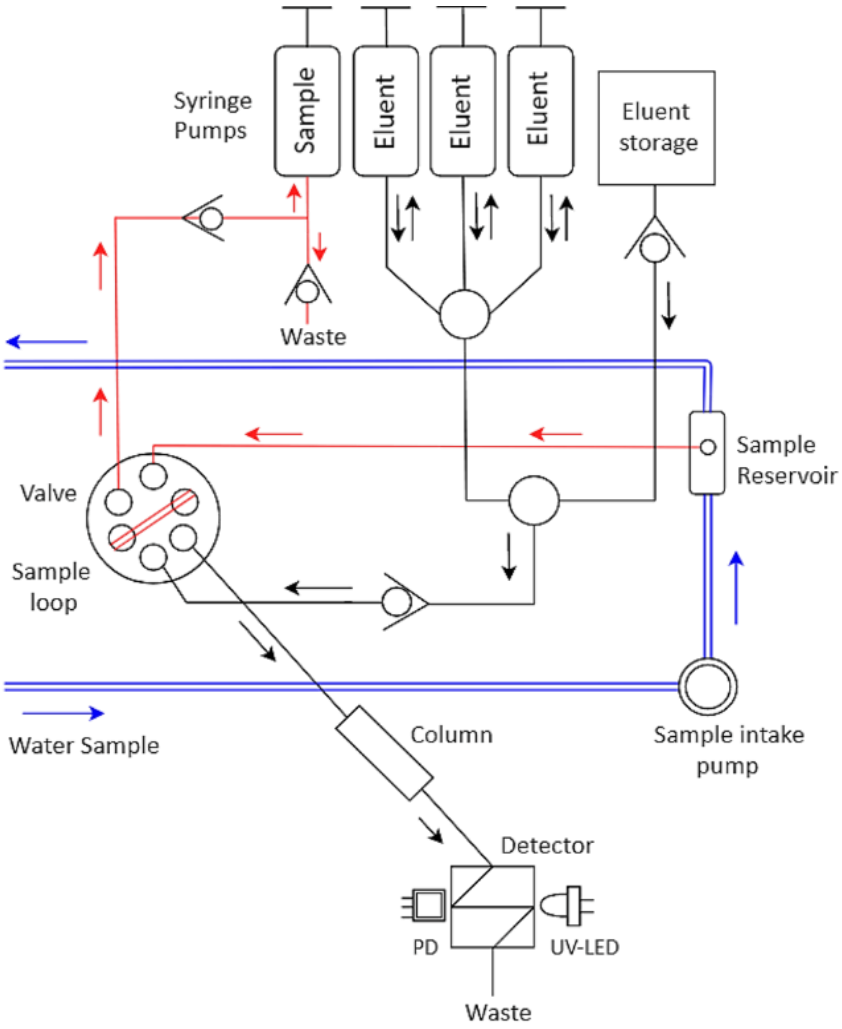

Figure 6.2: Schematic representation of analyser. The flow path of KOH eluent is shown in black. The flow path of sample through the sample reservoir is shown in blue. An aliquot of sample taken from the reservoir and introduced into the system via the sample loop is shown in red.

6.2.4. Sample intake system

The sample intake system was based on a loop utilising a low-power 12 V DC positive displacement pump from Chihai Motor (Shenzen, China). Sample was drawn from the environment through a coarse filter into a 3D printed sample reservoir of 10 mL internal volume and flushed back out into the water sample. After 1 min of flowing, the pump automatically powered off and the reservoir was full of sample. At this point, a sample aliquot was automatically drawn from the reservoir using the sample syringe via the sample loop of the six-way valve. This enabled the loop to be loaded with sample which was then injected into the eluent flow when the valve was switched to the injection position. By loading the loop in this manner, sample carry over was eliminated between sequential runs. A schematic of the automated sample intake is illustrated in Figure 6.3.

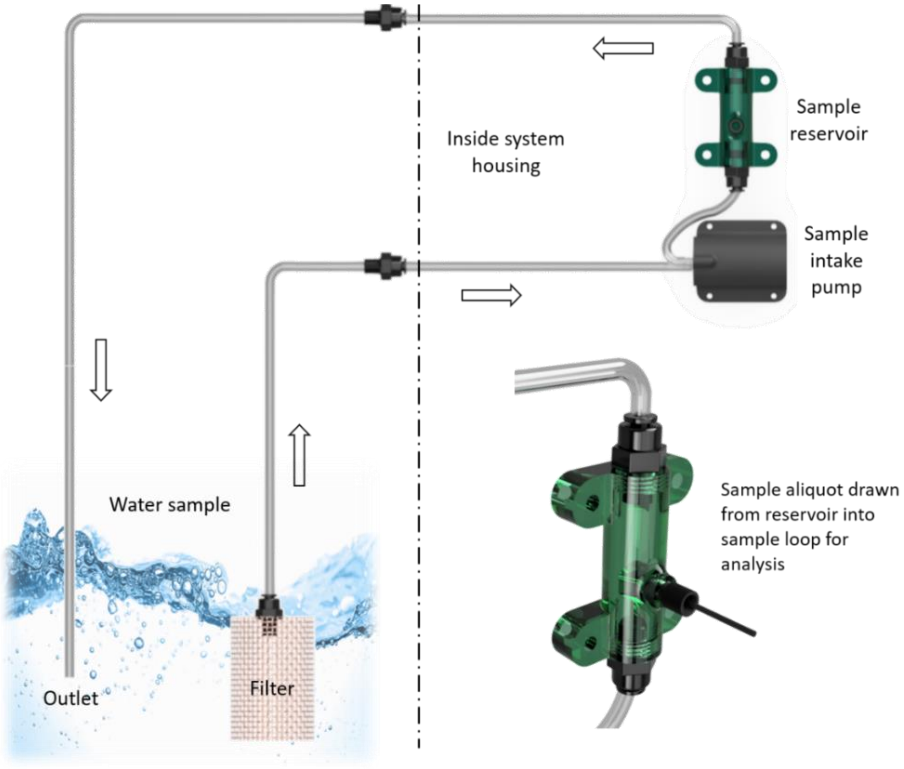

Figure 6.3: Schematic of automated sample intake system and render of sample reservoir shown inset. The configuration was based on a loop in which sample is drawn from the environment, into the sample reservoir and the sample is flushed back out into the water sample. When the pump is powered off, the reservoir is full with sample and a sample aliquot is then drawn from the reservoir using the sample syringe.

6.2.5. System control and data acquisition

The embedded system of the portable IC used a Teensy 3.6 microcontroller (Mouser Electronics, Munich) with an ARM Cortex-M4 processor running at 180 MHz. The Teensy 3.6 was selected for this prototype due to its high number of input/output pins, fast processor and low power consumption. The microcontroller was coupled with an AL8805 DC-DC LED driver (Sparkfun Electronics, Niwot, CO) to provide constant current to power the UVC LED and an ADS1115 16-bit analogue to digital converter (Adafruit Industries, New York, NY) to process the resultant signal from the photodiode. The syringe pumps and 6-way valve were actuated using TB6612FNG motor drivers (Sparkfun Electronics, Niwot, CO). A 12 V relay was used to turn the sample pump on and off. Internal system temperature and humidity readings were provided by a HTU21D-F sensor, while system timing was controlled by a DS3231 real-time clock (Adafruit Industries, New York, NY).

The firmware that was executed on the microcontroller was written in C++ and provided functionality which enabled the IC system to run automatically. The firmware was based on a configured sequence and set intervals. This configured sequence was an event-driven state machine. Switching of the 6-way valve was achieved by moving a stepper a set number of steps either clockwise or anti-clockwise, depending on injection or loading. The stepper motor rotated the desired number of steps, at a desired speed and was stopped when a limit switch was hit. The valve was switched to the injection position when the syringe pumps were delivering eluent. During the eluent delivery sequence, the firmware ensured the syringe pumps were flushing eluent at a constant flow rate of 0.8 mL min^{-1}. This was achieved using the integrated encoder on the 12 V DC motor actuating each syringe pump coupled with a proportional-integral controller in the firmware. The pulses from the encoder were counted over a 100-millisecond period using hardware interrupts. When the interrupt pin from each encoder read a high signal, an interrupt service routine was executed to increment a variable. The variable was read at a rate of 10 Hz and its value was used to calculate a rpm which the P.I. controller maintained.

When the syringe pumps were flushing eluent through the column, the data analysis function was executed. The LED was tuned on at a set intensity and the resulting signal from the photodiode was processed and written to a file on a micro SD card. This function passed the digital values generated by the analogue to digital converter through a running average filter. The running average values were sampled and written to a buffer at a rate of 20 Hz. This buffer was structured in a comma separated value (CSV) format which contained, along with the running average values, a raw value from the analogue to digital converter and an incrementing identifier value. Once the syringe pumps were emptied and the data analysis was complete, the data was written to the micro SD card for post processing. UniChrom software was used for processing of chromatograms and peak area integration.

6.2.6. Field deployments

In order to assess the performance of the portable IC in the field, the system was deployed *in-situ* at several locations, monitoring nitrate and nitrite levels in varying sample matrices. Firstly, the system was deployed within the Advanced Septic System Nitrogen Sensor Challenge, issued and managed by the US EPA and held within the Massachusetts Alternative Septic System Test Centre (MASSTC) [29]. Battelle (Columbus, Ohio, USA) were responsible for developing and implementing a Test/Quality Assurance Plan (T/QAP) for testing of the developed sensor system. The T/QAP was based on the International Organization for Standardization (ISO) Environmental Technology Verification (ETV) Standard - ISO 14034. Accordingly, within the challenge, the system was deployed *in-situ* within a septic water tank. Over a 7-day test period, the system performed analysis at an hourly sample frequency. Grab samples were taken at specified times and were analysed by a National Sanitation Foundation (NSF) certified test facility in Barnstable, Massachusetts. An assessment of nitrate and nitrite concentrations generated by the portable IC system versus the accredited lab results was carried out and reported. The system was also deployed within an effluent treatment plant located in Haapavesi, Finland. The sampling frequency at this location was twice per day over a two-month period. Grab samples were taken once every two weeks by the plant operators and these

samples were analysed by accredited benchtop instrumentation. Finally, the system was taken to perform on-site analysis at a freshwater stream located within Teagasc Johnstown Castle, Wexford, Ireland. Grab samples were also taken from this location and analysed using an accredited IC. Photographs of the portable system deployed at the various locations are shown in Figure E1 of the ESI.

6.3. Results and Discussions

6.3.1 Chromatographic Repeatability

The portable IC was set up within a laboratory setting and was configured to run once every 15 minutes for ~20 hours. An anion standard containing 15 mg L^{-1} NO_3^- and 10 mg L^{-1} NO_2^- was analysed continuously. A sample loop volume of 50 µL was selected as it represented an intermediate injection volume between the 150 µL sample volume used when analysing freshwater samples and the 10 µL sample volume which was used when analysing effluent and highly contaminated waters. The chromatographic repeatability achieved by the instrument is shown in Figure 6.4 as the chromatograms of sequential injections are overlaid. The peak area RSD values obtained for nitrite and nitrate over 82 runs were 3.87 % and 3.91 %, respectively. Retention time RSD values for nitrite and nitrate were found to be 3.59 % and 3.23 %, respectively. The eluent used was 120 mM KOH at a flowrate of 0.8 mL min^{-1} and an AG15 guard column was used for analytical separation. The 235 nm UV LED based detector was used for direct nitrite and nitrate.

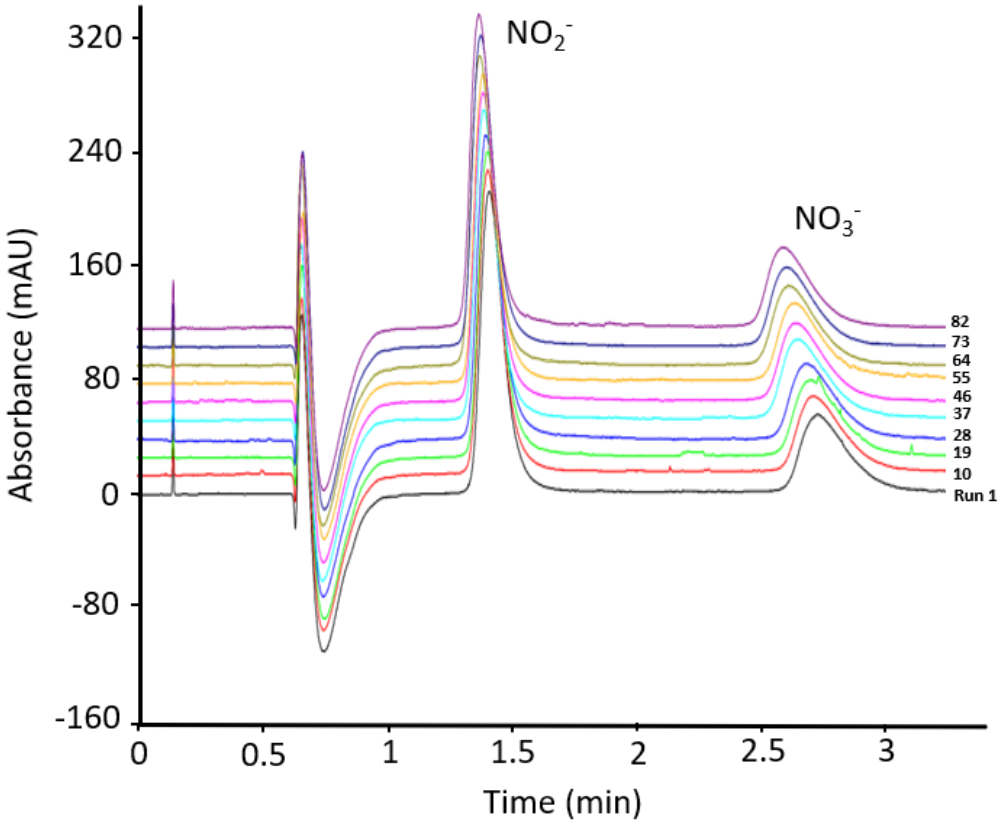

Figure 6.4: Selected chromatograms overlaid (offset by 15 mAU) following 82 sequential runs using portable IC set up. Each chromatogram represents 50 µL injection volume of standard containing 10 mg L^{-1} NO_2^- and 15 mg L^{-1} NO_3^-. Eluent was KOH with AG15 guard column for separation.

6.3.2. Analytical Performance

The portable IC system was based on the method and IC set up previously developed and reported by Murray *et al.* [27]. Using an AG15 guard column for separation, isocratic elution using KOH eluent and a low-cost 235 nm LED-based detector, selective detection of nitrite and nitrate was achieved with an elution time of < 3 minutes. By adapting the sample loop volume, the system had the ability to monitor a variety of sample matrices and a broad range of analyte concentrations. Using a 150 µL loop, the system had the ability to detect ppb levels of analyte. Using a 10 µL loop, highly contaminated water sources which contain high concentrations of analyte, such as effluent, could be analysed. The analytical ranges for nitrite and nitrate obtained using a 150 µL loop along with a 10 µL loop are presented in Table 6.1. Corresponding limit of detection (LOD)

values, calculated using a signal-noise-ratio (S/N) = 3, are also shown [31, 32]. Calibration curves for nitrite and nitrate using each loop are illustrated in Figure E2 and E3 of the ESI.

Table 6.1: Performance of portable IC using different sample loops

Analyte	**Sample Loop Volume**	**Linear Range (mg L^{-1})**	**R^2**	**LOD (mg L^{-1})**
Nitrite	150 µL	0.05 - 30	0.999	0.005
Nitrate		0.10 – 75	0.996	0.040
Nitrite	10 µL	0.30 – 100	0.999	0.17
Nitrate		2.5 - 500	0.998	1.30

6.3.3. *In-situ* analysis

The first set of data were obtained from the deployment carried out within MASSTC as part of the septic system Nitrogen Sensor Challenge. A test tank was set up which contained actual septic stream effluents. The tank was also spiked periodically with varying concentrations of nitrite and nitrate during the test period. The hourly concentrations of nitrite and nitrate obtained by the portable IC system over a 7-day period are shown in Figure 6.5. Concentrations obtained from grab samples which were analysed using accredited laboratory instrumentation are also shown within the figure. In terms of accuracy, the ideal performance target within the challenge was < 20% of true value. The total mean recoveries observed for nitrite and nitrate during the *in-situ* deployment within the septic water test tank were 83% and 99% respectively. For precision, the ideal RSD value for the challenge was < 20%. The highest RSD for determined nitrite concentrations was 5.64% and the highest for determined nitrate concentrations was 2.22%. The portable IC system met all the performance criteria set out for nitrite and nitrate within the challenge, highlighting the applicability of the system for septic water analysis.

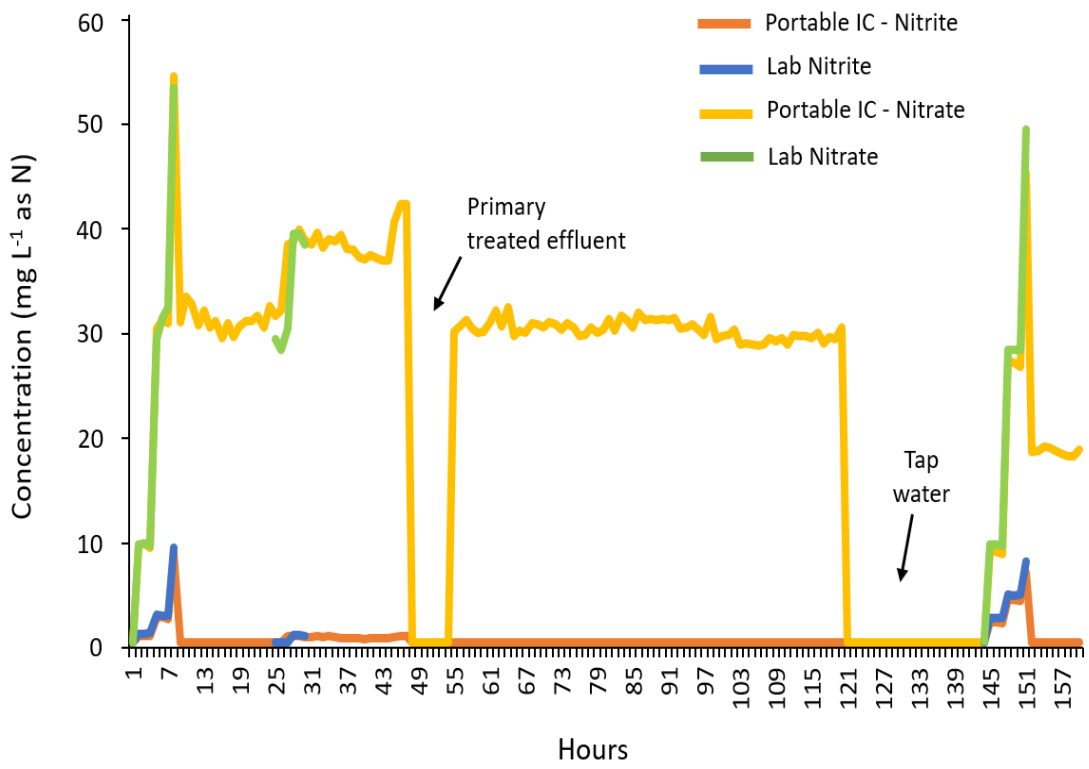

Figure 6.5: Portable IC data versus lab data over 7-day test period within septic tank water as part of the Advanced Septic System Nitrogen Sensor Challenge. The system employed a 10 µL injection volume, 120 mM KOH eluent, AG15 guard column for separation and the 235 nm LED based detector.

Following the MASSTC deployment, two additional deployments of the system took place. The second deployment took place within a wastewater treatment plant (WWTP) located in Haapavesi, Finland. The plant is responsible for treating sewage coming from dairy industry as well as the city of Haapavesi. The portable IC system was installed within the plant and was set to measure nitrite and nitrate within the effluent of the WWTP. It was determined that nitrite was not present within the effluent stream. The nitrate concentrations detected using the portable IC system, along with grab sample concentrations, over the course of two months are illustrated in Figure 6.6. Periodic grab samples were analysed using standard laboratory instrumentation. Finally, the portable analyser carried out on-site analysis over a 7-day period on the grounds of Teagasc, Johnstown Castle, Ireland. The system was deployed for the analysis of a freshwater stream which was surrounded by agricultural land. Once again, it was found that nitrite was not present within the sample. A comparison of nitrate concentrations

determined by the portable IC versus concentrations obtained following analysis using accredited instrumentation is illustrated in Figure 6.7.

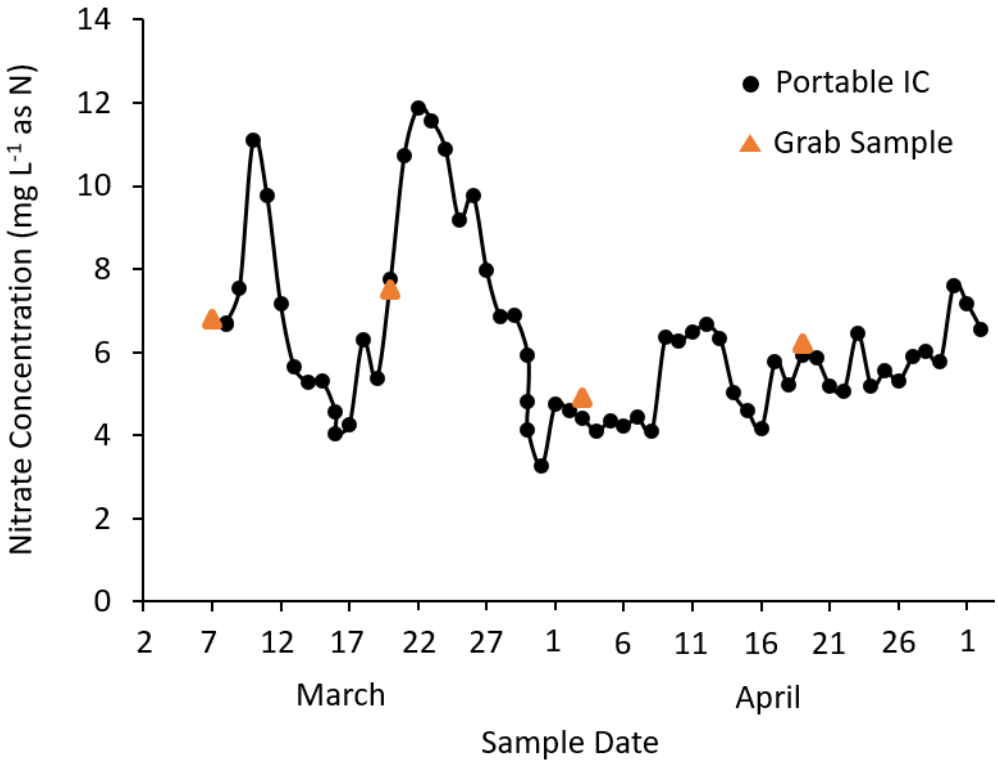

Figure 6.6: Data generated by the *in-situ* analyser following deployment within a WWTP located in Haapavesi, Finland. Data points generated by the IC system are shown in black, while grab sample concentrations are shown in orange. A 10 µL injection volume, 120 mM KOH eluent, AG15 guard column and the 235 nm LED based detector were used.

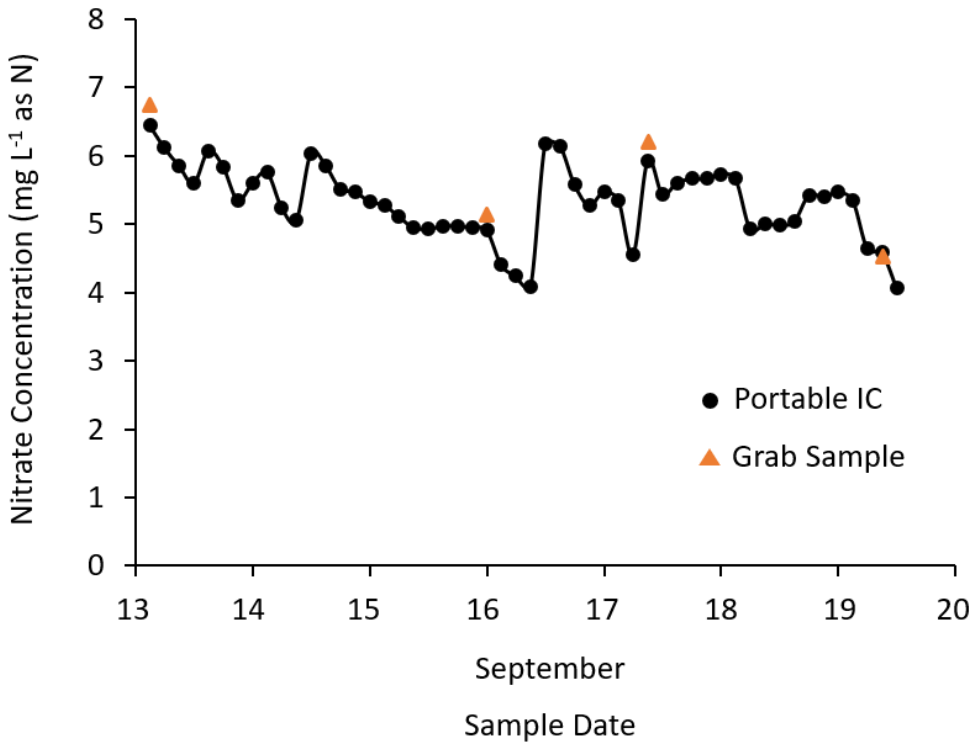

Figure 6.7: Data generated by the portable analyser following 7 days of on-site analysis of a freshwater stream. Data points generated by the IC system are shown in black and grab sample concentrations are shown in orange. A 150 µL injection volume, 120 mM KOH eluent, AG15 guard column and 235 nm LED based detector were used.

6.4. Conclusions

A low-cost, portable IC system for *in-situ* analysis of nitrite and nitrate was developed and demonstrated in the field. The system was based on a simple anion exchange method using KOH eluent in combination with an AG15 guard column to achieve anion separation. Selective, direct detection of nitrite and nitrate was attained through the use of a low-cost, 235 nm LED based absorbance detector. The system used custom syringe pumps for fluidic handling, which were fabricated through 3D printing and employed off-the-shelf components. In-house developed electronics and firmware were used to achieve system automation and data acquisition. The repeatability of the portable IC system was demonstrated and by varying sample injection volumes wide analytical ranges for nitrite and nitrate were demonstrated. The system was successfully deployed *in-situ* at various environmental sites including a septic

water tank, a WWTP and a fresh water stream, highlighting the suitability of the system to be deployed in varying sample matrices. The simple configuration and ease of assemble associated with the system opens the way towards scaled up *in-situ* deployments of analytical platforms. Future work and further development of the system will focus on modifying and adapting the system to facilitate mass manufacture. Injection moulding will be investigated as a route to manufacture for the syringe pumps. Currently, the UV detection cell is made by micromilling and bonding of PMMA and the windows are then chemically bonded. As a faster and simpler alternative, stereolithography (SLA) 3D printing of the optical cell will be explored with mechanical treaded sealing of the UV transparent windows. Other detection strategies, such as contactless conductivity detection, will also be explored for coupling with the separation capability of the system for potential detection of further analytes.

6.5. Acknowledgements

The authors would like to acknowledge financial support from the Irish Research Council, Grant No. EBPPG/2015/127 and the Australia Awards - Endeavour Research Fellowship, Grant No. 6389_2018. The LIFE Ecosense Aquamonitrix Project – Grant Number: LIFE 17 ENV/IE/000237 is also acknowledged. The authors would like to thank Prof Owen Fenton of Teagasc, Johnstown Castle, the USEPA, Battelle and the team at the Massachusetts Alternative Septic System Test Center (MASSTC) for providing access to environmental test sites and for their support.

6.6. References

[1] Li Y., Dvořák M., Nesterenko P. N., Stanley R., Nuchtavorn N., Krčmová L. K., Aufartová J., Macka M., Miniaturised medium pressure capillary liquid chromatography system flexible open platform design using off-the-shelf microfluidic components. *Anal. Chim. Acta* 2015, 896, 166-176.

[2] D. Mark, S. Haeberle, G. Roth, F. von Stetten, R. Zengerle, Microfluidic lab-on-a-chip platforms: requirements, characteristics and applications, *Chem. Soc. Rev*. 2010, 39, 1153-1182.

[3] A.D. Beaton, C.L. Cardwell, R.S. Thomas, V.J. Sieben, F.E Legiret, E.M. Waugh, P.J. Statham, M.C. Mowlem, H. Morgan, Lab-on-Chip Measurement of Nitrate and Nitrite for In Situ Analysis of Natural Waters, Environ. Sci. Technol. 46 (2012) 9548-9556.

[4] United Nations (2014) *International decade for action 'water for life' 2005-2015* [online], available: http://www.un.org/waterforlifedecade/quality.shtml [accessed 6 Dec 2018].

[5] J.R. Clinch, P.J. Worsfold, An automated spectrophotometric field monitor for water quality parameters: Determination of nitrate, Anal. Chim. Acta, 200 (1987) 523–531.

[6] H.W. Jannasch, K.S. Johnson, C.M. Sakamoto, Submersible, Osmotically Pumped Analyzers for Continuous Determination of Nitrate in Situ, Anal. Chem. 66 (1994) 3352-3361.

[7] L.R. Adornato, E.A. Kaltenbacher, T.A. Villareal, R.H. Byrne, Continuous in situ determinations of nitrite at nanomolar concentrations, Deep-Sea Research I, 52 (2005) 543–551.

[8] D. Thouron, R. Vuillemin, X. Philippon, A. Lourenco¸ C. Provost, A. Cruzado, V. Garcon, An Autonomous Nutrient Analyzer for Oceanic Long-Term in Situ Biogeochemical Monitoring, Anal. Chem. 75 (2003) 2601-2609.

[9] M.J. Moorcroft, J. Davis, R.G. Compton, Detection and determination of nitrate and nitrite: a review, Talanta, 54 (2001) 785– 803.

[10] M. Badea, A. Amine, G. Palleschi, D. Moscone, G. Volpe, A. Curulli, New electrochemical sensors for detection of nitrites and nitrates, J. Electroanal. Chem. 509 (2001) 66–72.

[11] J. Davis, M.J. Moorcroft, S.J. Wilkins, R.G. Compton, M.F. Cardosi, Electrochemical detection of nitrate and nitrite at a copper modified electrode, Analyst, 125 (2000) 737–742.

[12] S. Zhao, J. Tong, Y. Li, J. Sun, C. Bian, S. Xia, Palladium-gold modified ultramicro interdigital array electrode chip for nitrate detection in neutral water, Micromachines, 10 (2019) 223.

[13] K.S. Johnson, J.A. Needoba, S.C. Riser, W.J. Showers, Chemical sensor networks for the aquatic environment, Chemical Reviews, 107 (2007) 623-640.

[14] Endress+Hauser AG, Nitrite analyzer - Liquiline System CA80NO https://www.ie.endress.com/en/field-instruments-overview/liquid-analysis-product-overview/nitrite-analyzer-ca80no (accessed 15 May 2019).

[15] Systea S.p.A, WIZ Portable *In-situ* Probe For Water Analysis http://www.systea.it/index.php?option=com_k2&view=item&id=383:wiz-news&lang=en (accessed 15 May 2019).

[16] EnviroTech LLC, NAS-3X *In-Situ* Nutrient Analyzer https://www.bodc.ac.uk/ data/documents/nodb/pdf/ envirotech_nas_nutrient_analyser.pdf (accessed 12 May 2019).

[17] A.K. Hanson, Chemical Analyzer for Mapping Coastal Nutrient Distributions in Real Time. Oceans 2000 IEEE - Where Marine Science and Technology Meet (2000) 1975–1982.

[18] V.J. Sieben, C.F.A. Floquet., I.R.G. Ogilvie, M.C. Mowlem, H. Morgan, Microfluidic colourimetric chemical analysis system: application to nitrite detection, Anal. Methods, 2 (2010) 484-491

[19] A.D. Beaton, V.J. Sieben, C.F.A. Floquet, E.M. Waugh, S.A.K. Bey, I.R.G. Ogilvie, M.C. Mowlem, H. Morgan, An automated microfluidic colourimetric sensor applied in situ to determine nitrite concentration, Sens. Actuator B-Chem., 156 (2011) 1009-1014.

[20] C.F.A. Floquet, V.J. Sieben, A. Milani, E.P. Joly, I.R.G. Ogilvie, H. Morgan, M.C. Mowlem, Nanomolar detection with high sensitivity microfluidic absorption cells manufactured in tinted PMMA for chemical analysis, Talanta, 84 (2011) 235-239.

[21] Sea Bird Scientific, SUNA V2 Nitrate Sensor https://www.seabird.com/nutrient-sensors/suna-v2-nitrate-sensor/family?productCategoryId=54627869922, (accessed 16 May 2019).

[22] s::can Messtechnik GmbH, spectro::lyser spectrometer probe https://www.s- can.at/products/spectrometer-probes, (accessed 13 May 2019).

[23] YSI incorporated, IQ SensorNet NitraVis® Sensors https://www.ysi.com/nitravis, (accessed 14 May 2019).

[24] TriOS, OPUS UV spectral sensor https://www.trios.de/en/sensors.html, (accessed 14 May 2019).

[25] A. Ríos, M. Zougagh, M. Avila, Miniaturization through lab-on-a-chip: Utopia or reality for routine laboratories? A review, Anal. Chim. Acta, 740 (2012) 1–11.

[26] T.M. Schierenbeck, M.C. Smith, Path to Impact for Autonomous Field Deployable Chemical Sensors: A Case Study of in Situ Nitrite Sensors, Environ. Sci. Technol. 51 (2017) 4755−4771.

[27] E. Murray, P. Roche, K. Harrington, M. McCaul, B. Moore, A. Morrin, D. Diamond, B. Paull, Low cost 235 nm ultra-violet light-emitting diode-based absorbance detector for application in a portable ion chromatography system for nitrite and nitrate monitoring, J. Chromatogr. A 1603 (2019) 8-14.

[28] Alliance for Coastal Technologies, Nutrient Sensor Challenge. http://www.act-us.info/nutrients-challenge/index.php, 2017 (accessed 10 May 2019).

[29] US EPA, Advanced septic system nitrogen sensor challenge, https://www.epa.gov/innovation/advanced-septic-system-nitrogen-sensor-challenge-phase-ii-prototype-testing (accessed 15 May 2019).

[30] Integrated Ocean Observing System, ACT Nutrient Sensor Challenge. https://ioos.noaa.gov/news/act-nutrient-sensor-challenge-winners-announced/, (accessed 11 May 2019).

[31] E. Murray, Y. Li, S.A. Currivan, B. Moore, A. Morrin, D. Diamond, M. Macka, B. Paull, Miniaturized capillary ion chromatograph with UV light-emitting diode based indirect absorbance detection for anion analysis in potable and environmental waters, J. Sep. Sci. 16 (2018) 3224-3231.

[32] K.R. Elkin, Portable, fully autonomous, ion chromatography system for on-site analyses, J. Chromatogr. A 1352 (2014) 38-45.

Chapter 7:

Other experimentation and observations

"... even when we find not what we seek, we find something as well worth seeking as what we missed."

Robert Boyle, Of Unsucceeding Experiments, 1661

Chapter Overview

This chapter describes the experimentation and work carried out during the early stages of the PhD. This work yielded unexpected outcomes, unconducive to the development of a robust analyser, however, it was still informative and directed the research in a manner which enabled the final development of the portable, automated IC. At the commencement of the project, the ultimate aim was to develop a low-cost, deployable analytical system for the analysis of nutrients in environmental waters, with a specific focus on ion chromatography. The route to achieving this low-cost, portable IC system was to be based on the use of low back pressure monolithic columns and direct conductivity detection. This section discusses the rationale behind using monoliths, why it was decided not to proceed with the use of monoliths, and explains the transition from the use of conductivity detection to LED-based optical detection.

7.1 Monolithic columns and conductivity detection

Typical analytical columns for IC consist of silica or polymeric particles which are packed into the column. Generally, the smaller the particle size, the greater the efficiency. However, this is limited by the fact that there is a particular point at which the pressure drop across the column exceeds the operating conditions of the chromatographic instrument [1]. Therefore, the smaller the particles which are used, the greater the back pressure which occurs. The porous structure of monolithic columns has been shown to allow for higher flow rates at lower back pressure than particulate columns, while maintaining suitable efficiency [2-3]. The term “monolith” refers to a continuous material which is interlaced with channels allowing for the flow of liquid through the material. Both silica and polymeric based monolithic columns are available. When considering the analysis of small inorganic molecules, the bimodal pore size distribution of silica monoliths provides a greater surface area than polymeric monoliths [4]. The macroporous and mesoporous nature of a silica monolith is depicted in Figure 7.1. For this reason, silica monoliths were investigated towards achieving a portable IC system capable of rapid separations (< 2 min) at low back pressures.

In order to effectively separate inorganic anions using silica monolithic columns, post-creation modification of the monolith is required. This can be achieved using ion-interaction reagents or through the application of a surfactant coating to a reverse phase column. As an alternative approach, reagents can also be covalently or electrostatically bound to bare silica monoliths to convert the column into an IC phase [1]. The latter was the approach which was adopted within this project as silica monoliths were coated with the cationic surfactant didodecyldimethylammonium bromide (DDAB).

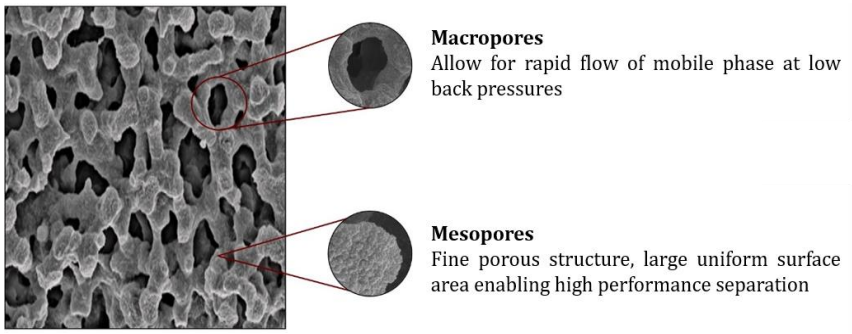

Figure 7.1: Scanning electron microscope (SEM) image of macropores (2 μm) and mesopores (13 nm) of silica monolithic column [5]

The monolithic coating work which was carried out is highlighted here. Using components from decommissioned Dionex DX 100 and 120 ion chromatograph systems, an IC test rig was setup and is shown in Figure 7.2. A C18 1 cm long Chromolith silica monolith (Merck KGaA, Germany) was coated with the cationic surfactant DDAB, using previously published coating procedures [6, 7]. The column was equilibrated with 1 % acetonitrile and then flushed with a DDAB/ACN solution at 1 mL/min until breakthrough of DDAB was observed, as determined by a rapid increase in conductivity. The column was then washed with water to remove any unretained DDAB. Finally, the column was equilibrated with eluent. As the goal was to generate a low-cost system, nonsuppressed, direct conductivity detection was selected as this allowed for a single column configuration without the necessity of a suppressor. Using the configuration shown in Figure 7.2, a range of various eluents were assessed with the coated monolith for the detection of anionic analytes. To enable direct conductivity detection, low-conductivity eluents are required. By using organic acids of low conductance, the analyte anions are of a higher ionic conductance than the eluent

competing anion, this allows for detection of analyte anions as they are eluted from the column into the conductivity detector.

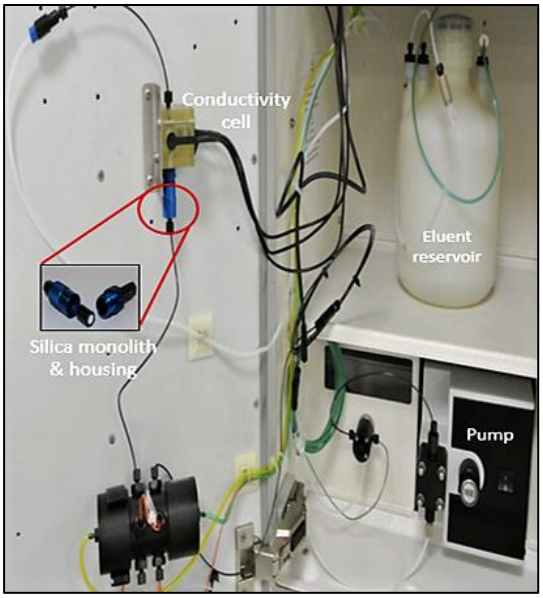

Figure 7.2: IC configuration assembled for monolith coating and anion analysis.

Monoliths have been coated with cationic surfactants in previous works and fast analysis of inorganic anions has been demonstrated [8-10]. Here rapid separation at low back pressures (< 10 bar) of multiple analytes were demonstrated using various eluents with the coated monolith and direct conductivity detection. Examples of chromatograms which were generated are illustrated in Figure 7.3. Chromatogram A shows the separation and detection of five common inorganic anions in under 1 minute using 5 mM 4-hydroxybenzoic acid eluent. Co-elution of early peaks was observed in the presence of phosphate. For chromatogram B, an eluent comprised of 2.5 mM phthalic acid / 2.3 mM Tris was used. Separation and detection of NO_2^-, NO_3^- and SO_4^{2-} was achieved, however, co-elution was observed in the presence of other anions.

As no suppressor is used with direct conductivity detection, the background conductivity originating from the eluent is high and this negatively impacts detection sensitivity. In addition, conductivity detection is non-selective which makes this approach prone to co-elution and interference, especially when considering rapid separation times. In an attempt to overcome these issues, LED-based optical detection was explored as a means of generating a simple and robust detector for coupling with an IC set up.

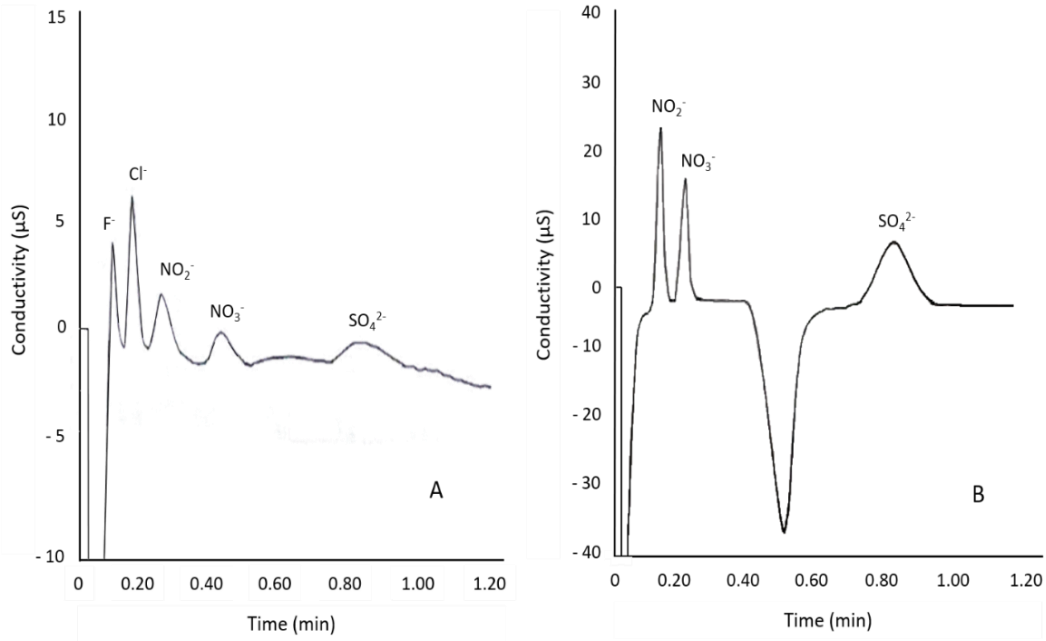

Figure 7.3: (A) Anion standard containing 5 mg/L F^-, Cl^-, NO_2^-, NO_3^- and SO_4^{2-} using 5 mM 4-hydroxybenzoic acid eluent; (B) Anion standard containing 10 mg/L NO_2^-, NO_3^- and SO_4^{2-} using 2.5 mM phthalic acid / 2.3 mM Tris eluent.

7.2 LED-based optical detection

An optical cell, shown in Figure 7.4, was adapted from a non-functioning UV-detector and an LED and photodiode were aligned and held in place enabling detection. Holders for the cell, LED and photodiode (PD) were 3D printed using a Markforged Mark Two printer.

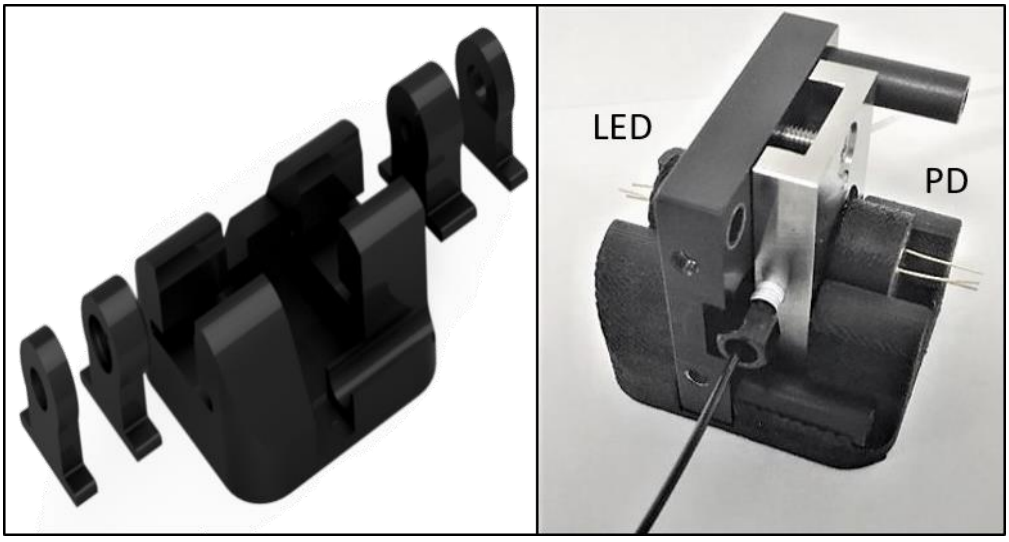

Figure 7.4: 3D printed optical cell housing and photograph of cell with LED/PD aligned

A simple test rig (Figure 7.5) was set up using the 1 cm RP silica monolith coated with DDAB, the DX 100 IC pump, a manual micro injection valve and the LED-based detector. Data acquisition and LED control was achieved using a custom interface unit as described in Chapter 4. Using this test rig the performance of the LED-based optical detector was established.

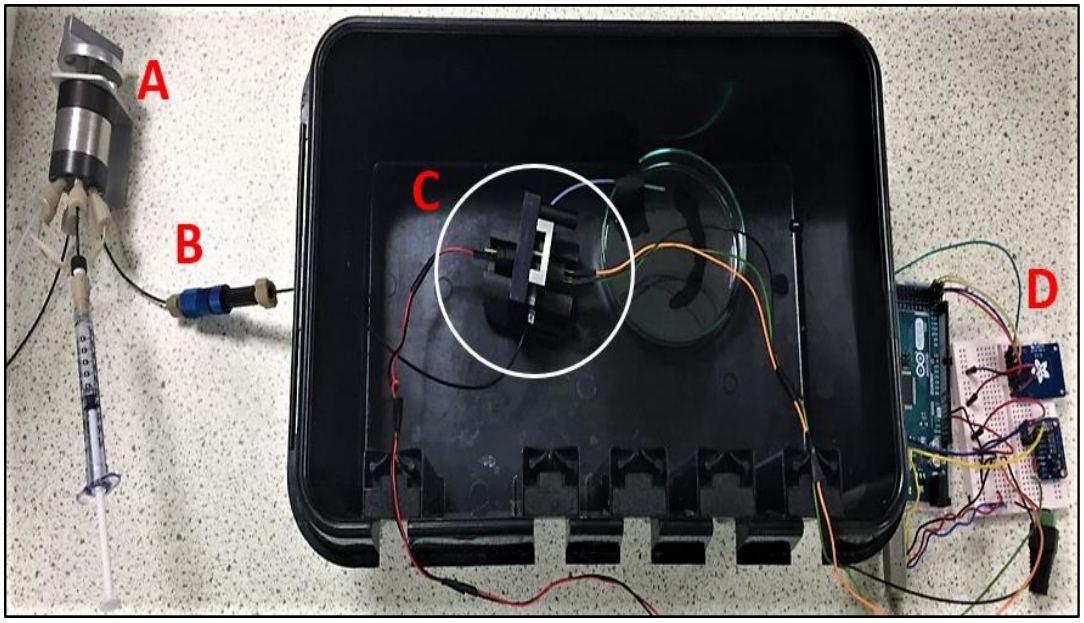

Figure 7.5: A: Micro injection valve, B: Coated silica monolith, C: Optical cell with LED/PD holder, D: Control system and acquisition

At the time of this work, UV-LEDs with a wavelength of 255 nm were the lowest wavelength LEDs available. Therefore, direct detection of nitrite and nitrate was not possible. As an alternative, indirect UV detection was employed using a 260 nm LED and a UV absorbing eluent. An example of a chromatogram generated using the optical cell and IC set up is shown in Figure 7.6. Fast separation and detection of multiple anions is achieved in under 3 minutes using sodium benzoate eluent, the coated monolith and the UV-LED based detector. Improved sensitivity was observed using the optical detector in comparison to direct conductivity detection. However, slight co-elution was also observed using the indirect UV detection approach due to its non-selective nature.

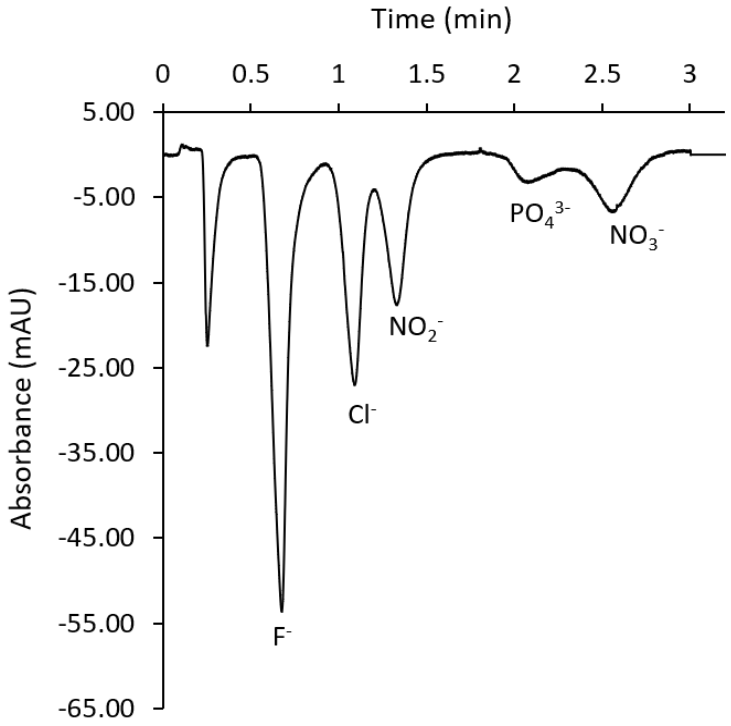

Figure 7.6: Chromatogram generated using IC set up with LED-based optical detector. Chromatogram represents a 25 µL injection volume of 5-anion standard containing 10 mg/L F^-, Cl^-, NO_2^-, PO_4^{3-} and NO_3^-. Eluent was 1.5 mM sodium benzoate at 0.8 mL/min.

7.3 Conclusion

Despite the demonstration of separation employing the coated monolith, when using surfactant coated columns, it has been shown that capacity gradually decreases over time due to slow leaching of the surfactant off the column [6]. This is problematic and raises concerns when considering long term, *in-situ* deployment. Covalently bonding latex particles functionalised with quaternary ammonium groups to the silica monolith achieves a more robust, stable anion exchange column [2]. However, this requires either manufacturing the functionalised particles or sourcing them from a supplier. Both tasks proved rather challenging and when considering the manufacturing of multiple columns for multiple systems, column reproducibility would be questionable. Thus, it was decided that particle-based anion exchange guard columns would be a more suitable approach. A guard column is utilised within Chapter 4 and facilitated the manufacture and deployment of the portable IC reported in Chapter 6.

The assembled optical detector successfully demonstrated the detection of inorganic anions and showed the potential application of LED-based optical detection. However, this detection cell was clearly not feasible when considering implementation within multiple systems as the detector cell was obtained and modified from a non-functioning benchtop UV-Vis system. With this knowledge, a low-cost optical detector was designed and fabricated as described in Chapter 4. Additionally, during the course of this research access to the deep UV 235 nm LED was made possible which enabled direct, selective detection of nitrite and nitrate.

7.4 References

[1] S.D. Chambers, K.M. Glenn, C.A. Lucy, Developments in ion chromatography using monolithic columns, J. Sep. Sci. 30 (2007) 1628-1645

[2] K.M. Glenn, C.A. Lucy, P.R. Haddad, Ion chromatography on a latex-coated silica monolith column, J. Chrom. A. 1155 (2007) 8–14

[3] N. Tanaka, H. Kobayashi, K. Nakanishi, H. Minakuchi, N. Ishizuka, Monolithic LC columns, Anal. Chem. 73 (2001) 420A–429A.

[4] T.J. Causona, I. Nischang, Critical differences in chromatographic properties of silica- and polymer-based monoliths, J. Chrom. A. 1358 (2014) 165–171.

[5] Merck Millipore (2017) *Chromolith HPLC Columns,* available: http://www.merckmillipore.com/IE/en/products/analytics-sample-prep/chromatography-for-analysis/analytical-hplc/chromolith-hplc-columns/Rk2b.qB.cMMAAAE_hPB3.Lxi,nav [accessed 28/08/17]

[6] S. Pelletier, C.A. Lucy, Achieving rapid low-pressure ion chromatography separations on short silica-based monolithic columns, J. Chrom. A. 1118 (2006) 12.

[7] P. Hatsis, C.A. Lucy, Improved sensitivity and characterization of high-speed ion chromatography of inorganic anions, Anal. Chem. 75 (2003) 995–1001.

[8] D. Connolly, D. Victory, B. Paull, Rapid, low pressure, and simultaneous ion chromatography of common inorganic anions and cations on short permanently coated monolithic columns, J. Sep. Sci. 27 (2004) 912–920.

[9] D. Connolly, B. Paull, Fast ion chromatography of common inorganic anions on a short ODS column permanently coated with didodecyldimethylammonium bromide, J. Chrom. A. 953 (2002) 299–303.

[10] B. Paull, P.N. Nesterenko, New possibilities in ion chromatography using porous monolithic stationary-phase media, TRAC Trends Anal. Chem. 24 (2005) 295–303.

Chapter 8: Conclusions and future perspectives

8.1 Overall summary and conclusions

Within this thesis, both the environmental and economic cost associated with nutrient pollution in environmental waters are highlighted and discussed. At present, measuring of nutrient levels in natural water predominantly relies on the physical collection of a spot sample that is then taken and analysed at a laboratory. As laboratory instrumentation is validated and often accredited, this approach is accepted and regarded as the standard for regulatory purposes. Nonetheless, multiple significant issues are associated with this methodology. The most important of which being the fact the results generated by lab analysis only show analyte concentration at the instant of sampling, meaning episodic events could be missed and conclusions could be drawn based on transitory analyte concentrations. It is clear, grab sampling alone is not sufficient enough to achieve effective nutrient monitoring, thereby *in-situ* analysers are a necessity. Yet, current systems on the market are complex and high cost making them unaffordable for many users and impractical when considering mass adoption and deployment.

A global need and a clear commercial demand exist for low-cost nutrient sensing platforms and this is exemplified by the large and growing total annual cost of nitrogen pollution, in the EU alone being estimated between €70 - €320 billion [1]. The global spending on water quality monitoring instruments is projected to be $3.6 billion by 2021. This spending is inclusive of new *in-situ* water quality monitoring instruments [2]. This PhD has been driven by this need and demand and has been focused on the development of simple, low-cost and reliable analytical systems which facilitate improved nutrient monitoring of environmental waters. Development of such systems will enable and assist decision makers to make operational and interventional decisions based on actual nutrient concentrations in water in near real-time. This offers the potential for the transition from the ineffective slow reactive model to a quick reactive and ultimately a preventative model.

A simple approach such as that described in Chapter 2 employing colorimetric chemistry within an on-site test kit is an example of an analytical system which has a complimentary role to play in nutrient monitoring. Although a visual test kit will not provide the accuracy of analysis carried out within a laboratory, a test kit such as this is very cheap and provides the user with rapid nitrate concentration estimates directly in the field.

The automated, portable IC system described in Chapter 3 offers greater potential in terms of filling the market gap which exists for low-cost *in-situ* nutrient sensing systems. The system is light weight, generates small volumes of waste, and effectively measures both nitrate and nitrite along with other inorganic anions. Although this system represents progress beyond state-of-the-art in a number of aspects, a considerable amount of future work is still required to reduce cost, waste and power consumption even further. Furthermore, low-cost data acquisition and communication systems need to be integrated with the platform.

Chapter 4 introduced a new low-cost UV optical detector, incorporating a 235 nm LED, which was designed and fabricated using rapid prototyping techniques. Fast, highly sensitive and selective detection of nitrite and nitrate was achieved using the developed detector with a simple, low backpressure IC set up with in-house built electronics. Similar to the configuration depicted in Chapter 3, the developed detector and direct IC method were coupled to a low pressure, low cost syringe pump to demonstrate the potential of the system for portable analysis. This chapter highlighted progression on from Chapter 3 and can be viewed as a significant stride towards achieving a low-cost, fully automated *in-situ* nitrate and nitrite analyser.

Following the demonstration of robust analysis for nitrate and nitrite in Chapter 4, strategies for fast ammonium analysis for potential integration with the IC method and UV detector were explored in Chapter 5. A multi-material 3D printed microfluidic heated reactor was developed and coupled with a modified Berthelot reaction for the determination of ammonium in water. A new

microdiamond infilled ABS polymer was presented in this chapter and was successfully used as the heater coating.

Chapter 6 presented the fully automated, low-cost portable IC system for nitrate and nitrite analysis which arose from the progressive developments which occurred throughout the previous chapters. This system was comprised of 3D printed pumps and components and incorporated the microfluidic optical detector introduced in Chapter 4. The system was validated and deployed within various water matrices in the US, Finland and Ireland. The system achieved high accuracy and precision in comparison to grab samples analysed by accredited instrumentation. The portable IC is lower in cost and less complex than other *in-situ* nutrient analysers, yet noteworthy analytical performance was achieved.

Finally, other experimentation and developments which took place during the PhD were presented in Chapter 7. Investigation into monolithic columns for rapid separation and analysis was carried out as these columns have shown promise in the past by others. However, particle-based anion exchange columns were seen as a more robust, simple solution as they are highly repeatable and can be readily purchased off the shelf. LED optical detection coupled with IC was also explored in this chapter and proved beneficial as it ultimately led to the microfluidic optical cell which was designed and reported in Chapter 4.

8.2 Next Steps

Following the successful deployment and demonstration of the portable IC within the nitrogen sensor challenge held in the US. Multiple IC systems were manufactured in-house for further deployment and testing around the world. At present, there are 25 IC systems, of the design reported in Chapter 6, which are deployed *in-situ*. These systems were deployed in Europe using funding received from the EU Ecosense Life project [3]. Partners within the project in addition to potential customers are operating and monitoring the systems to identify weak points and areas of needed amelioration in terms of robustness and longevity in the field. The locations in which the systems are deployed are graphically shown in Figure 8.1. The sample matrix at each location are as follows: in the USA it is septic tank water, in Spain effluent water, for Ireland it is river water, in Finland it is effluent and for New Zealand it is also effluent.

Figure 8.1: Illustration of locations (black points) around the world in which the developed portable IC system is currently deployed.

From the multiple deployments several key observations have emerged. The primary one being a potential failing in the 3D printed syringes after several months leading to eluent leakage. The cause of this issue has been identified as a minor movement in the pump drive plate and the contact point with the plunger of the syringe during operation. This movement over extended periods of time can cause wearing of the syringe and eventually syringe failure. To overcome this issue, several iterations of the syringe pumps have taken place and these changes will be integrated by the new product development (NPD) team prior to commercial release of the system. The other is regarding sample intake filtration, at present a coarse sintered glass filter wrapped in copper nickel alloy mesh has been used for filtration. This has performed well in all matrices with no significant biofouling observed with the exception of sewage sludge within biological digestion tanks. This is an extremely contaminated matrix and blockage of the filter occurred as shown in Figure 8.2. To carry out *in-situ* analysis of such a contaminated sample for long periods of time a sample intake filter such as this is not feasible. However, this matrix represents a niche sample type and from a commercial perspective the avenues of surface water, effluent and septic water are more impactful.

Figure 8.2: Before and after photographs of outermost sample intake filter following deployment in sewage sludge within biological digestion tank in Galindo Effluent plant, Spain, as part of the Life Ecosense Life Project.

8.3 Towards Commercialisation

At present, all efforts are focused on the portable IC system for nitrate and nitrite analysis. In terms of assessing the current development status of the portable IC, the concept of 'technology readiness level' (TRL) can be used to establish the systems distance from market and the tasks which need to be completed to achieve commercialisation. The concept of TRL was first introduced by the National Aeronautics and Space Administration (NASA) in the 1970s, with the TRL scale further detailed with definitions at each level in 1995. Nowadays, the TRL scale is routinely used as part of the EU Horizon 2020 framework program, the U.S. Department of Defense and many other organisations. TRL is now a proven method of communicating the status of new technologies [4].

The technological evolution of the nitrate and nitrite portable IC and journey from commencement of the PhD to now, with respect to the TRL scale, is graphically summarised in Figure 8.3. The current TRL of the system is TRL 7-8. The prototype system must now traverse the gap from prototype to product development and commercialisation. Key areas of focus and development in order to achieve this task are highlighted below:

- Design for Mass Manufacture: Components within the system must be modified to facilitate ease of system assembly and to ensure long term supply chain of system components.
- Data acquisition and user interface design and development: Incorporation of IoT technologies to enable remote access and development of smart phone applications for rapid on-site configuration will be investigated.
- Health and safety: Electronics to be CE marked and the system should be in line with CLP Regulation (CE) 1272/2008.
- Aesthetics and usability: Within the NPD and marketing departments of the company, the system must undergo design and other necessary changes to maximise the aesthetics of the system while maintaining usability.

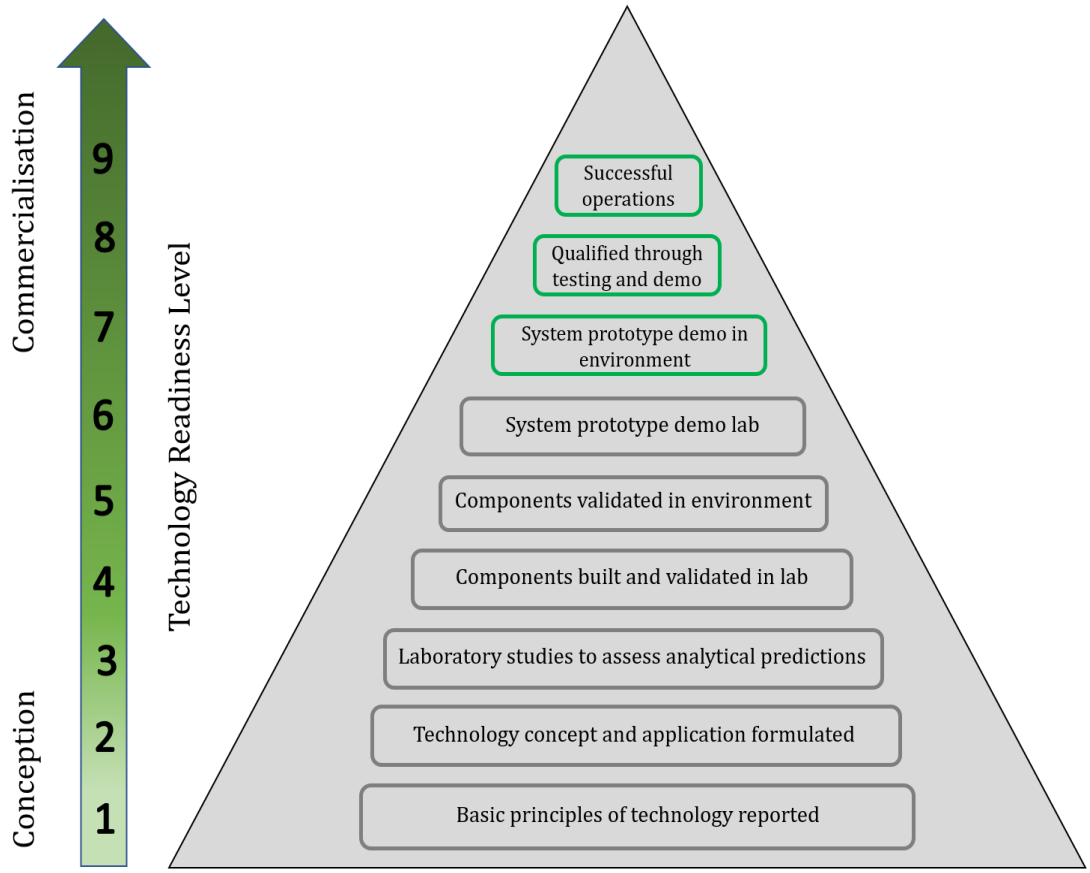

Figure 8.3: Concept in the process of technological evolution. The technology readiness level, adapted from Schierenbeck and Smith [6]. lists the stages of technology research and development that can be linked along the S-curve of Technological Process

8.4 Other Analytes

Phosphate is also a highly important analyte when considering nutrient pollution and a need yet exists for low cost *in-situ* phosphate sensing systems. The primary strategy of focus within our research group is based on colorimetry integrated onto microfluidic chips. This work is currently being carried out within the R&D department of TelLab and the PhD candidate has contributed to this work in relation to manufacturing of the microfluidic chips and the modification of colorimetric reagents for phosphate determination. The phosphate method employed is a variation of the molybdenum blue method coupled with an 880 nm LED and photodiode for detection. Photographs of the microfluidic colorimetric chip along with the portable platform assembled in-house are shown in Figure 8.4. A typical linear curve generated by the system in a laboratory setting is also demonstrated. Work will continue in this area with the aim of reducing system size towards potential integration with the nitrate and nitrite portable IC.

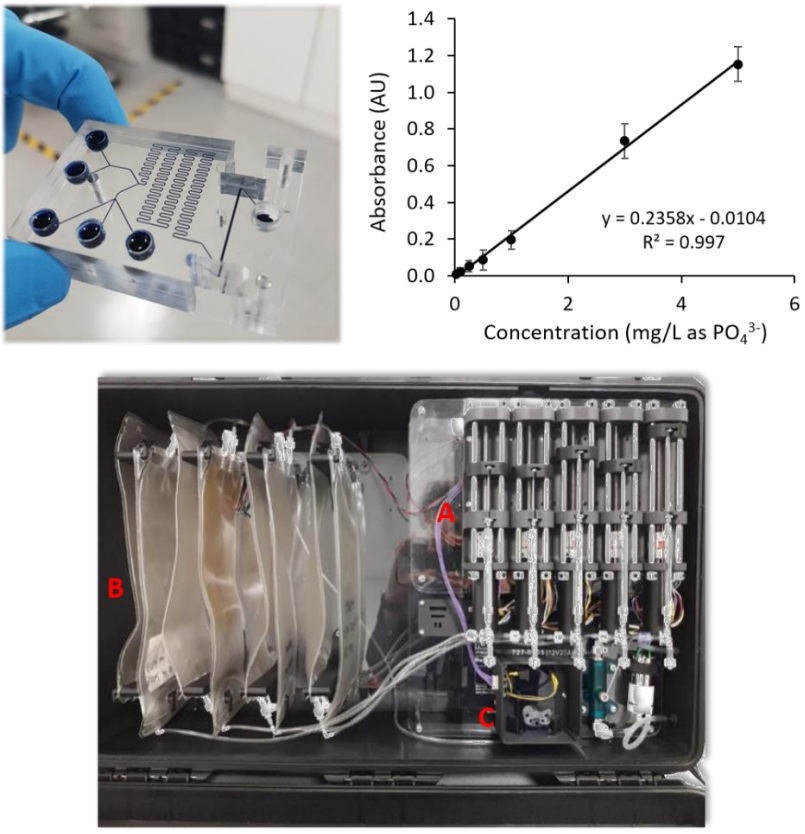

Figure 8.4: Photographs of microfluidic chip and portable platform for colorimetric phosphate analysis with typical linear curve observed. A: Pumps for reagent and standard delivery to chip, B: Storage bags for reagents, standards and waste, C: Housing for microfluidic chip and LED/PD detector.

Besides inorganic anions, the UV-LED based detector reported in chapter 4 also has the potential to enable detection of pharmaceutical compounds which contain a UV absorbing chromophore. To achieve integration of the detector with typical reverse phase chromatography, the PMMA polymer material in which the detector is made of must be replaced with a material compatible to non-polar eluents and solutions. A potential alternative to PMMA would be Teflon, due to its inherent resistance to organic solvents. A detector such as this with an integrated 235 nm UV-LED would enable low-cost detection of a broad range of pharmaceuticals. Drug compounds in the classes of anti-inflammatory, anti-fungals and anesthetics such as ibuprofen, tolnaftate and tetracaine, respectively, absorb strongly in the deep UV range which would allow for direct detection [6]. Also, anti-diabetic drugs such as Pioglitazone and Glimepiride along with sedatives such as benzodiazepines can be detected directly through UV detection [7]. Considerable development would be required to achieve this, but it is most certainly feasible and may add value when considering the field of process analytic technology.

8.5 References

[1] European Commission- Science for Environment Policy (2013). Nitrogen Pollution and the European Environment.

[2] TechNavio, Global Water Quality Sensor Market 2018-2022, Research and Markets, Dublin, Ireland, 2018.

[3] European Union LIFE Programme – Ecosense Aquamonitrix Project – Grant Number: LIFE 17 ENV/IE/000237 (2019) available: https://www.ecosensaquamonitrix.eu/ (accessed 11 May 2019)

[4] J.C. Mankins, Technology readiness assessments: A retrospective, Acta Astronautica, 65 (2009) 1216 – 1223

[5] T.M. Schierenbeck, M.C. Smith, Path to Impact for Autonomous Field Deployable Chemical Sensors: A Case Study of in Situ Nitrite Sensors, Environ. Sci. Technol. 51 (2017) 4755–4771.

[6] T.T. Nguyen, K. Rembert, J.C. Conboy, Label-Free Detection of Drug-Membrane Association using Ultraviolet-Visible Sum-Frequency Generation, J. Am. Chem. Soc. 4 (2009) 1401–1403.

[7] J.F.S. Petruci, M.G. Liebetanz, A.A. Cardoso, P.C. Hauser, Absorbance detector for high performance liquid chromatography based on a deep-UV light-emitting diode at 235 nm, J. Chromatogr. A 1512 (2017) 143-146.

Supplementary Information A

A colorimetric method for use within portable test kits for nitrate determination in various water matrices

Pictograph instructions, for ease of use when using the test kit, are illustrated in Figure A1 below. Additionally, the potential packaging design and a nitrate colour chart for estimation of nitrate concentrations present within a sample are highlighted in Figure A2.

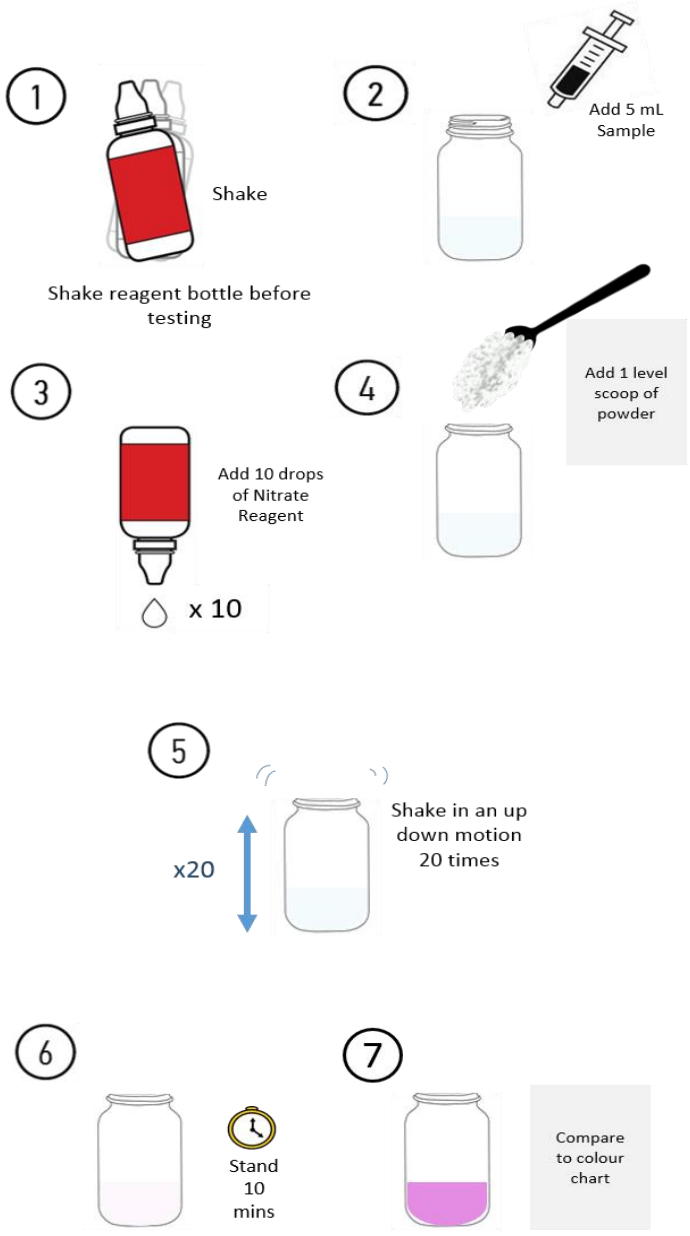

Figure A1: Pictograph instructions for the developed nitrate method

Figure A2: Potential packaging design and nitrate concentration colour chart

Supplementary Information B

Miniaturised capillary ion chromatography with indirect UV LED based detection for anion analysis in potable and environmental waters

Linearity and calibration plots generated using miniaturised IC system. Calibration plots for fluoride, chloride, nitrite and nitrate are graphically represented in Figure B1, B2, B3 and B4 respectively. The analytical parameters of the miniaturised IC system for the selected analytes are summarised in Table 3.3 within the main text of Chapter 3.

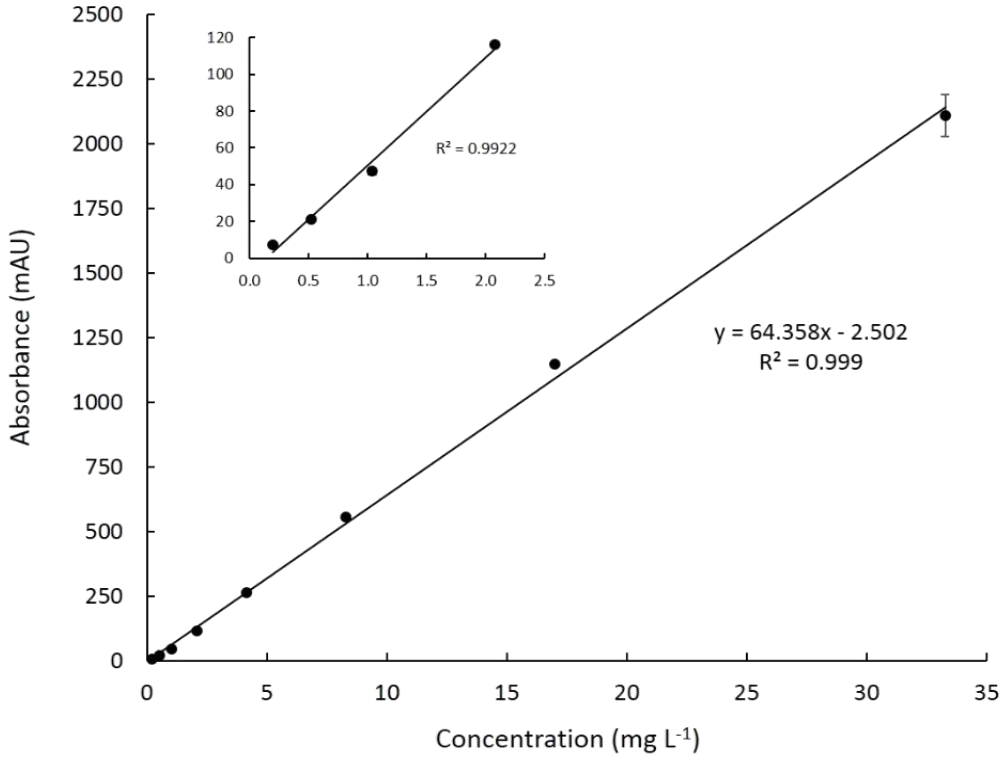

Figure B1: Calibration plot for fluoride determination using miniaturised capillary IC system. Linear range determined was 0.30 - 33.28 mg L^{-1} based on peak areas (error bars are standard deviations for *n*=3 replicates). Conditions are as stated in Figure 3.2 and 3.3.

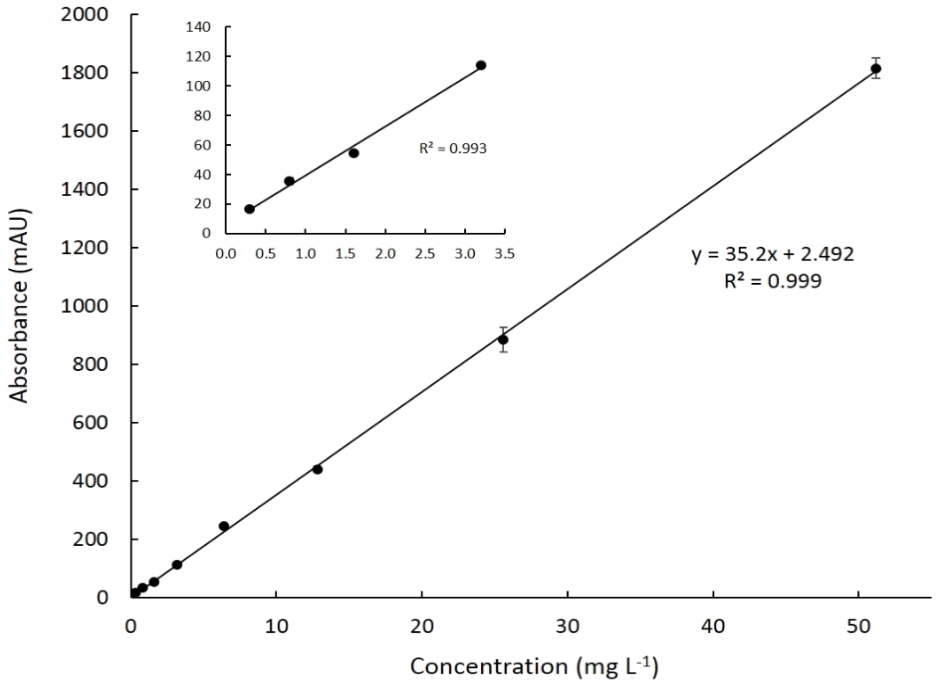

Figure B2: Calibration plot for chloride determination using miniaturised capillary IC system. Linear range determined was 0.30 - 51.20 mg L^{-1} based on peak areas (error bars are standard deviations for *n*=3 replicates). Conditions as stated in Figure 3.2 and 3.3.

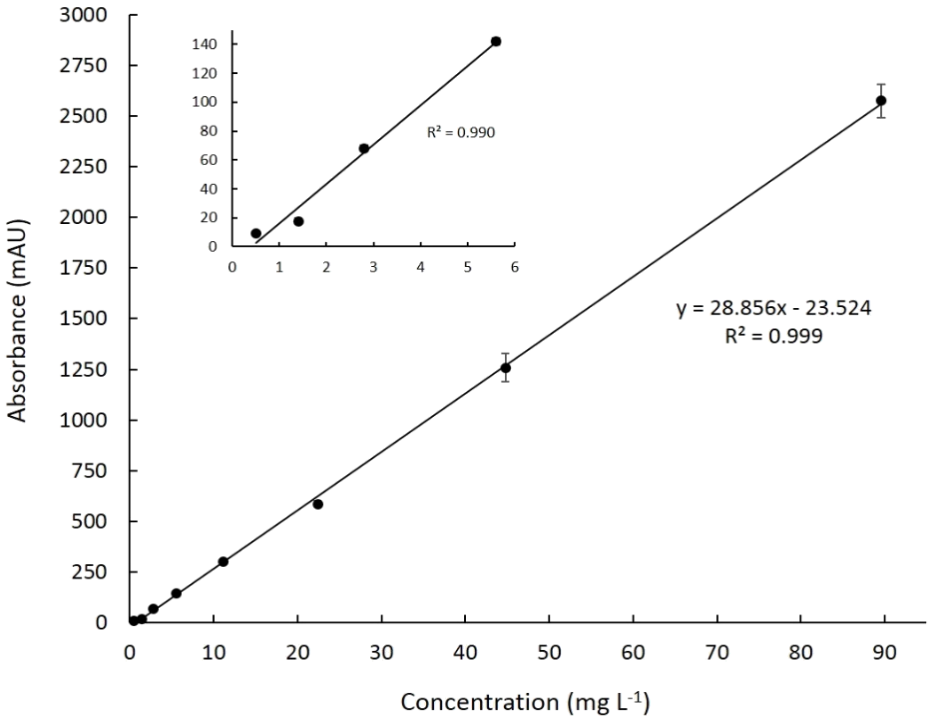

Figure B3: Calibration plot for nitrite determination using miniaturised capillary IC system. Linear range determined was 0.50 - 89.60 mg L^{-1} based on peak areas (error bars are standard deviations for *n*=3 replicates). Conditions as stated in Figure 3.2 and 3.3.

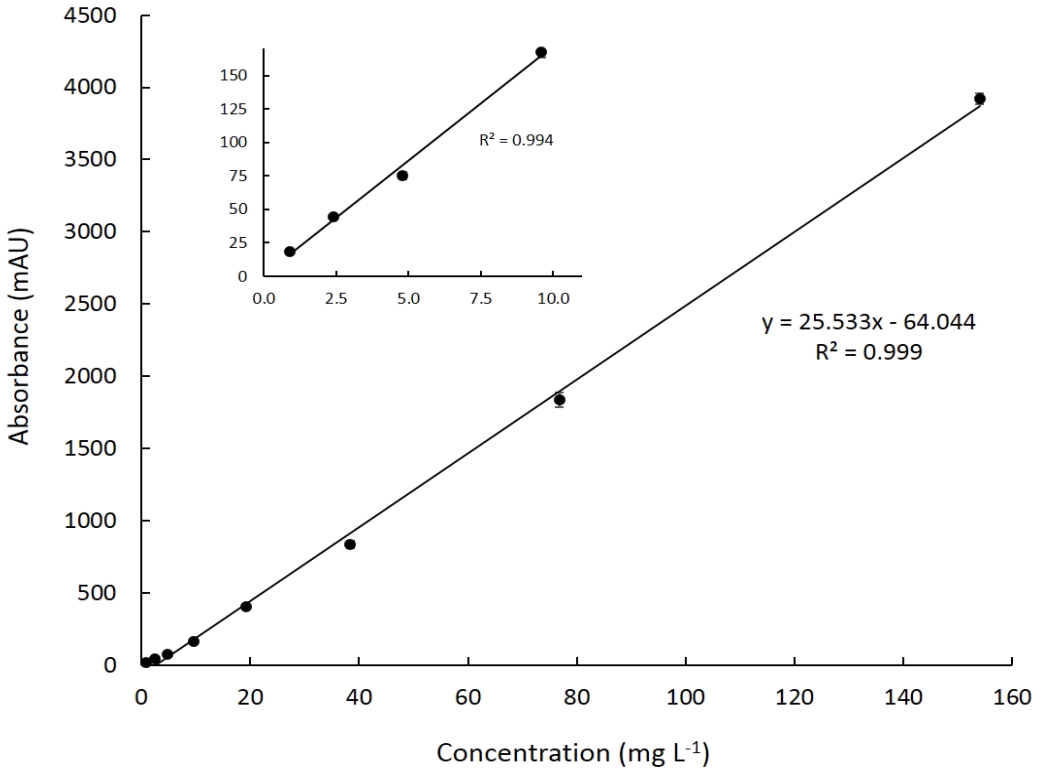

Figure B4: Calibration plot for nitrate determination using miniaturised capillary IC system. Linear range determined was 0.90 - 154.00 mg L^{-1} based on peak areas (error bars are standard deviations for *n*=3 replicates). Conditions as stated in Figure 3.2 and 3.3.

Supplementary Information C

Low cost 235 nm UV Light-emitting diode-based absorbance detector for application in a portable ion chromatography system for nitrite and nitrate monitoring

Temperature measurement of LED within detector during analysis using infrared thermal imaging camera.

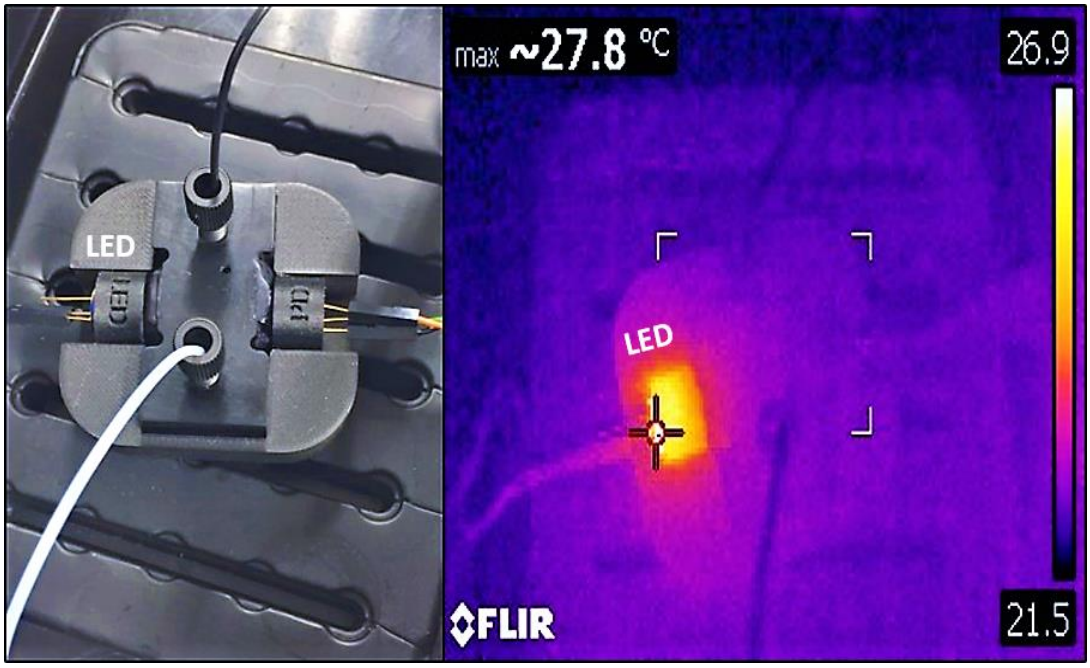

Figure C1: (Left) Photo of optical cell with 235 nm LED labelled within housing. (Right) Thermal image of the LED within detector after 1 hour of continuous operation.

Appendix C2: Equations associated with theoretical model for estimating effective pathlength and stray light.

Beer's law is highlighted in equation 1. This equation defines absorbance A for an ideal case of a monochromatic beam with no stray light as:

$$A = \log \frac{I^o}{I} = \varepsilon.l.c \qquad (1)$$

Where I^o is the incident radiant power and I is the emergent radiant power, ε is the molar absorptivity of the absorbing compound, l is the path length and c is the concentration of the absorbing compound. Following the taking of stray light I_s into account and for a light beam composed of n different wavelengths $\lambda_1, \lambda_2 \ldots \lambda_i \ldots \lambda_n$, absorbance can be written as:

$$A = \log \frac{\Sigma\ I_i^o + I_s}{\Sigma\ I_i + I_s} \qquad (2)$$

Where I_i^o is the incident radiant power at the wavelength λ_i and I_i is the emergent radiant power at the same wavelength. Rewriting equation 1 for each wavelength and substituting into equation 2 gives equation 3 below, where ε is the molar absorptivity at given wavelength λ_i.:

$$A = \log \frac{\Sigma\ I_i^o + I_s}{\Sigma\ I_i^o\ 10^{-\varepsilon.l.c} + I_s} \qquad (3)$$

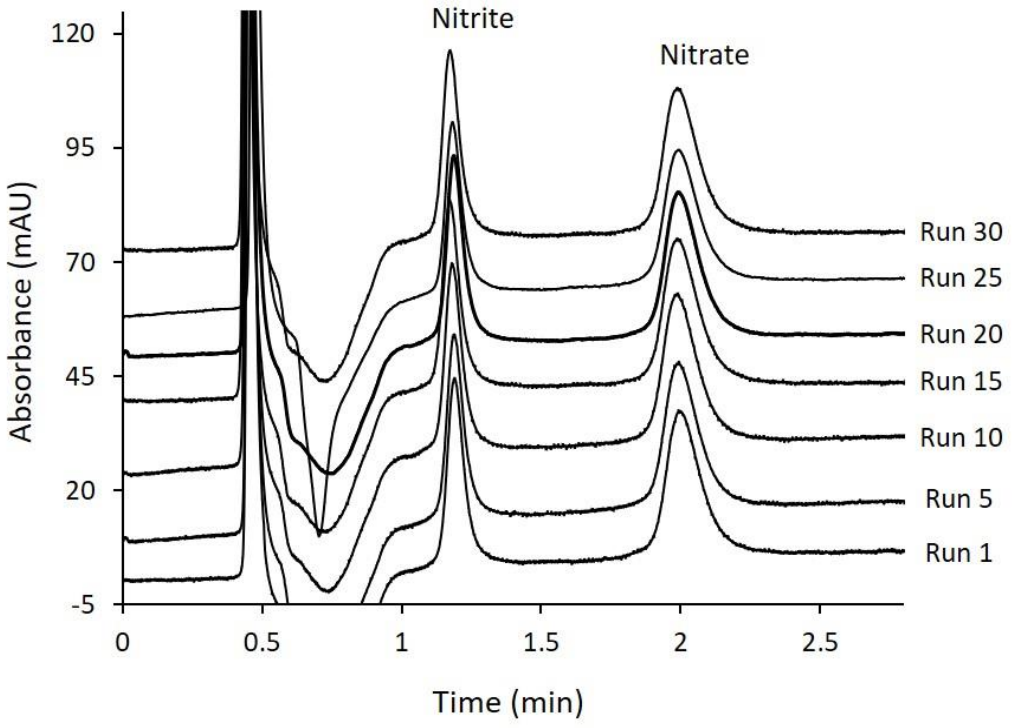

Figure C3: Selected chromatograms overlaid (offset by 10 mAU) following 30 sequential runs using IC set up with 235 nm LED and optical detector. Each chromatogram represents 150 µL injection volume of standard containing 0.5 mg L^{-1} NO_2^- and 2.5 mg L^{-1} NO_3^-. Eluent used was 100 mM KOH at a flowrate of 0.8 mL min^{-1} with AG15 guard column.

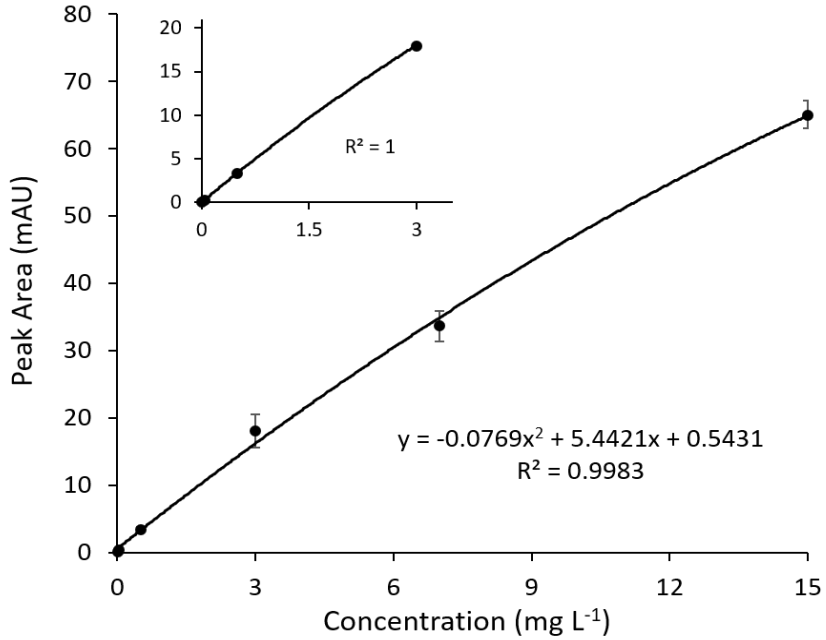

Figure C4: Calibration plot for nitrite determination. Range determined was 0.010 - 15 mg L^{-1} based on peak areas (error bars are standard deviations for *n*=3 replicates). Conditions are as stated in Figure 4.4 and 4.5.

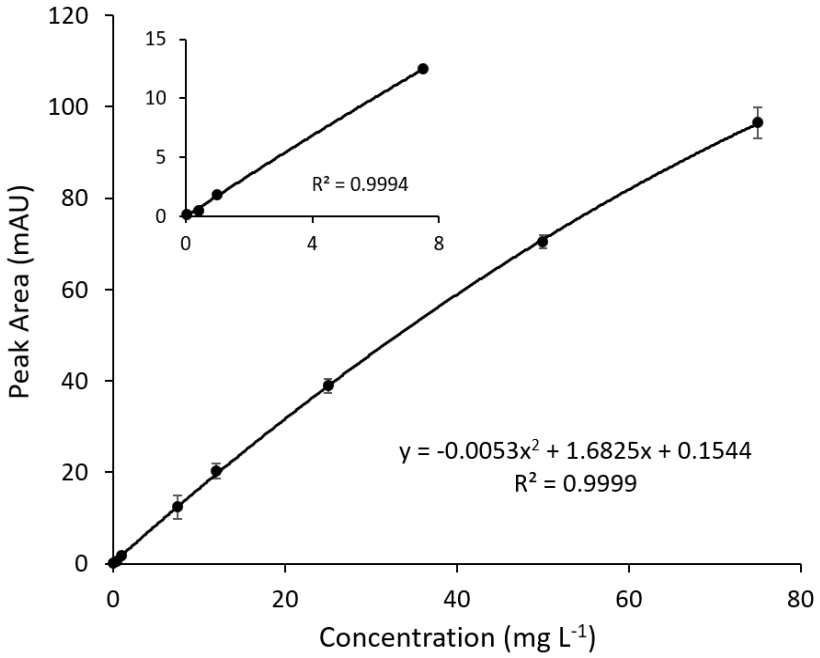

Figure C5: Calibration plot for nitrate determination. Range determined was 0.070 - 75 mg L^{-1} based on peak areas (error bars are standard deviations for *n*=3 replicates). Conditions as stated in Figure 4.4 and 4.5.

Table C6: Analysis of environmental sample A and environmental sample B carried out and reported by the environmental department of T.E. Laboratories Ltd.

Parameter (units)	**Sample A**	**Sample B**
Alkalinity (mg/L $CaCO_3$)	83	270
NH4 (by colourimetry, mg/L)	< 0.01	2.7
Antimony (µg/L)	< 0.10	0.26
Arsenic (µg/L)	< 0.10	1.2
Barium (µg/L)	< 0.03	30
Boron (µg/L)	< 0.03	68
BOD (mg/L)	3	6
Cadmium (µg/L)	< 0.03	< 0.03
Calcium (mg/L)	31	103
Chloride (mg/L)	19	22
Chromium (µg/L)	0.22	0.41
COD (mg/L)	6	20
Conductivity µS/cm @ 20˚C	327	599
Copper (µg/L)	1.19	3.4
Fluoride (mg/L)	0.23	0.11
Iron (µg/L)	128	71
Lead (µg/L)	< 0.05	0.14
Magnesium (mg/L)	7.2	10
Manganese (µg/L)	9.36	17
Mercury (µg/L)	< 0.01	< 0.01
Molybdenum (µg/L)	1.3	1.8
Nickel (µg/L)	0.64	4.3
Nitrate (mg/L)	5.03	58
Nitrite (mg/L)	0.50	0.15
pH (pH Units)	7.6	8.0
Molybdate React Phosphate as P	< 0.03	0.05
Potassium (mg/L)	4.51	15
Selenium (µg/L)	0.40	0.83
Sodium (mg/L)	9	11
Sulphate (mg/L)	13	37
Zinc (µg/L)	12.57	1.6

Table C7: Concentrations determined using IC set-up and UV detector, employing linear calibration curves to estimate concentrations, versus accredited IC (n=3).

Sample	***Analyte***	***IC Set-up (mg L^{-1})***	***Accredited IC (mg L^{-1})***	***Relative Error (%)***
A	Nitrite	0.94 ± 0.015	1.02 ± 0.011	-7.84
B	Nitrate	5.39 ± 0.040	5.07 ± 0.054	6.31
Environmental A	Nitrite	0.51 ± 0.007	0.50 ± 0.005	2.00
	Nitrate	5.07 ± 0.044	5.03 ± 0.037	0.79
Environmental B	Nitrite	0.14 ± 0.008	0.15 ± 0.010	-6.67
	Nitrate	63.10 ± 0.323	58.00 ± 0.541	8.80
EPA	Nitrate	55.82 ± 0.925	54.67 ± 0.891	2.10

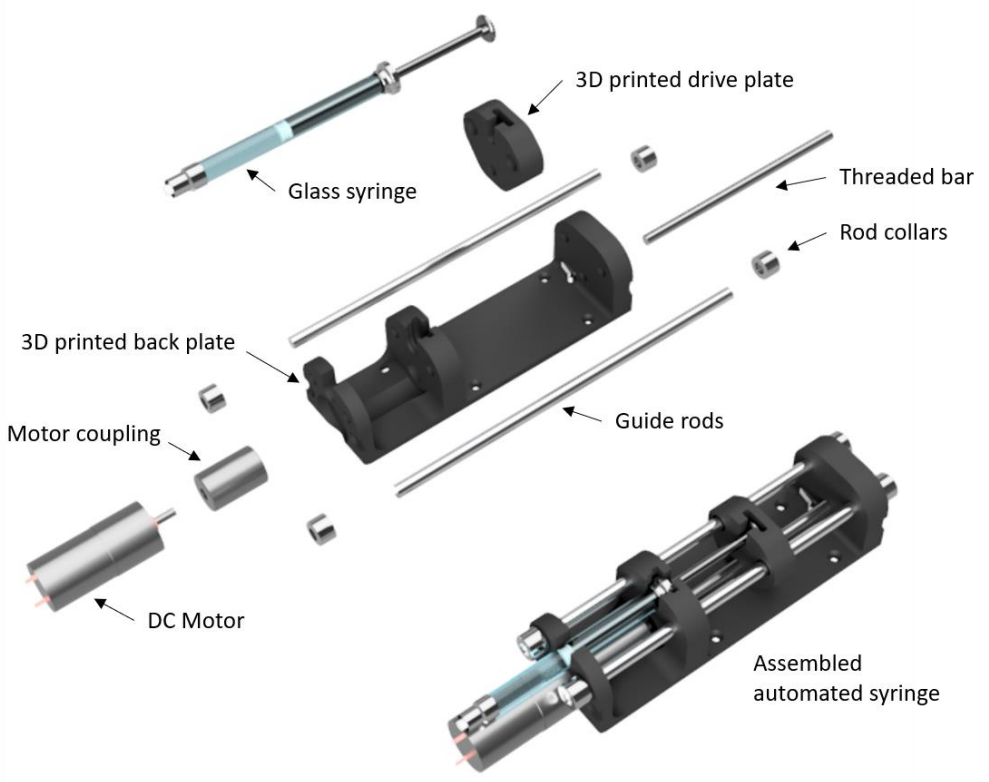

Figure C8: Exploded render highlighting design of low-pressure syringe pump which was coupled with simple IC configuration and UV detector.

Supplementary Information D

Integrated 3D printed heaters for microfluidic applications: ammonium analysis within environmental water

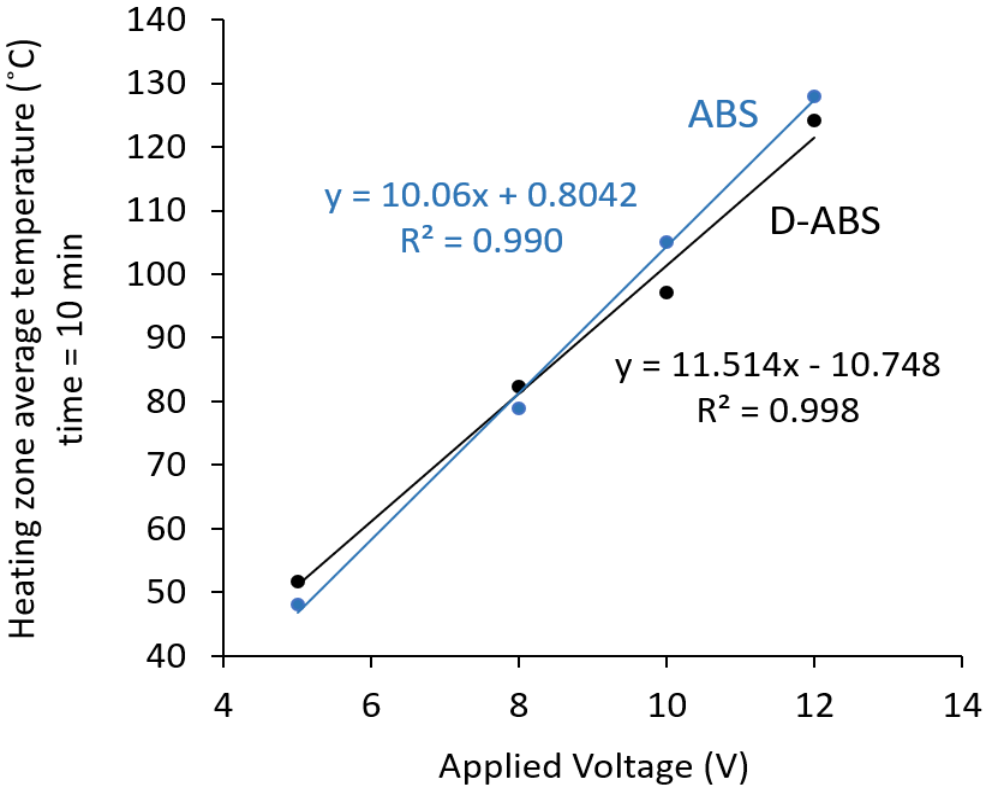

Figure D1: Heating zone average temperatures for ABS (blue line) and D-ABS (black line) heaters, recorded at 10 min, versus voltage. Temperature of heating zones for both ABS and D-ABS heaters increased linearly with increasing voltages.

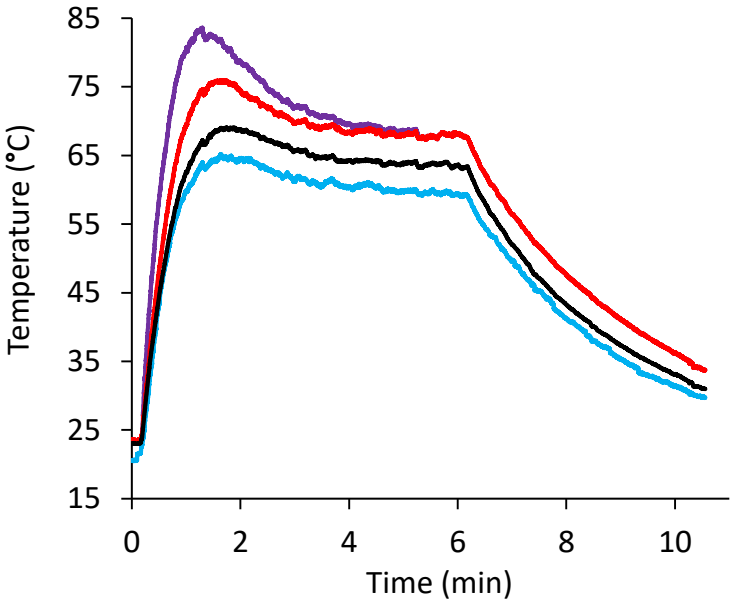

Figure D2: Time vs. temperature plot when PID is implemented at a temperature setpoint of 60ºC. The plot shows that after an initial fluctuation the temperature is stabilized after about 5 minutes. The temperature shown here, acquired through an IR camera, differs from the one sensed by the PID sensor yet it is stable, nonetheless.

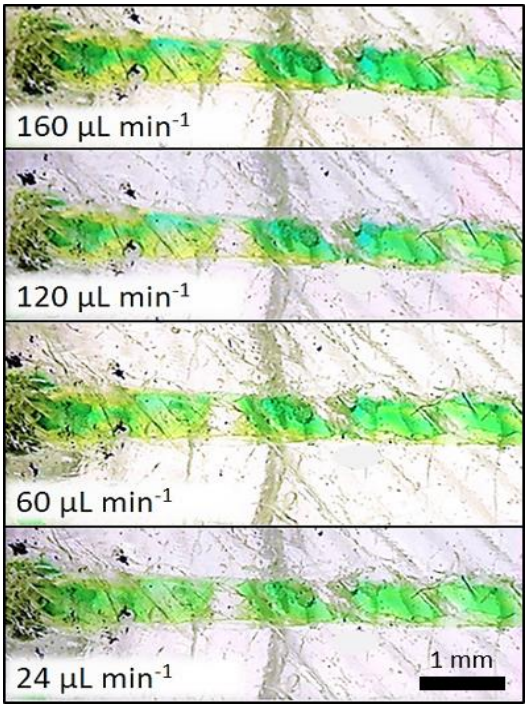

Figure D3: Demonstration of mixing using blue and yellow dyes within chip at various flow rates (160, 120, 60 and 24 µL min^{-1}) enabling residence times of 1.2, 1.6, 3.3 and 8 min respectively. As flowrate decreases, the dyes merge and a green colour is observed in a shorter distance along the fluidic channel.

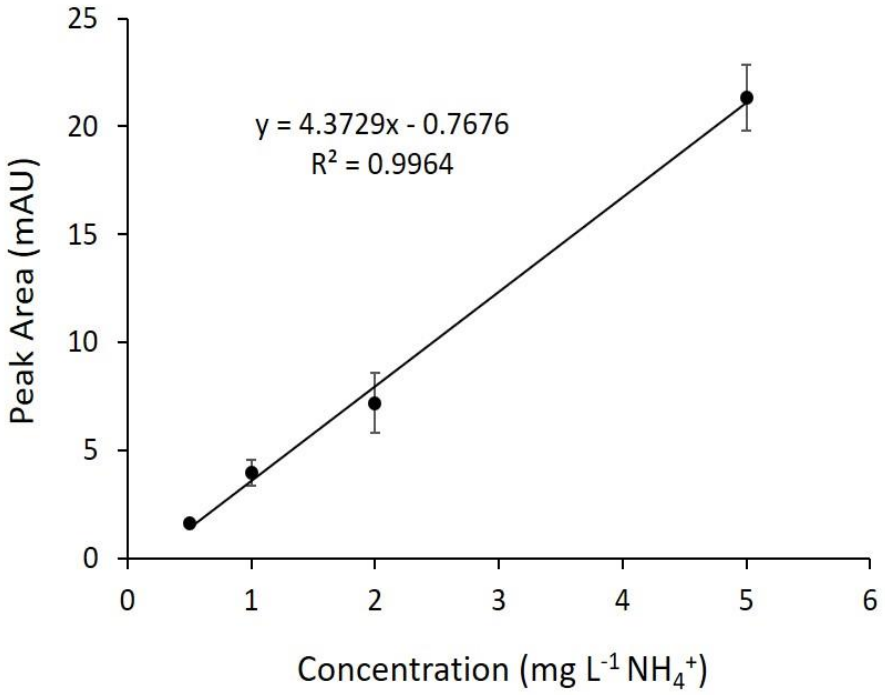

Figure D4: Calibration curve using the FIA system with optimised heating conditions and the modified Berthelot reaction. (error bars are standard deviations for n=3 replicates).

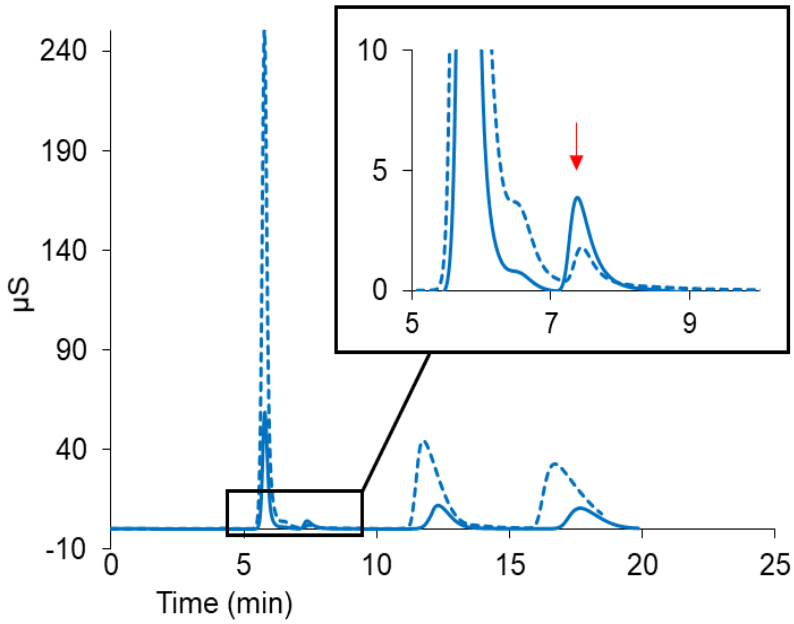

Figure D5: Ion chromatograms of the two samples (sample #2 - solid line - and #3 - dotted line). NH_4^+ peak is highlighted inset by a red arrow within the enlarged section.

Supplementary Information E

Fully automated, low-cost ion chromatography system for in-situ analysis of nitrite and nitrate in natural waters

Figure E1: (A) Photograph of the portable IC system deployed in the US and picture of the water test tank. (B) Photo of system deployed in Teagasc Johnstown Castle analysing surface water. (C) Photo of portable IC system sampling from process water at effluent treatment plant in Haapavesi, Finland.

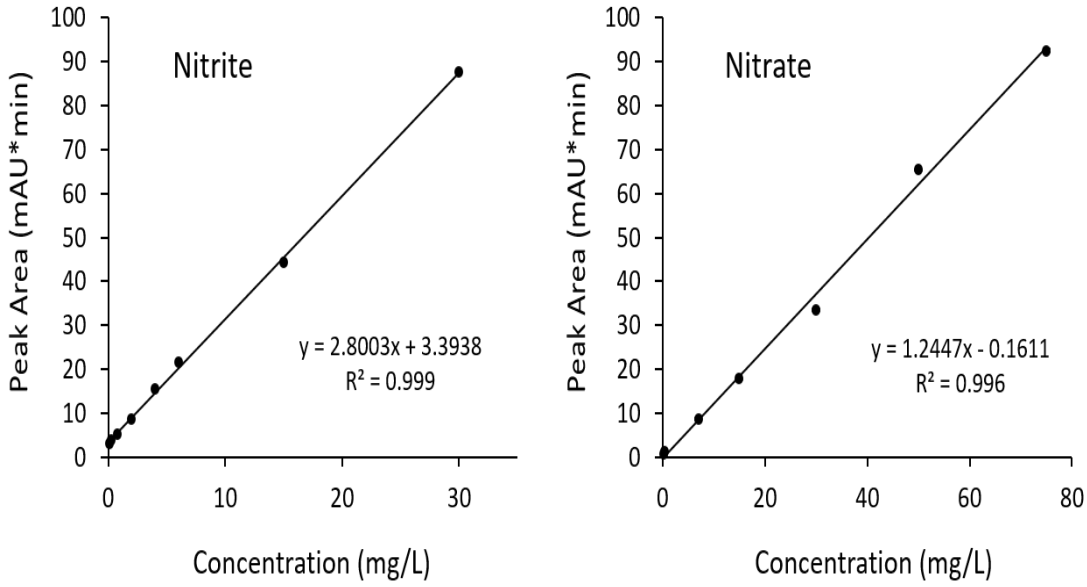

Figure E2: Calibration plots for nitrite and nitrate obtained for portable IC system using 150 µL sample loop

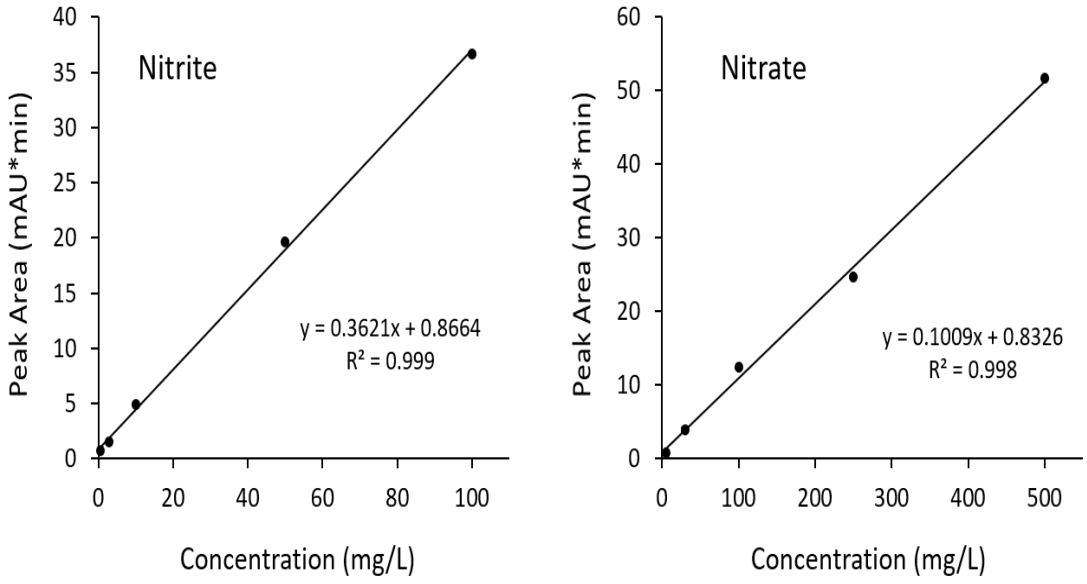

Figure E3: Calibration plots for nitrite and nitrate obtained for portable IC system using 10 µL sample loop